

HYD-RESPONSES: daily hydro-meteorological catchment-level time series to analyse HYDrological drought dynamics in RESPONSE to (cumulative) water deficits in Swiss catchments.

Christoph Nathanael von Matt^{1,2}, Benjamin David Stocker^{1,2}, and Olivia Martius^{1,2}

¹Institute of Geography, University of Bern, Bern, Switzerland

²Oeschger Center for Climate Change Research, University of Bern, Bern, Switzerland

Correspondence: Christoph Nathanael von Matt (christoph.vonmatt@unibe.ch)

Abstract.

The HYD-RESPONSES dataset (<https://doi.org/10.5281/zenodo.14713274>; von Matt et al., 2025) (<https://doi.org/10.5281/zenodo.14713274>; von Matt et al., 2026) provides new daily catchment-level time series for key hydro-meteorological variables necessary to study drought conditions, including precipitation, snow water equivalent, temperature, soil moisture, (potential) evaporation, and streamflow. The dataset covers 184 small to large Swiss catchments of the surface water monitoring network operated by the Federal Office for the Environment (FOEN). The catchments range across a variety of streamflow regime types, mean altitudes, biogeographic regions, and anthropogenic influences. The ~~data set provides daily average streamflow derived from measurements by the FOEN and daily hydrometeorological data (precipitation, temperature, radiation, snow and soil moisture) on the catchment level extracted from spatially gridded~~ data dataset comprises daily mean streamflow observations obtained from the Federal Office for the Environment (FOEN), complemented by daily hydrometeorological variables aggregated at the catchment scale. Complementary variables are derived from from spatially gridded products provided by MeteoSwiss (~~RhiresD, TabsD, TmaxD, TminD, SrelD~~), MeteoSwiss and Spatial Climate Analyses), the WSL Institute for Snow and Avalanche Research SLF (SPASS), SLF (OSHD), and the European Centre for Medium-Range Weather Forecasts ECMWF (ERA5-Land [reanalysis](#)).

In addition, derived indicators describing snowfall, snowmelt, (potential) water balance and streamflow are provided. ~~Information on precipitation, evaporation-driven and streamflow deficits are provided in form of~~ Deficits related to precipitation, evaporation, and streamflow are quantified using both standardized and non-standardized (drought/deficit) indices. Standardized indices include the SPI, SPEI and SMRI and are provided on multiple aggregation scales from 1 to 24 months (mostly in 3-monthly steps). Non-standardized indices are provided as cumulative (water) deficits in (potential) water balance (CWD and PCWD) and streamflow (CQD). For all variables and indices, the climatology and the (standardized) anomalies are available on various time scales (daily, monthly, seasonal, and yearly). Drought event time series containing drought event numbers and drought event durations, are provided for streamflow droughts identified by using two percentile-based event definitions (fixed and variable threshold) and for cumulative water deficits (CWD, PCWD and CQD).

Detailed catchment descriptors covering hydro-climatological and hydro-terrestrial aspects as well as streamflow characteristics are provided for all catchments. The dataset can be used to study weather-driven streamflow extremes, to train

data-driven machine-learning algorithms, to study drought propagation, and for comparative analyses of catchment responses in disturbed and undisturbed catchments. The dataset is compatible with the recently published [CAMELS-CH dataset "Catchment Attributes and MEteorology for Large-sample Studies" dataset for hydrological Switzerland \(CAMELS-CH\)](#) and with additional catchment descriptors provided by the FOEN.

30

1 Introduction

In recent years, the frequency of droughts has increased in Europe and Switzerland with notable drought years in 2003, 2011, 2015, 2018, 2020. Most recently, in 2022, conditions were characterized as unprecedented in terms of compound heat and drought in the last 500 years over large parts of Europe (BAFU, 2016; BAFU et al. (Eds.), 2019; BUWAL, BWG, Me-
35 teoSchiweiz, 2004; Scherrer et al., 2022; Tripathy and Mishra, 2023). Under climate change, this trend is likely to continue with projected increases in drought frequency, dry spell duration, and drought severity for both individual and combined drought types (Brunner et al., 2019c, a; Calanca, 2007; Kotlarski et al., 2023; Muelchi et al., 2021a; von Matt et al., 2024). Increasing drought impacts on various sectors are expected. This has prompted Swiss national authorities to establish a national drought early warning system (DEWS, see <https://www.trockenheit.admin.ch/en>; BAFU (Eds.), 2021; CH2018, 2018;
40 Haile et al., 2020; Henne et al., 2018; Naumann et al., 2021; Brunner et al., 2019a; Otero et al., 2023; Ranasinghe et al., 2021; Tschurr et al., 2020; BAFU, 2022; Swiss Confederation, 2025).

Droughts are an inherently multivariate phenomenon with often non-linear drought propagation from meteorological conditions to impacts on ecosystems, infrastructure, and economy. Individual drought events may differ in their hydro-climatological, hydro-meteorological, hydro-terrestrial and anthropogenic [characteristics-drivers](#) (Brunner et al., 2023; Hao and Singh, 2015;
45 Mishra and Singh, 2010; Zhou et al., 2021; Floriancic et al., 2020; Massari et al., 2022). The consideration of multiple hydro-climatic, hydro-meteorological, hydro-terrestrial and anthropogenic ([disturbance](#)) factors is therefore key to understand catchment-specific drought responses and sensitivities and to provide information for drought early warning, preparations, and interventions (e.g., Apurv et al., 2017; Apurv and Cai, 2020; Baez-Villanueva et al., 2024; Brunner et al., 2022, 2021; Ding et al., 2021; Peña-Angulo et al., 2022; Peña-Gallardo et al., 2019; Sutanto and Van Lanen, 2022; Tjiedeman et al., 2018; Van Lanen et al., 2013; Savelli et al., 2022; Van Loon and Laaha, 2015; von Matt et al., 2024).

Novel high-resolution observational datasets provide a unique opportunity to combine multiple hydro-meteorological variables to analyze and monitor drought dynamics and the evolution of drought impacts of individual events at the catchment-level. For example, the propagation of meteorological to hydrological droughts or the evolution of droughts from the development to the recovery phase can be studied (Brunner et al., 2021; Brunner and Chartier-Rescan, 2024; Parry et al., 2016; Raposo et al., 2023;
55 Brocca et al., 2024a; Brunner et al., 2021; Stocker et al., 2023; Poussin et al., 2021). The Federal Office for Climatology and Meteorology (MeteoSchiweiz) provides a suite of high-resolution essential climate variables spatially interpolated to a regular grid from a dense measurement station network (MeteoSchiweiz, 2024). Further, new high-resolution snow climatologies produced by both MeteoSchiweiz and the WSL Institute for Snow and Avalanche research SLF have recently become available, providing a

novel opportunity to analyze the long-term influence of snow processes, which are crucial for streamflow (drought) generation in Alpine catchments in Switzerland (Staudinger et al., 2014, 2017; Avanzi et al., 2024; Brunner et al., 2023; Koehler et al., 2022; Michel et al., 2023; Marty et al., 2025).

Observation-based evapotranspiration and soil moisture data is sparse in Switzerland. Hence, information on these variables is often extracted from hydrological model simulations Brunner et al. (2021); Melsen and Guse (2019); Samaniego et al. (2013, 2018). The ERA5-Land reanalysis dataset, provided by the European Centre for Medium-Range Weather Forecasts (ECMWF) (Muñoz-Sabater et al., 2021), offers a compromise between high spatial resolution and long temporal coverage and is better suited for hydro-meteorological analyses and modelling over more complex terrain such as Switzerland than the ERA5 reanalysis datasets (Muñoz-Sabater et al., 2021). A frequently used approach for analyzing drought propagation from meteorological (precipitation) to agricultural (soil moisture) and hydrological (streamflow and/or groundwater) droughts relies on standardized drought indices based on e.g., precipitation and/or evaporation (by using the standardized precipitation index (SPI) or the standardized precipitation evaporation index (SPEI) (Raposo et al., 2023; Barker et al., 2016; Peña-Gallardo et al., 2019; Zhou et al., 2021). These standardized drought indices are typically aggregated over varying retrospective time scales (months to years) and are useful proxies for various factors that determine catchment-scale water balances, including soil moisture, streamflow, groundwater, and snow processes (Bachmair et al., 2018; Tschurr et al., 2020; European Commission, 2020; Cammalleri et al., 2019; Staudinger et al., 2014). Longer aggregation scales hereby reflect response scales of storage components with longer memory, while shorter scales reflect streamflow and/or soil moisture in smaller catchments, mainly influenced by pluvial processes (Bachmair et al., 2018; Baez-Villanueva et al., 2024; Haslinger et al., 2014; Myronidis et al., 2018; Staudinger et al., 2014; Tschurr et al., 2020; WMO and GWP, 2016; Yihdego et al., 2019; Cammalleri et al., 2019; Bachmair et al., 2016; European Commission, 2020). Standardized drought indices are now widely used in DEWS (Bachmair et al., 2016; Kchouk et al., 2022; Raposo et al., 2023; Tjiedeman et al., 2020) and will also be used in the Swiss DEWS (L. Benelli, pers. comm.).

Recent studies focused on assessing the benefits of non-standardized (deficit) indices in tracking the drought propagation signal across drought types (see e.g., Brunner and Chartier-Rescan, 2024; Sur et al., 2020; Wu et al., 2020). Non-standardized indices provide physically interpretable and consistent information on deficits which remain inter-comparable across systems ~~as a result of non-transformation~~ (Van Loon, 2015; Raposo et al., 2023; Wu et al., 2020). Examples are the Hydrological Anomaly Index (HAI), the Water Balance Drought Index (WBDI), the cumulative water deficits (CWD), and the potential cumulative water deficit (PCWD) (Stocker et al., 2023; Sur et al., 2020; Wu et al., 2020). Non-standardized indices allow direct quantification of (precipitation) deficits or surpluses associated with the drought propagation into and recovery from a (hydrological) droughts (Wu et al., 2020) and hence provide valuable information for proactive water management and decision-making (Xu et al., 2023; Parry et al., 2018).

Here, we present a novel dataset with high-resolution observational daily catchment-level time series for key hydro-meteorological variables (including precipitation, snow water equivalent, temperature, soil moisture, (potential) evaporation and streamflow), standardized and non-standardized (drought/deficit) indices (SPI, SPEI, SMRI, CWD, PCWD, CQD) and (streamflow) drought events covering 184 small to large catchments in Switzerland. The HYD-RESPONSES

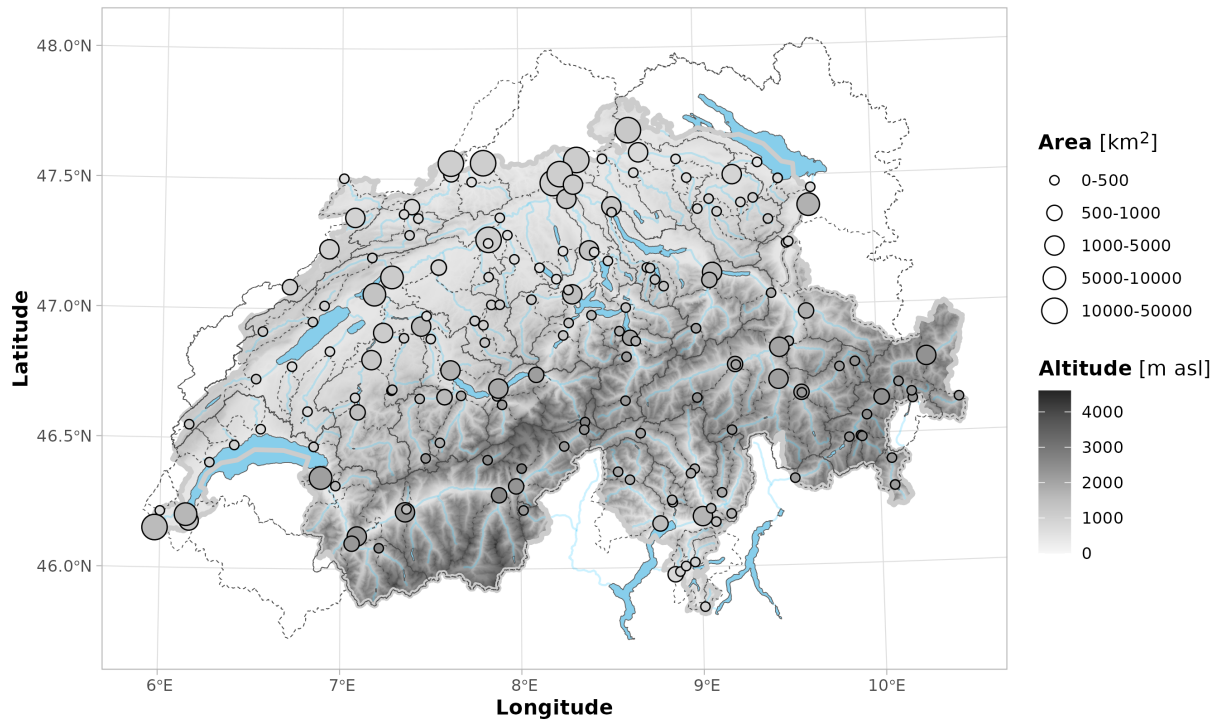


Figure 1. Overview of the study area and catchments included in the HYD-RESPONSES dataset. Catchment outlets (circles) are coloured by mean catchment altitude [m a.s.l.] and the point size scales with the catchment area [km²]. Dashed lines show the catchment outlines. Generalized streamflow networks and lakes are shown in light blue.

dataset can be combined with existing hydro-meteorological time series datasets and catchment descriptors such as CAMELS-CH (Höge et al., 2023a) [which provides large-sample hydro-meteorological data for hydrologic Switzerland and is the Swiss version of the "Catchment Attributes and MEteorology for Large-sample Studies" \(CAMELS; see e.g., Clerc-Schwarzenbach et al., 2024\)](#). The remaining paper is structured as follows: In section 2 the study region and the catchments are presented. Section 3 introduces all datasets used to compile the HYD-RESPONSES dataset. Section 4 elaborates on the processing of hydro-meteorological data. Section 5 is the analogue for the processing and extraction of catchment descriptors. Section 6 finally discusses the dataset and points to potential caveats and cautionary notes while section 7 presents multiple complementary datasets which are valuable in combination with the HYD-RESPONSES dataset. Section 8 provides a concluding summary. Three exemplary use cases to illustrate the nature and potential of the HYD-RESPONSES dataset are provided in Appendix A.

2 Study region and catchments

105 The 184 catchments (Fig. 1) provided in the HYD-RESPONSES dataset span a wide range of catchment areas (0.56–35'878 km²), glaciation percentages (0–56 %), altitude ranges (467–2937 m a.s.l.) and 18 streamflow regime types (~~n=18~~) (see Fig. 2). ~~More than half~~ A bit more than half of the catchments 51 % (n=94(51%)) of the catchments are small to ~~mid-sized~~ mid-size with an area of between 10 km² and 500 km². Only 9 (4 %) catchments are smaller than 10 km² and 56 (30.4 %) catchments are larger than 500 km². The dataset contains eight very large catchments with areas between 10000 km² and 50000 km² (max. area = 35'878 km²), associated with the three largest rivers in Switzerland: Aare, Rhine and Rhone. Most catchments (82.5 %) have less than 5 % glaciated area. ~~The~~ In terms of mean catchment height (elevation), the catchments are distributed relatively equally between 500 and 2500 m a.s.l. ~~with fewer (77 out of 98) catchments at elevation ranges above 1500 m a. s.l. (see Fig. 2c).~~ Only eight catchments are higher than 2500 m a.s.l. and only one catchment is at very low elevation (catchment Wiese, Basel). Streamflow regime types were classified and adjusted by the FOEN based on data from the Hydrological Atlas of Switzerland Table 5.2 (https://hydrologischeratlas.ch/downloads/01/content/Tafel_52.pdf). Catchments smaller than 500 km² are characterized by considering mean altitude and catchment glaciation percentage to reflect the contribution of specific streamflow (drought) generating processes (glacial, nival, pluvial). Catchments larger than 500 km² are generally classified as *mixed regime (>500 km²)* type and contain catchments characterized by a combination of streamflow (drought) generating processes. For more information see also Aschwanden and Weingartner (1985) and Fig. 2e.

110

115

120 Note that 12.5 % (n=23) of the catchments have at least 5 % of catchment area lying outside of the Swiss national borders as the dataset consists of catchments of the entire hydrological Switzerland (catchments that drain in(to) Switzerland). Furthermore, the Swiss streamflow monitoring network is designed such that multiple measurement stations may be located along the same river. As a result, upstream catchments can be nested within larger downstream catchments, leading to hierarchical dependencies.

125 3 Input data products

In this section, the input datasets used to produce and compile the HYD-RESPONSES dataset are presented and reference literature for further reading and more detailed information is provided. Original data products are provided by the Federal Office for Climatology and Meteorology (MeteoSwiss), the Federal Office for the Environment (FOEN), the Swiss Federal Office of Topography (Swisstopo), the Federal Office for Agriculture (FOAG), the WSL Institute for Snow and Avalanche Research (SLF) and the European Centre for Medium-Range Weather Forecasts (ECMWF).

130

3.1 Catchment-level time series data from streamflow observations

Daily average streamflow measurements at the catchment outlet were provided by the FOEN via the Hydrological Service (www.hydrodaten.admin.ch) for more than 200 stations. The data availability is station-specific and depends on the installation and FOEN-internal data quality checking. The HYD-RESPONSES dataset only provides a subset of 184 catchments

Table 1. (Spatially gridded) [Data](#) products used for the time series extraction. [Full variable names and associated units are provided in Table B1 \(glossary\) in Appendix B.](#) Note that the variable short names correspond to the layer/product names in the respective dataset.

Dataset	Variables	Period	Spatial resolution	Temporal resolution	Producer
Spatial Climate Analyses	TabsD, RhiresD TminD, TmaxD, SrelD	1961–2023 1971–2023	1 × 1 km	daily	MeteoSwiss
Snow Climatology for Switzerland (SPASS)	SWECLQMD	1961–2022	1 × 1 km	daily	MeteoSwiss & SLF
Climatological snow data since 1998 (OSHD)	swec, romc	1998–2023	1 × 1 km	daily	SLF
ERA5-Land	tp, t2m, e, pev, smlt, sd, ssr, ro, sro, swv11, swv12, swv13, swv14	1950–2023	0.1 × 0.1° (ca. 9 × 9 km)	hourly	ECMWF
Streamflow time series	Q	Station specific	catchment-level (outflow point data)	daily	FOEN

135 ~~by considering and considers~~ only stations for which an analysis of hydrological drought dynamics in response to cumulative water deficits was deemed to be meaningful in correspondence with the FOEN (Caroline Kan; see Fig. 1). ~~Stations were excluded in case of i) Q measured at~~ [Namely stations which provide reliable streamflow \(Q\) time series and are associated with a physical/natural catchment.](#) Stations have therefore be excluded if they i) [only provide](#) water-level ~~stations (information (no Q, 3 stations), ii) Q measured at NADUF-stations (are not part of the main streamflow measurement network (e.g., stations~~ 140 [from other networks such as the National Surface Water Monitoring Programme \(NAWA BAFU, 2023\).](#) 4 stations), iii) secondary stations (11 stations), iv) stations with potential return ~~streamflow (= negative)streamflow (Q values, 2 stations), v) Q measured at derivations (2 stations), vi) stations with no~~ [without](#) watershed delineation (i.e., subterranean; 1 station) and vii) uncertainties in time series composition due to displacement and/or temporarily missing Q of contributing stations (4 stations). ~~A The~~ complete list of included stations is provided in Tables ~~??, ??, ?? and ?? (Appendix)~~ [B6, B7, B8, B9 and B10 in](#) 145 [Appendix B.](#)

3.2 Catchment-level time series data derived from spatially gridded products

~~Meteorological variables (except for evaporation) were assembled~~ [Hydro-meteorological variables used in this study were compiled from multiple complementary data sources, combining station-based spatial climate analyses, dedicated snow model products, and reanalysis data \(Table 1\). This multi-source approach allows both comprehensive coverage of relevant variables](#)

150 and comparative analyses between different data products.

Meteorological variables derived from station-based observations were obtained from the high-resolution (1×1 km) spatial climate analyses provided by MeteoSwiss (MeteoSwiss, 2024)~~(see Table 1). The variables.~~ These include average 2 m temperature (TabsD), daily minimum and maximum 2 m temperature (TminD, TmaxD), daily precipitation sums (RhiresD),
155 and daily sunshine duration (SrelD) (Frei, 2014; Frei and Schär, 1998; MeteoSwiss, 2021a, b, c). ~~The data~~ Data availability is product-specific and covers the period ~~1961–2023~~ 1961–2023 for RhiresD and TabsD and ~~1971–2023 for the other products~~ (1971–2023 for TminD, TmaxD, SrelD) and SrelD. The spatial climate analyses ~~products used here only generally~~ cover the Swiss territory ~~; except for only, with the exception of~~ RhiresD, which ~~covers catchments located outside Switzerland, but draining also includes catchments outside Switzerland that drain~~ through Swiss territory. Note that RhiresD is not available
160 for catchments covering regions in France and Italy before 1992 due to limited meteorological station availability and ~~hence limited reduced~~ data reliability (MeteoSwiss, 2021a). Catchments with ~~a significant area in France or Italy may therefore be handled with care and/or potentially be excluded from analysis before~~ substantial areas in these regions should therefore be treated with caution or excluded from analyses prior to 1992 (see ~~Section ??~~ Sect. 6.2).

165 Snow water equivalent (SWE) data ~~was were~~ compiled from two independent high-resolution (1×1 km) snow datasets. The ~~first and main product resulted from the joint research project “A primary source is the~~ spatial Snow Climatology for Switzerland (SPASS) ~~” developed jointly~~ by MeteoSwiss and SLF (Michel et al., 2023; Marty et al., 2025). ~~The preliminary version was produced in 2022 and~~ This dataset provides modelled and bias-corrected daily SWE ~~data for the period for~~ September 1961–September ~~2022. The spatial extent is restricted to the Swiss territory. The SPASS SWE is based on the daily 2022,~~
170 derived using the SnowQM model based on TabsD and RhiresD~~products (see above) and makes use of a quantile-mapping approach. The.~~ The SnowQM model is presented in detail in Michel et al. (2023). The ~~second snow product is based on spatial coverage is restricted to Switzerland. A second snow dataset is derived from~~ the Swiss Operational Snow-hydrological Snow-Hydrological model system (OSHD)~~and is provided by the,~~ provided by WSL (SLF)~~(Mott, 2023; Mott et al., 2023).~~ The OSHD data provides information on both SWE and, which supplies SWE and modelled snowmelt runoff for the period
175 ~~1998–2022~~ 1998–2022 (Mott, 2023; Mott et al., 2023).

All ~~other remaining~~ hydro-meteorological variables, including evaporation, potential evaporation, soil moisture, and additional variables ~~already covered by the previously introduced datasets overlapping with the datasets described above,~~ were extracted from the ERA5-Land reanalysis ~~dataset~~ provided by ECMWF (Muñoz-Sabater et al., 2021). Several variables
180 are ~~therefore covered by multiple source data and are all included thus available from multiple sources and are retained~~ in the HYD-RESPONSES dataset to ~~allow comparative analyses between the different data products. Time series covered by multiple data sources include temperature variables~~ enable inter-product comparisons. Variables covered by more than one data source include air temperature (TabsD, TminD and TmaxD from MeteoSwiss, t2m from ERA5-Land), precipitation (RhiresD from MeteoSwiss, precipitation from ERA5-Land), ~~potential and total evaporation (ERA5-Land), sunshine duration (SrelD),~~

185 snow water equivalent (SWE; from SPASS, OSHD, and ERA5-Land) ~~, modelled snow melt and modelled snowmelt~~ (from
OSHD and ERA5-Land) ~~and streamflow (FOEN). Additional variables extracted from ERA5-Land include four~~. Additional
ERA5-Land-specific variables include soil water volume levels (swvl) at four depths, total solar radiation (ssr) ~~and~~, total runoff
(ro), and surface runoff (sro). ~~For a more detailed description of variables, see the data~~ Detailed variable descriptions are
provided in the dataset documentation on Zenodo (~~von Matt et al., 2025~~) (von Matt et al., 2026). A glossary ~~of for the~~ variable
190 abbreviations is provided in Table B1.

~~The ERA5-Land data is provided at an hourly temporal~~ are available at hourly resolution for the period
~~1950–2023 and can be accessed 1950–2023~~ via the Copernicus ~~climate data store~~ Climate Data Store (CDS)
(<https://cds.climate.copernicus.eu/datasets/reanalysis-era5-land>). ~~We preferably included data from~~ ERA5-Land ~~over~~
195 ~~data from~~ consists of numerical model output from the ECMWF land surface model which itself is driven by downscaled and
elevation-corrected meteorological forcing from ERA5 due to the (Muñoz-Sabater et al., 2021). The higher spatial resolution
~~of ERA5-Land~~ ($0.1 \times 0.1^\circ$, ~~ca.~~ approximately 9×9 km). ~~To ensure consistency with the other hydro-meteorological input~~
~~datasets, the hourly results in an enhanced soil moisture representation and river discharge estimations making~~ ERA5-Land
~~data was aggregated to daily values (see Section 4.1).~~ more suitable for analyses based on the hydrological cycle than ERA5
200 (Muñoz-Sabater et al., 2021).

~~Overview of the spatial raster products used to extract daily time series. (a) Mean daily temperature (TabsD, MeteoSwiss),~~
~~(b) Daily precipitation sum (RhiresD, MeteoSwiss), (c) Daily snow water equivalent of the Swiss snow climatology (SPASS)~~
~~(SWE, MeteoSwiss & SLF), (d) Daily evaporation sum (aggregated from hourly ERA5-Land data, ECMWF). Note that the~~
205 ~~second snow climatology product (OSHD) is not shown. Contours in white/black show catchment 2034 – Broye, Payerne,~~
~~Caserne d'aviation for the day with the highest observed catchment average values for each specific product for the year~~
~~2022. White squares show the catchment outlet where daily streamflow is measured. Extracted and derived time series over the~~
~~year 2022 are shown for the same catchment in Figure 6. The procedures used to extract time series from all gridded datasets~~
~~are detailed in Section 4.~~

210 3.3 Catchment-level time-invariant data (catchment descriptors)

Datasets used to compile an extensive set of catchment descriptors include station metadata and information on time series
availability and homogeneity provided by the FOEN as well as spatial (polygon) data on hydro-terrestrial characteristics
(e.g., soil characteristics, hydro-geology) provided by the FOEN, FOAG and Swisstopo (see ~~Tab.~~ Table 2). Most information
is available from www.opendata.swiss, the FOEN Hydro-Service (www.hydrodaten.admin.ch), or can be downloaded and
215 inspected via www.map.geo.admin.ch (Swisstopo). Direct links to the datasets are provided below ~~in section 10.~~ and in section
Code and data availability.

Table 2. Data products used to extract catchment descriptors.

Dataset	(Extracted) Variables	Producer
Digital soil suitability maps of Switzerland	soil wetness, soil depth, permeability, water holding capacity, nutrient content and skeletal content	FOAG
Hydrogeological map of Switzerland	aquifer type (loose or solid rock), aquifer genesis and aquifer productivity	FOEN
Lithological map for Switzerland	dominant rock type classes (loose, sedimentary and crystalline rock)	Swisstopo
Springs and swallow holes in karst regions	number of springs (per km ²)	FOEN
swissALTI3D (DEM) aspect, slope Swisstopo swissTLM3D Hydrography	Drainage density	Swisstopo
Biogeographic regions of Switzerland	Biogeographic regions	FOEN
Catchment metadata	time series availability, breakpoint analysis, area, mean height, outlet coordinates and streamflow regime type	FOEN

The digital soil suitability maps [of Switzerland](#) provide information on a set of different soil characteristics assessed on 25 different geological and geomorphological units which are further discriminated by different landscape elements depending on aspect, slope and bedrock. The maps were first assessed in 1980 and revised in 2000 (BLW, 2022; Swisstopo, 2020). The different soil characteristics include soil wetness, soil depth, permeability, water storage capacity, nutrient content and skeletal content.

The hydro-geological map of Switzerland provides information on groundwater resources in Switzerland (Schürch et al., 2007), including information on aquifer type (loose or solid rock), aquifer genesis and aquifer productivity. The map was originally produced and published for the Hydrological Atlas of Switzerland (HADES, <https://hydrologischeratlas.ch/>). The hydro-geological information was further complemented with the lithological map for Switzerland (produced by Swisstopo), which provides a general overview of dominant rock type classes (loose, sedimentary and crystalline rock). The maps are available via opendata.swiss (hydrogeological map, lithological map) or can also be accessed via the Hydrological Service of the FOEN (<https://www.bafu.admin.ch/bafu/de/home/themen/wasser/zustand/karten/geodaten.html>). The number of springs and swallow holes in karstic regions provides additional information related to aquifers and the contribution of subsurface water storage. The layer provides main discharge source locations in karstic regions and is available via opendata.swiss (produced by FOEN). ~~Standard topographical characteristics such as slope and aspect were derived from the high-resolution digital elevation model (swissALTI3D) publicly available via Swisstopo at a resolution of 2 m (Swisstopo, 2022).~~ The swissTLM3D Hydrography provides topological information on the different water bodies of Switzerland (including flowing and stagnant waters) and originates from the swissTLM3D dataset provided by and accessible via Swisstopo.

Basic catchment characteristics

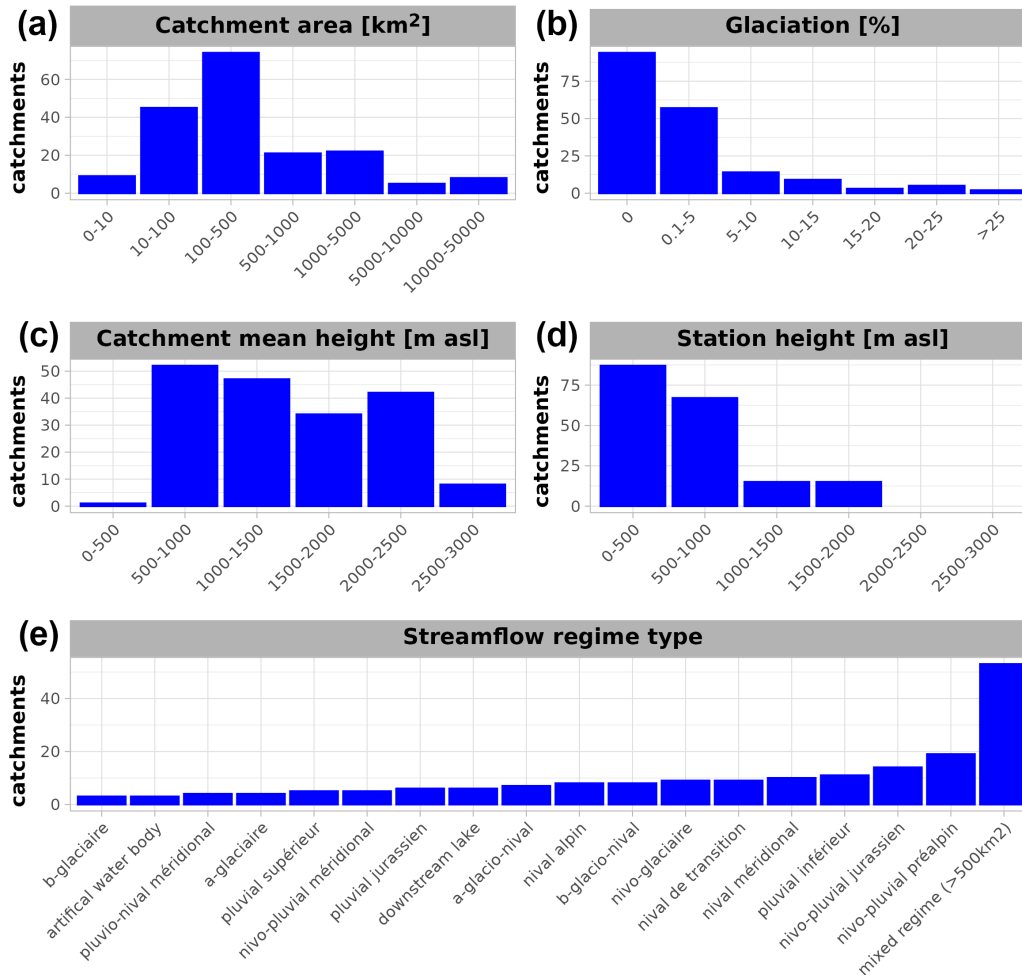


Figure 2. General catchment characteristics provided by the FOEN. **a)** Catchment area in km², **b)** Glaciation percentage (of catchment area), **c)** catchment mean height [m a.s.l.], **d)** height of the streamflow gauge measurement station [m a.s.l.] and **e)** streamflow regime types. The Y-axis shows the frequency number of catchments in each category.

The biogeographic regions of Switzerland provide six regions differentiated by similarity of flora, fauna, bryophytes and ornithological information as well as homogeneous surface water catchments (BAFU (Eds.), 2022). Biogeographic (eco-)regions often correspond well to catchment groups with similar streamflow regime types and are therefore frequently used for catchment regionalization (e.g., Jehn et al., 2020; Guo et al., 2021). The biogeographic regions are available via opendata.swiss.

Finally, general information on the gauging stations and streamflow time series (availability and homogeneity) were provided as accompanying (meta-)data by the FOEN. Time series homogeneity was ~~assessed by a FOEN-internal breakpoint analysis for time series homogenization~~ derived by the FOEN using breakpoint tests following the method of Bai and Perron (1998). Breakpoints are identified by partitioning the time series based on the number of potential breakpoints and subsequent modeling of the time series by piecewise linear regression (see Bai and Perron, 1998). The optimal breakpoints are found by minimization of the sum of squared residuals. Resulting breakpoints are indicative to changes in the mean annual 7d mean flow (M7Q) and were further plausibilized by the FOEN based on catchment meta information and known (potentially) relevant anthropogenic influences such as the construction of (reservoir) dams, hydropower and wastewater treatment plants (for more information see BAFU, 2024). General station information includes catchment area, mean ~~height~~ catchment height (elevation), glaciation percentage, outlet coordinates and streamflow regime type (among others) (see Figs. 1 and 2). Catchment outlines (polygons provided by the FOEN) and catchment outlets (point shapes) are provided in the coordinate system CH1903/LV03 (EPSG:21781).

Note that the digital soil suitability maps, swissTLM3D hydrography, biogeographic regions of Switzerland as well as information on springs and swallow holes in karst regions are restricted to Swiss national territory. Catchments with a significant area outside of Switzerland should be treated with caution regarding descriptive variables extracted from these datasets (see Sect. 5 for a comprehensive overview on extracted descriptors). The hydrogeological and lithological maps of Switzerland to a large extent also cover areas outside of Switzerland. Only catchments of the Rhine (catchments 2091, 2143, 2288, 2289) and Wiese (catchment 2199) are not entirely covered. However, with a coverage of at least >94%, descriptors extracted from these datasets may still prove valuable for these catchments.

Methodological details on the extraction and preparation of catchment descriptors are presented in Section 5.

4 ~~Data-processing~~ Processing of hydro-meteorological data

This section describes the methodology used for aggregating spatially gridded ~~data products and catchment descriptors on the catchment level~~ (time series) data product, the methods used to derive additional indicators, standardized drought indices, and presents the definition and declaration of (hydrological) drought events. Guidance on the reliability of indicators is provided through a three-level classification based on the origin of the underlying data, the extent to which variables rely on (model) assumptions, and the degree of processing applied to derive the hydro-meteorological data, (drought) indices, and events. Level 1 consists of direct, unaltered measurement data and is therefore considered the most reliable. Level 2 includes data directly extracted from publicly available spatially interpolated hydro-meteorological datasets and data subjected to only minimal (post-)processing (e.g., temporal aggregation). Level 3 comprises all variables, indicators, and indices derived by the authors, irrespective of the degree of validation or verification performed. For both Level 2 and Level 3 data, additional annotations are provided for variables whose derivation is based on a (strong) modeling component. A summary of the classification is

Table 3. Three-level reliability classification used for hydro-meteorological data in the HYD-RESPONSES dataset.

<u>Level</u>	<u>Description</u>
<u>Level 1 (L1)</u>	<u>Direct, unaltered measurement data. These data are considered the most reliable, as they are not subject to interpolation, modeling assumptions, or additional processing.</u>
<u>Level 2 (L2)</u>	<u>Data extracted from publicly available, spatially interpolated hydro-meteorological datasets and data subjected to only minimal post-processing, such as temporal aggregation. Variables whose derivation relies on strong underlying (modeling) assumptions are explicitly annotated.</u>
<u>Level 3 (L3)</u>	<u>Variables, indicators, and indices derived by the authors, irrespective of the degree of validation or verification performed. Variables whose derivation relies on strong underlying (modeling) assumptions are explicitly annotated.</u>

provided in Table 3.

275 The naming of the unaltered variables directly retrieved from measurement data (streamflow) or extracted from spatially
interpolated hydro-meteorological datasets is based on the layer names used in the original input datasets (see variables listed
in Table 1 and the glossary provided in Table B1). Derived variables and (standardized) drought indices are named by a suffix
representing the type of indicator followed by all contributing variables where ERA5-Land variables are kept in lowercase
while variables from other products start with upper-case letters. Naming for derived variables based on the snow products
280 make use of the product name (SPASS) or the combination of product and variable names (OSHD) as identifier for clear
distinction. All extracted and derived variables and their suggested reliability level are listed in the Tables B2, B3, B4 and B5
in Appendix B.

Time series of all categories are illustrated in Fig. 6 showing the exceptional drought year 2022 for the example catchment
2034 - Broye, (Payerne, Caserne d'aviation) located in the western Swiss Plateau region (see catchment contours in Fig. A4).

285 A detailed analysis of the event year 2022 demonstrating the utility of the time series provided in the HYD-RESPONSES
dataset is provided in Sect. A2 in Appendix A.

4.1 Time series extraction

Based on the spatially gridded hydro-meteorological input products (see ~~Section~~ Sect. 3.2), catchment-level time series were
290 extracted using the R-packages *terra* (Hijmans, 2023) and *exactextractr* (Baston, 2023). First, the hourly ERA5-Land data
was aggregated to daily resolution following the standards used by the MeteoSwiss spatial climate analyses (e.g., RhiresD
and TabsD). For this, instantaneous ~~and accumulation/flux variables~~ variables and variables representing accumulations or
fluxes are distinguished. For instantaneous variables, we provide daily average values. For ~~accumulation and flux~~ variables

representing accumulations and fluxes, we provide ~~variables~~–daily sums. Flux variables (mainly precipitation and evapo-
295 transpiration) ~~were further aggregated consistently with~~ are aggregated using the same temporal convention as the RhiresD
precipitation sums, i.e., from 06 UTC (day) to 06 UTC (day + 1) (see MeteoSwiss, 2021a). Instantaneous variables and
ERA5-Land temperature were averaged from 00 UTC to 00 UTC ~~, which is consistent with the other~~ again following the
convention used in equivalent MeteoSwiss products (e.g., TabsD; MeteoSwiss, 2021b). Daily catchment-average time series
were then extracted by using the catchment outlines (polygons) provided by the FOEN. Units were homogenized across time
300 series. ~~The units~~ Both units and full standard variable names are listed in Table B1 (glossary).

The length of the time series depends on the dataset that they were derived from (see Table 1 for details). Streamflow
time series are provided for three different catchment-specific time periods: (1) the original time series (entire period), (2)
the most recent gap-free time-period time series and (3) the most recent homogeneous time series (in case of significant
305 and plausible breakpoints; otherwise equal to the gap-free time series) (see Fig. 3). The breakpoint information is provided
by FOEN (~~for more information see BAFU, 2024~~). ~~(see Sect. 3.3)~~. Information on the start of the streamflow monitoring by
~~limnographs~~ water level sensor is also provided. The streamflow data should only be considered reliable after the initialization
of a limnograph sensor. In case of no breakpoints the gap-free period is equal to the homogeneous period. The homogeneous
period is usually the shortest (e.g., in case of breakpoints or limnograph water level sensor initialization; see for example
310 catchment 2349 in Fig. 3). In the case of gaps but no breakpoints, both the homogeneous and the gap-free periods are identical
(see, i.e., catchments 2239, 2386 and 2368 in Fig. 3). Indicators and (non-)standardized (drought/deficit) indices derived from
the hydro-meteorological time series are available for the longest common period of all contributing variables.

4.2 Derived indicators

4.2.1 Streamflow

315 Derived indicators related to streamflow consist of the 7-day average streamflow (moving average) M7Q ~~(Fig. 6i)~~. The M7Q
(or M7) is often used in low-flow studies and is also used for the official low-flow statistics in Switzerland by the FOEN (see
e.g., BAFU, 2024; Muelchi et al., 2021a; von Matt et al., 2024).

4.2.2 Snow related variables

In addition to variables providing direct information on (modelled) snowmelt, also daily differentiated SWE (Δ SWE) time se-
320 ries are provided for both SPASS and OSHD. Snowfall (Δ SWE > 0) and snowmelt (Δ SWE < 0) time series are provided sep-
arately. Note that ~~the SPASS~~ SWE is reset in the SPASS dataset at the end of every snow year (every September 1st) to avoid
unrealistically high ~~snow water equivalent accumulation (“snow towers”)~~ (Michel et al., 2023). ~~This accumulation of snow~~
water equivalents (“snow towers”; see Michel et al., 2023). As snowfall and snowmelt were derived from daily differences in
SWE (Δ SWE), this reset can result in ~~large snowmelt amounts (an artificially large negative Δ SWE < 0) around value on~~
325 September 1st. st that does not represent actual physical snowmelt. To prevent this model artifact from affecting the derived

~~snowmelt time series~~, Δ SWE values on September 1st ~~were therefore~~ ~~st~~ ~~were set to missing values and~~ replaced by a linear interpolation ~~between the day before and the day after~~ ~~using the~~ Δ SWE values from the preceding and following days. Snow-corrected precipitation series ($P + \Delta$ SWE) were calculated by combining time series of total precipitation (RhiresD and ERA5-Land) and Δ SWE time series (SPASS, OSHD) as well as time series with modelled snowmelt information (SPASS, OSHD and ERA5-Land). Negative snow-corrected precipitation amounts (e.g., RhiresD < Δ SWE) were set to zero.

4.2.3 Water balance

(Potential) Water balance indicators ($P - E$ and $P - PET$) were derived by combining the total and snow-corrected precipitation time series with the ERA5-Land evaporation and potential evaporation time series.

4.3 Cumulative water deficits

~~Cumulative (potential)~~ (Potential) Cumulative water deficits (CWD and PCWD) are non-standardized indicators tracking evaporation-driven deficits in the (potential) water balance. CWD and PCWD were derived from the daily water balance indicator time series (see ~~Section ??~~ Sect. 4.2.3) using the *cwd* R-package (Stocker et al., 2023; Stocker, 2021). A deficit starts when the water balance is negative (i.e., ~~$P - E < 0$~~ $P - E < 0$) and is accumulated as long as the deficit remains uncompensated (deficit > 0). Note that no surplus information is tracked. Once the deficit is compensated, the values remain at zero (CWD = 0). Example time series are shown for both CWD and PCWD in Fig 6k,l. In some cases, ~~PCWDs~~ (especially for $P - PET$ based only on ERA5-Land variables), i.e., $tp - pev$, PCWDs are not compensated each year and can persist over multiple years. Both CWDs and PCWDs are hence also provided on a yearly calculation basis (annual reset on December 31st). Non-standardized indices preserve units (here millimetres) and are physically interpretable in terms of absolute deficit amounts. Cumulative water deficits do not rely on a predetermined calculation time window, which allows the user to track both deficits accumulated over short periods in time (below one month) and deficits accumulated over very long periods.

Water-balance based non-standardized drought indices are widely in use in ecohydrological, land-atmosphere interaction research and catchment-memory studies both with and without temporal resets (see e.g., Biegel et al., 2025; Cui et al., 2022; Stocker et al., 2023). Being more strongly tied to the actual physical water availability, non-compensated CWDs may provide valuable information on carry-over effects in multi-year drought contexts and/or long-term shifts in climatic water balance (Stocker, 2021; Fowler et al., 2022; Saft et al., 2015). PCWDs in contrast are based on potential water balance and (absolute) carry-over deficits should hence be treated with caution. CWD and PCWD time series which are annually reset provide complementary year-to-year information, which may better align in contexts of annual low-flow statistics and allows for a year-to-year comparison across years and catchments.

4.4 Standardized (drought) indices

Standardized (drought) indices depict the anomaly of a deficit over a fixed retrospective period-time window (e.g., 1 month). The ~~hydrometeorological~~ hydro-meteorological indicator time series is first aggregated over the given period-window and

then transformed to a standard normal distribution by fitting a suitable candidate distribution (Tijdeman et al., 2020; Stagge et al., 2015). Standardized indices therefore provide information on both anomalously dry and wet conditions, which are often defined by thresholds corresponding to standard deviations (STD). As such, values below -1 STD indicate drier than normal conditions (moderate droughts), while values above $+1$ STD indicate wetter than normal conditions (moderate wetness) (McKee et al., 1993; Tschurr et al., 2020). The HYD-RESPONSES dataset provides daily time series for three standardized (drought) indices: the Standardized Precipitation Index (SPI, McKee et al., 1993), the Snowmelt and Rain Index (SMRI, Staudinger et al., 2014), and the Standardized Precipitation Evaporation Index (SPEI, Vicente-Serrano et al., 2010). ~~SPI and SMRI represent precipitation-driven deficits, as they are based on total (SPI; Ponly) or snow-corrected (SMRI; P+ Δ SWE) precipitation-time series~~ SPI represents deficits driven by precipitation only (derived from P), while the SMRI tracks deficits in liquid water input originating from both rainfall and snowmelt (derived from P+ Δ SWE) precipitation-time series accounting for seasonal snowfall and snowmelt dynamics (Staudinger et al., 2014; Baez-Villanueva et al., 2024). The SPEI ~~accounts for~~ represents deficits driven by ~~evaporation and is derived from the potential water balance (P-PET)~~ evaporative demand (derived from P-PET) and hence indirectly accounts for temperature effects (Vicente-Serrano et al., 2010; Mwinjuma et al., 2026; Gebrechorkos et al., 2025)

360
365
370 . Daily time series for all three indices (SPI, SPEI, SMRI) are provided for aggregation ~~periods-windows~~ ranging from 1–24 months (31–730 days). Exemplary SPI and SMRI time series for all aggregation windows are shown in Fig. 6g,h. All indices were calculated using the ~~SCI -package~~ R-package (Stagge et al., 2015; Gudmundsson and Stagge, 2016) with custom modifications accounting for the daily time series resolution. All candidate distributions provided within the ~~SCI -package~~ R-package (*gamma, genlog, gumbel, lnorm, norm, gev, pe3, weibull*) were tested for suitability. The distributions were fitted for each day of the year (DOY) based on the reference period 1991–2020. This results in a fit for each DOY derived from the same (window of) values for each distribution. Monthly SPI fits (SPI-1) are for example based on the 30 daily values up to the specific DOY for each of the 30 years in the reference period 1991–2020. The suitability of candidate distributions was assessed based on three indicators: the Shapiro-Wilks normality tests (*p*-values; Shapiro and Wilk, 1965), the number of flags returned by the fitting function ~~(usually indicating convergence issues)~~ fitSCI (see SCI R-package; Gudmundsson and Stagge, 2016), and the number of missing and/or implausible values. Implausible values are defined as values above or below ~~$+3$ (-3)~~ ± 3 STD following Stagge et al. (2015). Estimating more extreme standardized index values from a 30-year climatology requires substantial extrapolation of the fitted distribution and is therefore associated with large uncertainty, particularly given the strong temporal autocorrelation of drought indices. Values beyond ± 3 correspond to events with return periods far exceeding the length of the reference record and cannot be robustly quantified (see Stagge et al., 2015).

375
380
385 The returned flags in distribution parameter fitting were mainly related to convergence issues (non-convergence) (flag 3, see SCI R-package Gudmundsson and Stagge, 2016). Without a valid fit, the transformation to standardized index values is not possible resulting in missing values on the flagged DOYs in all time series years. As in Staudinger et al. (2014), one best-fitting distribution (over all DOYs) is chosen for all catchments ~~and~~ to allow for catchment comparability. The distribution was selected among the distributions satisfying the following conditions: (1) the transformed values are not significantly different from a normal distribution for the majority of catchments (*p*-values > 0.05 for at least 75 % of the catchments), (2) fewer than 5 DOYs flagged and (3) fewer than 50 implausible and/or missing values in the transformed

390

time series (combined consideration of missing values due to flags and unrealistically high/low values). The distribution selection procedure is illustrated for the SPEI in Fig. 4. The results of the Shapiro-Wilks tests (p -values) and information on missing/improbable values and flags are also provided in the HYD-RESPONSES dataset and can be used to identify catchments with non-satisfying properties within the overall best-fitting distribution (see Fig. 4). Following Stagge et al. (2015), values of all standardized (drought) indices time series were restricted to the interval [-3, 3] STD.

The *Gamma* distribution was chosen for the SPI for all variables (RhiresD, ERA5-Land), which is consistent with other studies and ~~WMO recommendations~~ recommendations of the World Meteorological Organization (WMO) (WMO and GWP, 2016; Stagge et al., 2015; Tschurr et al., 2020; von Matt et al., 2024). The SMRI was fitted by the *genlog* ($lnorm$) distribution for the snow-corrected precipitation series based on SPASS (ERA5-Land and OSHD). For the SPEI, the *genlog* distribution was found to perform best across time scales (see Fig. 4). ~~Following Stagge et al. (2015), values of all standardized (drought) indices time series were restricted to the interval -3, 3STD.~~

SPI, SPEI and SMRI provide complementary (and standardized) information on hydroclimatic variability and drought-related processes facilitating integrated analyses of drought development and propagation and allowing consistent comparisons across catchments, regions and climates (Mwinjuma et al., 2026; Gebrechorkos et al., 2025; Tijdeman et al., 2022). Standardized indices are frequently employed in drought monitoring and early warning systems (DEWS; Tijdeman et al., 2020; Kchouk et al., 2022), drought propagation analysis or as proxy for various storage processes (Haslinger et al., 2014; Cammalleri et al., 2019; Raposo et al., 2023; Peña-Gallardo et al., 2019; Barker et al., 2016). Example use cases for drought event analysis and catchment response patterns are provided in sections A2 and A3 in Appendix A.

4.5 Climatology & Anomalies

Climatologies and anomalies are provided for all time series ~~including the standard~~, including the time series of extracted variables (see sections 3.1 and 3.2) variables directly extracted from spatially gridded data products with no modifications except for spatial and temporal aggregation where required (see Sect. 4.1), derived indicators (Section Sect. 4.2), standardized (drought) indices (Section 4.4) drought indices (Sect. 4.4), and cumulative water deficits (Section Sect. 4.3 and 4.6).

Both climatologies and anomalies are based on the reference period 1991–2020. The climatology is provided for two variants: i) using moving windows and ii) for fixed ~~periods~~ time windows. The variants are available at the following time scales: daily (only i), monthly (both), seasonal (both), and annual (only ii). The moving window climatology was calculated by using a moving window of 31 days ($day - 15$, $day = 0$, $day + 15$) for the monthly, a 3-month window (91 days) for the seasonal and a 6-month (183 days) window for the extended season time scale. The moving window climatology is calculated for DOYs 1–366 with NA-values set for February 29th in the case of non-leap years. Example time series for monthly anomalies in 2 m temperature, precipitation, evaporation, soil moisture, snow water equivalent, snowmelt and (potential) cumulative water deficits are shown in Fig. 6a-f,m-n.

The regular climatology is available for monthly, seasonal (DJF, MAM, JJA, SON), extended season (~~Mai–October~~ May–October, November–March) and annual time scales. Using the moving window climatology, standardized anomalies have been derived by ~~calculating z-scores $((value - \mu)/\sigma)$ first subtracting the climatological mean (μ) and then~~

dividing by the climatological standard deviation (σ) (also known as *z-scores*). The following climatological statistics are provided: minimum, maximum, mean, median, standard deviation, 5th, 25th, 75th and 95th percentiles. For the 7-day average streamflow series (M7Q) we also provide the 2nd, 10th and 15th percentiles which are frequently used in streamflow drought analysis and monitoring (see e.g., Van Loon, 2015; Stahl et al., 2020; Sarailidis et al., 2019; BAFU, 2025)

430 .

4.6 Cumulative streamflow deficits

Time series of cumulative streamflow deficits (CQD) were calculated based on negative streamflow anomalies (drought phases) by using the same procedure as for cumulative water deficits (see ~~Section~~ Sect. 4.3). CQD time series are provided for both fixed and variable threshold definitions. Fixed thresholds (e.g., a constant percentile threshold) are used for critical flow levels that do not change seasonally (e.g., directly linked to physical/actual low-flow or water scarcity situations) whereas variable thresholds (e.g., seasonally varying percentiles) account for seasonality and changing flow regimes, allowing drought phases and deficits to be identified relative to expected (seasonal) conditions ("anomalies", Stahl et al., 2020; Van Loon, 2015; Brunner et al., 2019a; von Matt et al., 2024). Hence, variable threshold definitions are often used to analyse seasonally varying streamflow (drought) generating processes or to understand drought propagation mechanisms (Brunner et al., 2023, 2022; Hammond et al., 2022). For the fixed threshold definition, daily M7Q anomalies were derived for ~~the yearly Q347-threshold events (\approx the yearly events exceeding the Q347 threshold, defined as the daily flow rate exceeded for 347 days per year (i.e., the 347-day exceedance flow, roughly corresponding to the 5th percentile, see Section ??~~th streamflow percentile; see Sect. 5.3). For the variable threshold definition, daily M7Q anomalies were calculated for the following monthly (31 days) and seasonal (91 days) percentiles: 2nd, 5th, 10th, 15th, 25th, 50th (median) and mean. Cumulative deficits are physically interpretable and in the case of cumulative water deficits [mm] and streamflow deficits [m^3/s] also physically comparable in terms of total runoff depth [mm]. Figure 6j shows CQDs for both fixed and variable threshold definitions for the year 2022 for catchment 2034 - Broye, (Payerne, Caserne d'aviation).

440

445

4.7 Identification of drought events

We define drought events as coherent phases of non-zero deficits for cumulative deficits (CWD, PCWD and CQD) and as negative M7Q-based streamflow anomalies for streamflow droughts. Streamflow drought phases were extracted for the same percentiles and time scales as used for CQDs (see ~~section~~ Sect. 4.6), namely for monthly (31 days) and seasonal (91 days) percentiles: 2nd, 5th, 10th, 15th, 25th, 50th (median) and the mean. ~~For each event definition~~ Streamflow events were also extracted for the fixed (yearly) Q347 threshold (see Sect. 4.6 and 5.3).

An event starts on the first day values fall below the threshold value and lasts until values exceed the threshold again (see Fig. 5). For each variant, the event time series consists of consecutively numbered event phases and information on the event duration since the start (i.e., an event with a duration of 5 days is represented in the time series as: "1 1 1 1 1" (event phase number), "1 2 3 4 5" (duration since start)). Additional event characteristics (e.g., lowest value during a phase) can easily be derived by the

455

460 [user in combination with the indicator time series](#). A minor pooling ~~for~~ of hydrological drought events is introduced by using [the 7-day average streamflow \(M7Q\) time series which merges closely successing and potentially dependent individual events to one single event as a result of the smoothing of large day-to-day fluctuations](#) (Tallaksen and Van Lanen, 2004; Hisdal and Tallaksen, 2000; Tallaksen et al., 1997; Sarailidis et al., 2019). [Streamflow drought events based on both fixed and variable threshold definitions were used for the event shadings in Fig. 6.](#)

5 Catchment descriptors

465 Catchment descriptors were extracted from spatial datasets containing information on hydro-terrestrial characteristics (e.g., soil suitability maps), catchment (station) metadata (see [Section Sect. 3.3](#)) and the extracted hydro-meteorological time series (e.g., climatology; see [Section Sect. 4.5](#)). All catchment descriptors provide only static (time-invariant) catchment information. Catchment descriptors are provided as single-value catchment-level information. [An example use case of catchment grouping/regionalization based on catchment descriptors is presented in Sect. A1 in Appendix A.](#)

470 5.1 ~~Extraction of catchment~~ [Field-based](#) descriptors

Spatially non-overlapping polygon datasets (e.g., soil suitability maps) typically provide categorized values for variable-specific classes (e.g., soil depth classes are *shallow*, *medium*, *deep*, *very deep*). To extract catchment-level information, polygon-based information was first rasterized to a spatial grid identical to the MeteoSwiss spatial climate analyses grid products (in both extent and resolution). The rasterization was done by using the *rasterize* function of the *terra* R-package (Hijmans, 2023).
475 ~~Slope and aspect values were derived from the swissALTI3D digital elevation model (DEM, see section 10 for a download link) by using the standard terra R-package function terrain (Hijmans, 2023). A custom categorization was then applied to the resulting grid values (e.g., for slope 0–30, 30–60, etc.).~~ The percentage overlap with the catchment area was then assessed for all variable-specific classes by using the *exact_extract* function (as for time series) and adjusting the aggregation function to fractions ("frac"; see Baston, 2023).
480 Catchment area overlap fractions are provided for all categories. Descriptors with multiple classes can also be reduced to a single dominant category represented by the largest percentage overlap ("proportion"). An example is shown for the biogeographic regions in Fig. 7. ~~However, the class a.~~ [Reducing a specific catchment descriptor to one single \(dominant\) category \(e.g., derived via largest overlap percentage\) may however lead to a loss in explanatory power as the category with the largest overlap does not necessarily correspond to may not necessarily be the most representative , as multiple categories can share similar proportions of the catchment area or most influential for streamflow \(drought\) analysis.](#)
485

5.2 ~~Derivation of other catchment~~ [Feature-based](#) descriptors

~~Additional catchment descriptors were derived from the remaining descriptive input products (catchment metadata, karstic sources, catchment outlines and hydrography) and the calculated hydro-climatology (see Section 4.5).~~ Two descriptive variables related to catchment shape and drainage were derived in R by using the catchment outlines, namely the *basin shape*

490 *index* (BSI) and *drainage density*. The HYD-RESPONSES dataset provides two BSI variants. The first variant is derived based on a ratio between area and [basin length \(\$A/L^2\$ \) known as form factor \(Horton, 1932\)](#) and the second variant is based on a ratio between the catchment area and the area of the circle with the smallest radius encircling the entire catchment (A_{catch}/A_{circle}) [known as circularity ratio \(Miller, 1953\). Both indices range from 0 to 1. Both are frequently used \(also in combination\) as morphometric catchment indicators \(see e.g., Das et al., 2022; Pisupati and Ratnakar, 2025\). Albeit providing](#)

495 [similar information, the form factor is primarily controlled by basin length and hence provides information on catchment elongation, while the circularity ratio is more sensitive to basin shape accounting for complex/irregular shapes resulting in larger areas \(for more information on basin shape indices see Das et al., 2022\). For more information see Das et al. \(2022\)](#)

–The drainage density denotes the ratio between the catchment area and the total length of streamflow channels (both natural and stormwater drainage infrastructure; Dingman, 1978; USGS, 2023). The drainage density was calculated by using the

500 [swissTLM3D hydrography dataset \(see ~~section~~ Sect. 10 for a download link\)](#). Both indices (BSI and drainage density) are frequently used in flood-related studies but may also provide valuable information during low-flow periods as high-intensity precipitation events are a relevant factor for (streamflow) drought recovery (Eekhout et al., 2018; Floriancic et al., 2022; Lee and Ajami, 2023; Matanó et al., 2024; Qiu et al., 2021; Tarasova et al., 2024; Vicente-Serrano et al., 2022; Wu et al., 2022; Xu et al., 2023). Further, also the overlap percentage with the Swiss territory (swissBOUNDARIES3D, see [~~section~~ Sect. 10](#)

505 [for a download link](#)) is provided for each catchment and can be used to exclude catchments with significant portions outside of Switzerland which goes along with a limited coverage in both hydro-meteorological and catchment descriptor input datasets (see [Sections Sect. 3.2 and 3.3](#)) [–for ca. 12.5 % of catchments \(see Sect. 2\)](#). Information on karstic sources is provided as the number of sources per catchment and km^2 .

5.3 [Time series-based and climatological descriptors](#)

510 Several indices related to streamflow characteristics (low flow, responsiveness, baseflow and flow stability) are provided in the HYD-RESPONSES dataset. The Q347 (Aschwanden, 1992; Aschwanden and Kan, 1999) is a low flow index used as the basis for water abstraction restrictions in Switzerland and corresponds to the [5th streamflow percentile \(low flows\) daily flow rate exceeded for 347 days per year. The Q347 was](#) derived from the flow duration curve (FDC) [–The Q347 was derived](#) by using the [hydroTSM R-package \(Zambrano-Bigiarini, 2020\) and corresponds roughly to the 5th streamflow percentile \(95th percentile of](#)

515 [365 days \$\approx\$ 347, hence Q347\)](#). The baseflow index (BFI; Nathan and McMahon, 1990) is a widely used index linked to multiple catchment characteristics such as aquifer type, productivity and soil characteristics. The BFI provides information on the (base-)flow sustained during dry periods (e.g., by subsurface storages; Tallaksen and Van Lanen, 2004; Bloomfield et al., 2021; Van Loon and Laaha, 2015). The BFI was derived using the *baseflow* function of the *lfstat* R-package (Laaha and Koffler, 2022) and is shown in Fig. 7. Stoelzle et al. (2020) introduced the delayed-flow index (DFI) which breaks down the BFI into

520 individual hydrograph components. The components include fast, intermediate, slow and base responses and potentially reflect various storage processes contributing to the overall streamflow response (e.g., snowmelt and groundwater). The DFI was derived by using the *delayedflow* R-package (<https://modche.github.io/delayedflow/>; see also Stoelzle et al., 2020). The last two indices related to streamflow behaviour are the "flashiness" or R-B-index (Baker et al., 2004) which represents the ratio of

the sum of day-to-day streamflow changes divided by the total streamflow and the flow-stability index which relates the mean annual minimum flows (MAM_q) to the mean annual flow (MAM/MQ ; MAM_q/MQ). The remaining catchment descriptors were derived from the extracted hydro-meteorological time series and/or their respective climatology. Information on average precipitation, temperature, evaporation, snow water equivalent, streamflow, the fraction of precipitation falling as snow and the runoff fraction (Q/P) are provided ~~, partly on both monthly and yearly time scales~~ on yearly scales for identifying broad climatic (i.e., water balance) and physiographic controls on hydrological behavior. Finally, monthly Pardé coefficients (PCs) are provided which indicate the contribution of monthly mean streamflow to the annual mean streamflow.

6 ~~Three example use cases~~ Discussion

6.1 Relevance and Applications

The HYD-RESPONSES dataset addresses fundamental challenges in hydrological drought analyses by compiling and harmonizing multiple data sources into a coherent catchment-scale framework, enabling multi-variable drought analyses in Switzerland. Drought (deficit) indices derived from two high-resolution snow climatologies for Switzerland (SPASS, OSHD) also allow for in-depth quantitative analyses on the contribution of snow processes to cross-seasonal drought propagation in Alpine catchments (Staudinger et al., 2014, 2017; Brunner et al., 2023). A combined use of standardized indices (SPI, SPEI, SMRI at 1–24 month scales) and non-standardized cumulative deficits (CWD, PCWD, CQD) facilitate multi-scale (drought) deficit and catchment response sensitivity assessments and allows for a concurrent anomaly-based and physically interpretable characterization of drought deficits (Raposo et al., 2023; Van Loon, 2015; Wu et al., 2020; Baez-Villanueva et al., 2024; Stocker et al., 2023). By providing time series for many relevant variables for drought monitoring (precipitation, temperature, evaporation, soil moisture and streamflow; see e.g., WMO and GWP, 2016) at daily temporal resolution, the HYD-RESPONSES dataset may also be used for training machine learning models such as Random Forests (RFs; e.g., Floriancic et al., 2022) or Long Short-Term Memory models (LSTMs; see Kratzert et al., 2018; Lees et al., 2022; Kratzert et al., 2023) which have recently emerged as promising approach for rainfall-runoff modeling (Kratzert et al., 2018, 2019; Lees et al., 2022). Three example applications of the HYD-RESPONSES dataset are illustrated in Sect. A1, A2 and A3 in Appendix A.

Although the dataset was developed for Switzerland, the methodological framework — combining in-situ observations, gridded products, and reanalysis into catchment-scale time series — is transferable, with requirements that scale with data availability. Replication requires four essential components: (1) streamflow observations with defined catchment boundaries, (2) meteorological forcing data (precipitation, temperature), (3) snow information for mountain regions, and (4) static catchment descriptors (e.g., information on soils, geology, topography). While the first component is often limiting, the second component is decisive for the applicability of the dataset on specific use cases. Switzerland can leverage from high-density observational station networks resulting in high-quality spatially gridded hydro-meteorological products (see e.g., MeteoSwiss, 2024). With known biases in mind (especially over complex terrain), ERA5-Land is a viable alternative

by providing temporally and physically consistent variables at sufficiently high spatial resolution for comparative catchment studies and machine learning applications aiming for generalizable results in regions where observational networks are less dense (Muñoz-Sabater et al., 2021; Dalla Torre et al., 2024; Scherrer et al., 2023). For local operational drought management or absolute deficit quantification, reliable high-resolution observational products remain however preferable. Several recent developments address observational data limitations, including the Caravan global community dataset (Kratzert et al., 2023), rapidly advancing machine learning-based bias correction methods for downscaling reanalysis products such as ERA5-Land (Menapace et al., 2025; Najafi et al., 2026; Zhang et al., 2025) or advances in developing high-quality remote sensing-based products for soil moisture (e.g. SMAP; see Brocca et al., 2024b; An et al., 2025), snow (e.g., ICESat-2 Besso et al., 2024), evaporation (see e.g., Anderson et al., 2024) and terrestrial water storage (e.g., GRACE-FO; Rodell and Reager, 2023).

6.2 Limitations and cautionary notes

The HYD-RESPONSES time series are provided for product-specific periods, and the spatial coverage is restricted to Swiss territory for most of the higher resolution MeteoSwiss and SLF products (TabsD, TminD, TmaxD, SPASS, SrelD, OSHD) as well as many catchment descriptor input datasets. Full coverage over the entire hydrological Switzerland is only available for ERA5-Land (all variables) and the MeteoSwiss RhiresD product (after 1992; see MeteoSwiss, 2021a). Catchments with significant areas outside of the Swiss national borders —approximately 12.5 % of the catchments (see Sect. 2) — may therefore be considered with caution or used solely for time series based on ERA5-Land variables only. Time series for standardized drought indices are provided only for the transformation variant based on the best-fitting distribution across all catchments to allow for catchment comparability (see e.g., Staudinger et al., 2014). The best-fitting distribution may however vary across catchments and climates (see e.g., Stagge et al., 2015). The HYD-RESPONSES dataset therefore also provides information on fits, missing values, and flags which can be used to exclude catchments with unsatisfying fitting and transformation properties from analyses. Field- and feature-based catchment descriptors were aggregated at catchment level via summarization (e.g., karstic sources) or percentage overlaps (see Sect. 5.1). Maximum percentage overlaps with catchment area may however only insufficiently account for spatial differentiation which could enhance the representation of factors most influential to streamflow evolution by accounting for spatial proximity to the stream/river courses (Tarasova et al., 2024; Floriancic et al., 2022).

Several known limitations are further related to the datasets used to compile the HYD-RESPONSES data. ERA5-Land is a state-of-the-art reanalysis product provided at a higher spatial resolution than the standard ERA5 reanalysis (Hersbach et al., 2020; Muñoz-Sabater et al., 2021). The higher spatial resolution results in a better depiction of soil moisture, lakes, river discharge estimations, and the orographic enhancement of precipitation (Muñoz-Sabater et al., 2021). ERA5 and ERA5-Land datasets however share most of the parameterizations, as ERA5-Land consists of output from the ECMWF land surface model driven by downscaled and elevation-corrected ERA5 data (Muñoz-Sabater et al., 2021). Despite the advantage of higher spatial resolution over ERA5, a grid resolution of 9 km still has limitations over complex high-altitude terrain. The extracted time series related to snow water equivalent should be used with caution, as snow depth in ERA5-Land is

of mixed quality depending on geographical location and altitude (Dalla Torre et al., 2024). Scherrer et al. (2023) showed that ERA5-Land overestimates SWE at high elevations with larger biases in the southern compared to the northern Alps. Higher-resolution datasets such as SPASS (Marty et al., 2025) and OSHD (Mott, 2023; Mott et al., 2023) should hence be preferred over ERA5-Land. Note however that all snow-related datasets have problems in representing small SWE amounts at low altitudes (Scherrer et al., 2023; Michel et al., 2023; Marty et al., 2025). Caution is also required when using the snow-corrected precipitation (water input) time series. The time series corrected by the Δ SWE series consider both snowfall (Δ SWE > 0) and snowmelt (Δ SWE < 0), while the correction based on snowmelt variables only accounts for snowmelt (smlt in ERA5-Land and romc in OSHD; see Table 1 and Tables B1 and B2 and Sect. 4.2.2). Snowmelt-corrected precipitation time series may therefore be of limited use during the main snow accumulation season but can still provide valuable information during the snowmelt season.

Another limitation of the ERA5-Land dataset is the parameterization of subgrid-scale processes and the representation of subsurface storages that affect evapotranspiration (e.g., fixed maximum storage volume assumption; see Muñoz-Sabater et al., 2021). Key processes such as dynamic groundwater-vegetation interactions, irrigation withdrawals, and adaptive rooting strategies are hence not represented and may lead to biases in evapotranspiration responses (Muñoz-Sabater et al., 2021; Dalla Torre et al., 2024; Wood et al., 2025; Stocker et al., 2023). Although ERA5-Land compares more favorably with in situ soil moisture and evapotranspiration observations than previous reanalyses (e.g., ERA5), considerable discrepancies remain, especially in dry summers and in regions with heterogeneous land cover (Scherrer et al., 2022; Fluhrer et al., 2025). Given these limitations, drought indicators based on ERA5-Land evapotranspiration should generally be interpreted with caution. This limitation is further compounded by the fact that the validation of long-term soil moisture and evapotranspiration remains challenging due to the scarcity of consistent observational datasets, particularly at high spatial resolution and over multi-decadal time scales (Hirschi et al., 2020; Yi et al., 2024; Mukherjee et al., 2018). Many state-of-the-art evapotranspiration products are limited in temporal or spatial extent and can be affected by gaps and cloud contamination (e.g., remote sensing-based products; see Yi et al., 2024). ERA5-Land thus remains one of the few datasets providing spatially consistent and continuous long-term evapotranspiration estimates with sufficiently high spatial resolution over Switzerland.

Additional caution is warranted when using HYD-RESPONSES water balance time series (and indicators derived from them) when they were derived by combining ERA5-Land evapotranspiration with (snow-corrected) precipitation from independent data sources (RhiresD, OSHD, and SPASS). While ERA5-Land variables are internally consistent, the combination with independent data sources may lead to systematic biases in absolute deficit estimates. This limits the interpretability of absolute cumulative deficits but does not invalidate the approach for comparative, process-oriented drought analyses across regions and catchments (e.g., drought propagation, catchment response sensitivities). Relative measures of cumulative deficits, their temporal evolution, and their normalization through ratios (e.g., CWD/PCWD)

can still provide valuable insights, even when absolute magnitudes are uncertain. In such contexts, relative anomalies, temporal evolution, and spatial patterns are more informative than absolute deficit magnitudes. Studies have further demonstrated coherent representation of major drought events (e.g., drought years 2003 and 2018) across datasets, which supports the usability of combined indicator time series when known limitations are adequately taken into account (Scherrer et al., 2022; Wood et al., 2025). Note that the HYD-RESPONSES dataset also provides complementary water balance and SPEI time series derived from ERA5-Land variables only, providing consistent metrics and opportunity for comparisons among data products. Guidance on the usage and reliability of all HYD-RESPONSES time series products is provided by a classification based on three reliability levels (see Sect. 4 and Table 3). The levels are based on the origin of the underlying data, the extent to which variables rely on (model) assumptions, and the degree of processing applied to derive the hydro-meteorological time series.

7 Complementary datasets

Complementary datasets provide a wide range of additional catchment descriptors and hydro-meteorological time series. An overview of datasets and variables is provided in Table 4. The FOEN provides additional geodata related to both surface and groundwater via the Hydrological Service (<https://www.bafu.admin.ch/bafu/de/home/themen/wasser/zustand/karten/geodaten.html>). The datasets include additional catchment descriptors with information on population density, catchment areas covered by forest and agriculture (among others) as well as information on water quality aspects and sewage. The FOEN further operates both a groundwater monitoring network (NAQUA) providing continuous groundwater measurements for selected point locations (BAFU, 2019) and a water quality measurement network (NAWA) providing information on concentration and loads of important dissolved compounds (e.g., pH, electric conductivity, nutrient contents; BAFU, 2023).

The “Catchment Attributes and Meteorology for Large-sample catchment Studies” (CAMELS) datasets aim at providing a consistent set of hydro-meteorological time series and catchment descriptors over a large sample of hydrological catchments on country level (Clerc-Schwarzenbach et al., 2024). The catchments in the Swiss version of the CAMELS data (CAMELS-CH; Höge et al., 2023a) are largely congruent with our dataset. The only exception is station 2646, which is only contained in the HYD-RESPONSES dataset. Note that the HYD-RESPONSES dataset provides only a sample subset of 184 catchments. The CAMELS-CH dataset provides valuable complementary catchment-level information on glacier changes (based on GLAMOS, for details see Höge et al., 2023a), land use, hydro-geological and hydro-terrestrial information (e.g., the contributions of various grain size categories and bulk-density) as well as anthropogenic disturbances (e.g., hydropower and reservoir capacities). CAMELS-CH further provides modelled time series based on the hydrological model PREVAH (see e.g., Höge et al., 2023a; Viviroli et al., 2009). The CAMELS-CH dataset is freely available from Zenodo (<https://zenodo.org/records/10354485>; Höge et al., 2023b).

The CombiPrecip dataset (MeteoSwiss) provides high-resolution (10 minutes, 1×1 km) precipitation fields derived from a combination of radar and station measurement data (Sideris et al., 2014). The CombiPrecip dataset could be a valuable addition

Table 4. Datasets compatible and complementary to the HYD-RESPONSES dataset.

<u>Dataset</u>	<u>Short description</u>	<u>Provider</u>
Accompanying catchment information	<u>Includes catchment proportions of forests, agricultural (crop) land, population, built-up area and more</u>	FOEN
<u>Groundwater measurement network (NAQUA)</u>	<u>Groundwater measurements</u>	<u>FOEN</u>
<u>Water quality measurement network (NAWA)</u>	<u>Information on water quality parameters</u>	<u>FOEN</u>
CAMELS-CH (Höge et al., 2023b)	<u>Swiss version of the Catchment Attributes and Meteorology for Large sample catchment Studies (CAMELS) dataset</u>	via Zenodo
MeteoSwiss CombiPrecip (CPC)	<u>High-resolution precipitation fields at ground based on a combination of radar and measurement data</u>	MeteoSwiss
HydCheck (Streeb et al., 2024)	<u>Detailed evaluation of influences and disturbances of the streamflow at NAWA measurement stations</u>	FOEN

for studying drought recovery where extreme precipitation is often considered an important factor (Wu et al., 2022).

660 The HydCheck project (Streeb et al., 2024) evaluated the influence of (anthropogenic) disturbance factors on streamflow at stations of the National Surface Water Quality (NAWA) Programme (BAFU, 2023). The evaluated NAWA stations are largely (87.5% of the stations) congruent with the HYD-RESPONSES dataset. The HydCheck dataset provides catchment-level information on the magnitudes for all evaluated disturbance categories including water storage and regulation, hydropower, sewage water, constructions, agriculture as well as drinking and groundwater. The overall impact on several hydrological
665 properties including low-, mid- and high-flow regimes as well as short-term effects and hydraulics is provided as categorical information (from "not disturbed" to "strongly disturbed"). For more information see Streeb et al. (2024).

As part of the planned Swiss National drought early warning system (DEWS), both a high-resolution remote-sensing based evaporation product (V. Humphrey, pers. comm.) and an automatic soil moisture measurement network are under development at MeteoSwiss, ETH Zurich and WSL and may become a valuable addition in a future.

670 **8 Conclusions**

The HYD-RESPONSES dataset contains data for 184 Swiss catchments that cover a variety of streamflow regimes, mean altitudes, catchment areas, and anthropogenic influences/disturbances. The catchments cover all biogeographic regions of Switzerland. The HYD-RESPONSES dataset provides daily streamflow data and daily hydro-meteorological time series extracted from gridded data products of MeteoSwiss (TabsD, RhiresD, TmaxD, TminD, SrelD), Meteoswiss and SLF (SPASS).

675 [SLF \(OSHD\) and ECMWF \(ERA5-Land\)](#). The variables include temperature, precipitation, evaporation, sunshine duration, solar radiation, snowmelt, snow water equivalent, soil moisture, surface runoff, runoff, and streamflow. [HYD-RESPONSES](#) further provides derived variables related to streamflow (e.g., M7Q), water balance (e.g., P-E) and snowfall. Additionally, three standardized drought indices (SPI, SPEI, SMRI) for accumulation windows from 1 to 24 months and information on the (non-standardized) cumulative water deficit (CWD), the potential cumulative water deficit (PCWD) and cumulative streamflow deficit (CQD) are provided.

680 The dataset also provides information on (streamflow) drought events (occurrence and duration). For each catchment, the drought events have been identified based on fixed and on seasonally varying percentile thresholds.

The combination of data sources, the information on hydro-meteorological variables (mainly temperature, precipitation and snow), the derived indices (water balance, cumulative water deficits, standardized drought indices, climatology and anomalies) allow for a multi-purpose use and various analytical approaches such as time series analysis (e.g., Kratzert et al., 2018; Lees et al., 2022), drought propagation and catchment sensitivity analysis (e.g., based on principal component analysis and clustering; Jehn et al., 2020) and changes in rainfall-runoff relationships during hydrological droughts (e.g., Wu et al., 2021).

685 The [HYD-RESPONSES](#) dataset can easily be combined with complementary datasets such as [CAMELS-CH](#) (Höge et al., 2023a) and [HydCheck](#) (Streeb et al., 2024). The catchment time series vary in length (subject to station initialization), the hydrological time series are provided for the entire measurement period along with information on data homogeneity (see [BAFU \(2024\)](#) for more details).

690 Limitations exist for catchments extending beyond the Swiss borders. The catchment descriptors were extracted from datasets mainly covering Swiss national territory. The [MeteoSwiss](#)-based datasets cover only Switzerland except for [RhiresD](#), which covers the entire hydrological Switzerland from 1992 onward. In summary, the dataset provides a state-of-the-art data basis to study droughts in Switzerland.

9 Code and data availability

The [HYD-RESPONSES](#) dataset is freely available (CC BY 4.0) from Zenodo (<https://doi.org/10.5281/zenodo.15748821>; von Matt et al., 2026). Regular updates are not planned. An R tutorial on how to use and combine the different data products is provided with the dataset but can also be accessed on GitHub (<https://github.com/codicolus/HYD-RESPONSES>).

700 As of now, [MeteoSwiss](#) gridded spatial analyses products ([MeteoSwiss, 2021a, b, c](#)) are not available for free but will be available for free in the course of 2025 ([MeteoSwiss, 2025](#)). The preliminary snow climatology for Switzerland ([SPASS](#); see [Michel et al., 2023](#); [Marty et al., 2025](#)) was provided directly by [MeteoSwiss](#) and is not yet available for public use. The [SLF](#) snow climatology ([OSHD](#); [Mott, 2023](#); [Mott et al., 2023](#)) was published under the [WSL Data Policy](#) and can be downloaded via [Envidat](#) (<https://www.envidat.ch/#/metadata/climatological-snow-data-1998-2022-oshd>). The hourly [ERA5-Land](#) dataset ([Muñoz-Sabater et al., 2021](#)) is accessible via the [Copernicus Climate Data Store \(CDS\)](#) (see <https://cds.climate.copernicus.eu/datasets/reanalysis-era5-land?tab=download>). Daily streamflow time series can be requested

via the Hydrological Service of the FOEN via <https://www.bafu.admin.ch/bafu/de/home/themen/wasser/zustand/daten/messwerte-zum-thema-wasser-beziehen.html>. The soil suitability maps (FOAG), the hydrogeological map (FOEN) and the lithological map (Swisstopo) are available from <https://opendata.swiss> or directly via Swisstopo (<https://www.swisstopo.admin.ch/de/geokarten-500-vektor>). Directly available from Swisstopo are also the datasets swissTLM3D Hydrography (<https://www.swisstopo.admin.ch/de/landschaftsmodell-swisstlm3d#swissTLM3D---Download>) and swissBOUNDARIES3D (<https://www.swisstopo.admin.ch/de/landschaftsmodell-swissboundaries3d>). Further available via <https://opendata.swiss> are the Biogeographic regions (<https://opendata.swiss/de/dataset/biogeographische-regionen-der-schweiz-ch>; see also BAFU (Eds.), 2022) and information on karstic springs and swallow holes (also produced by the FOEN; <https://opendata.swiss/de/dataset/quellen-und-schwinden-in-karstgebieten>). Data used for the overview map of the study region (Fig. 1) is available for free from Swisstopo and FOEN. Datasets used include: the digital height model DHM25 (<https://www.swisstopo.admin.ch/de/hoehenmodell-dhm25>) and the general hydrological background map (downloadable via <https://opendata.swiss>; see <https://opendata.swiss/en/dataset/generalisierte-hintergrundkarte-zur-darstellung-hydrologischer-daten>).

720

The software used to compile the datasets are all open-source and contain the following R-packages available via CRAN: *tidyverse* (<https://cran.r-project.org/web/packages/tidyverse/index.html>; Wickham et al., 2019), *exactextractr* (<https://cran.r-project.org/web/packages/exactextractr/index.html>; Baston, 2023), *sf* (<https://cran.r-project.org/web/packages/sf/index.html>; Pebesma, 2018), *lfstat* (<https://cran.r-project.org/web/packages/lfstat/index.html>; Laaha and Koffler, 2022), *SCI* (<https://cran.r-project.org/web/packages/SCI/index.html>; Gudmundsson and Stagge, 2016; Stagge et al., 2015) and *stars* (<https://cran.r-project.org/web/packages/stars/index.html>; Pebesma and Bivand, 2023).

Available via Github are the R-packages *cwd* (Stocker (2021); available via: <https://github.com/stineb/cwd>), and *delayedflow* (Stoelzle et al. (2020); available via: <https://modche.github.io/delayedflow/>).

Author contributions. CNvM conceptualized the project proposal, acquired funding from the FOEN, performed the formal analysis and drafted the article. OM and BS provided guidance on the methodological aspects. CNvM, OM and BS assisted with writing the paper and revisions.

Competing interests. The contact author has declared that none of the authors has any competing interests.

Acknowledgements. [The HYD-RESPONSES project was funded by the Federal Office for the Environment \(FOEN\). The preliminary SPASS dataset was kindly provided by Regula Muelchi \(MeteoSwiss\). We thank Caroline Kan \(FOEN\) for her help with the catchment selection.](#)

735 Appendix A: [Exemplary use cases](#)

The different data types can be combined to comprehensively analyse hydrological streamflow droughts in response to various hydro-meteorological indicators. This section presents three use cases: catchment regionalization, in-depth event analysis, and composite analysis. A comprehensive R-tutorial on how to read and combine the different data products is provided with the dataset but can also be accessed via Github (<https://github.com/codicolus/HYD-RESPONSES>).

740 A1 Catchment grouping

For some applications, catchments need to be grouped by similarity, as measured by a set of [catchment descriptors related to hydro-meteorological, terrestrial characteristics](#) and/or anthropogenic [catchment descriptors disturbances](#) (e.g., Tarasova et al., 2024). As an example application, we show the distribution of catchment coverage fractions across biogeographic regions for the soil characteristics *soil depth, skeletal content, water logging, permeability, and water storage capacity* (Figure A1).

745 The percentage coverage distributions reveal notable differences in soil characteristics and their subcategories. Catchments in the Swiss Plateau region are characterized by larger coverages of deep to very deep soils with a mostly poor to medium skeletal content, normal soil permeability and good water storage capacities (see Fig. A1). Alpine catchments, on the other hand, are characterized by shallower soils (especially the Southern Alps) and a higher skeletal content. Soils in the Alps further have almost no water logging and a low water storage capacity. Soils with a (weakly) inhibited permeability or with a very
750 good water storage capacity are infrequent across all biogeographic regions. ~~An other example for catchment grouping is the~~

~~Whereas soil characteristics reflect differences in terrestrial catchment characteristics, the streamflow regime types are more indicative of hydro-climatic streamflow generation processes (see Sect. 2, Fig. A2). In Alpine environments, snow- and glacier processes are important contributors to streamflow generation. Hence, both Western and Eastern Central Alps show predominantly glacial and nival streamflow regime types of which 86 % are shared among regions (see Fig. A2a,b). In contrast to the Central Alps, the hydro-climatology of the Southern Alps is more Mediterranean with the Alps often described as "Alpine divide" between the warmer and drier conditions in the South and more temperate Atlantic influences in the North (NCCS, 2025; Haslinger et al., 2019). Despite similar streamflow generating processes, the streamflow regime types in the Southern Alps are differentiated from their counterparts in the Central Alps (*méridional*, see Fig. A2d) and, in contrast to the Central Alps, can also include stronger contributions of pluvial processes. The Northern Pre-Alps show the largest variability of streamflow regime ~~type classification for Switzerland (see e.g., Aeschwanden and Weingartner, 1985; Weingartner and Schwanbeck, 2020). Figure A1 in Appendix A shows the incidence of streamflow regime types across biogeographic regions~~(Fig. A2c). As transitional region between Alps and lowlands, streamflow regime types also show a large variety of processes contributing to streamflow generation including glacial, nival and pluvial processes. The Jura is a subalpine mountain range characterized by a strongly karstified geology. The
765 ~~variability of streamflow regime types is the lowest among biogeographic regions and consists mainly of locally specific types (*jurassien*) influenced by a mixture of nival and pluvial processes (Fig. A2e). The Swiss Plateau region is equivalent to the lowlands and hence is dominated by pluvial streamflow regime types (Fig. A2f).~~~~

Note that whereas catchments smaller than 500 km² allow for a more distinct discrimination in streamflow regime types and hence streamflow generating processes, catchments with an area larger than 500 km² are influenced by a multitude of streamflow generating and/or storage processes (e.g., groundwater contributions) and are hence provided as *mixed regime* (>500 km²) type (see Sect. 2). The mixed regime type is the most prevalent among catchments (see Fig. 2 and occurs across all biogeographic regions (Fig. A2) being the most frequent regime type in Western and Eastern Central Alps as well as in the Northern Pre-Alps.

The catchment grouping to biogeographic regions presented here is again based on maximum overlap of catchment area with the specific biogeographic region (see also Fig. 7a). Biogeographic regions are frequently used for grouping catchments into groups of similar streamflow (generation) characteristics and provides usable results (see e.g., Brunner et al., 2019b; Muelchi et al., 2021b; von Matt et al., 2024). In specific cases where a categorization into biogeographic regions may not be unambiguous (see Sect. 5.1), categorization may be reconsidered by the user via alternative grouping (e.g. directly on streamflow regime types), alternative categorization approach (other than maximum overlap) or expert judgement. As such the streamflow regime types *nivo-pluvial jurassien* and *pluvial jurassien* could for example be recategorized to the Jura region (see Fig. A2f).

A2 Detailed Event analysis

The combination of hydro-meteorological indicators, standardized (drought) indices (SPI, SPEI, SMRI), ~~cumulative~~ (potential ~~water (balance)~~ cumulative water and streamflow deficits (CWD, PCWD, CQD) and accompanying climatological anomalies allow for a detailed analysis of specific (streamflow) drought events. Drought-generating processes vary across catchments depending on hydro-climatological and terrestrial catchment characteristics, the season as well as on anthropogenic disturbances (e.g., Brunner et al., 2022; Van Loon and Van Lanen, 2012; Van Loon, 2015; Apurv et al., 2017). Except for glacier melt and groundwater, the HYD-RESPONSES dataset provides time series for all relevant hydro-meteorological indicators required to analyse (streamflow) drought generation, drought propagation as well as drought type classification.

Figure 6 illustrates time series for the year 2022 of a subset of relevant hydro-meteorological variables for catchment 2034 - Broye, Payerne, Caserne d'aviation. This catchment is located in the western Swiss Plateau region (highlighted in Fig. A4).

The year 2022 was an exceptional year with unprecedented combined heat and drought conditions over Europe (Tripathy and Mishra, 2023). The Broye catchment experienced low-flow conditions beyond a 100-year return period (BAFU (Eds.), 2023). In the Broye catchment, the lowest 7-day average streamflow values were observed between July and August (see Fig. 6i) Several streamflow drought events were identified for both yearly fixed (purple shading) and variable (green shading) threshold definitions ~~-(see Fig. 6 (all panels))~~. The longest events occur during the annual low-flow season for both definitions.

The year 2022 was also one of the warmest years on record with three heatwaves occurring in mid-June, mid-July and in the beginning of August (Imfeld et al., 2022). During the longest streamflow drought event in July 2022 (~~M7Q row in Figure~~ see Fig. 6i), evaporation anomalies begin to decline and become negative towards the end of the event (~~ET row in see~~ Fig. 6c). Concurrent strong negative soil moisture anomalies at shallow and deeper levels (see Fig. 6d) suggest that the successively decreasing evaporation anomalies may be related to increasingly depleted soil moisture storages resulting in limited

water availability for evaporation. Interactions between (subsurface) storage processes are however complex and also include groundwater–soil moisture interactions (e.g., Orth and Destouni, 2018).

805 ~~Hydro-meteorological time-series for the Swiss Plateau catchment 2034–Broye, Payerne (Caseerne d’aviation) for the year 2022. Color shadings in all panels highlight drought periods based on two definitions: yearly Q347 (pink, fixed threshold approach) and a moving monthly 15th percentile threshold (green, variable threshold approach). (a) Moving monthly anomalies of the 2-m-temperature (T2m), positive anomalies are shown in red and negative anomalies in blue. (b) Moving monthly anomalies of the precipitation (P, RhiresD) (c) Moving monthly anomalies of the evaporation (ET, ERA5-land). (d) Moving monthly anomalies of the soil moisture volume (ESM-ERA5-land), soil moisture anomalies are depicted for a near-surface SM-level (black, 0–7 cm) and the deepest level (blue, 100–289 cm) available from ERA5-Land. (e) Moving monthly anomalies of the snow-water equivalent (SWE-SPASS). (f) Moving monthly anomalies of the snowmelt (smlt, SPASS). (g) SPI colored by aggregation scales from 1- to 24-months. (h) SMRI colored by aggregation scales from 1- to 24-months. (i) Seven-day average streamflow (M7Q). (j) The CQD time series shows the corresponding accumulated M7Q deficits for both the fixed threshold approach (black) and the variable threshold approach (blue). (k) Absolute cumulative water deficit (CWD). (l) 815 Potential cumulative water deficit (PCWD). (m) Monthly anomalies of the CWD (CWD anomaly). (n) Monthly anomalies of the PCWD. Time series of the cumulative water deficits for both absolute values and monthly anomalies are shown for both standard (black, $P-E$ (P_e)) and snowmelt-corrected (blue, $P-E+\Delta SWE$ ($P_{smltSPASS_e}$)) variants. The same is shown for cumulative potential water deficits which are based on the potential water balance ($P-PET$ (P_{pev}) and $P-PET+\Delta SWE$ ($P_{smltSPASS_{pev}}$)).~~

820 The HYD-RESPONSES dataset further provides information on cumulative (atmospheric) water deficits represented by standardized and non-standardized (drought) indices. For the Broye catchment, the 2022 streamflow drought events identified with the variable threshold (green shading) correlate well with shorter aggregation scales (1- to 3-monthly) SPI and SMRI indices in spring and summer. The correspondence between short-term precipitation deficits and streamflow droughts is, however, not consistent throughout the year. During the variable threshold streamflow droughts in mid-March to April, both SMRI-1 and 825 SMRI-3 reach more negative values than their SPI equivalents, which ~~suggests a contribution of lacking snowmelt indicates that lacking snowmelt contributed~~ to the streamflow drought generation (see Fig. 6g,h). Lacking snowmelt as contributing factor is further confirmed by considering the larger and rather persistent negative anomalies in both SWE and snowmelt in the preceeding 1 to 3 months (see Fig. 6e,f).

Cumulative deficits in actual (CWD, Fig. 6k) and potential (PCWD, Fig.6l) water balance as well as streamflow (CQD, 830 Fig. 6j) provide complementary information to the SPI, SMRI and SPEI in the form of non-standardized and hence physically interpretable deficit amounts. Cumulative streamflow deficits (CQD) show only two phases without deficit compensation for both drought definitions (Fig.6j). A shorter CQD phase coincides with the drought events in spring (variable threshold) and the shorter drought event in June (fixed threshold), while a longer phase coincides with the remaining shorter and longer streamflow drought phases in July and August before CQD is compensated by September 2022. For both CQD phases, the 835 CQD is larger for streamflow droughts based on a variable threshold definition. Above average precipitation (+130 %; BAFU (Eds.), 2023) was reported in September 2022 and corresponds well with the compensation of CQD and is also reflected in the

positive monthly (31d) precipitation anomalies (P anomaly, Fig. 6b). Similar to the longest streamflow drought phases, also the largest ~~deficits in (actual) cumulative deficits in~~ water balance (CWD) occurred between May–August ~~2022. Larger CWDs during the warm season are consistent with the~~ 2022 (in terms of both absolute deficits and anomalies, see Fig. 6k,m). Based
840 on the seasonal climatology of both temperature and evaporation ~~with the~~ (highest values during summer), larger absolute CWDs are generally expected to occur during the warm season (not shown). Major CWD phases match streamflow drought phases remarkably well, especially for the variable threshold definition with one exception in April. The two longer streamflow drought phases in May–June further show the benefits of considering anomalies in the CWDs. While absolute CWDs were not compensated in between the streamflow droughts, the CWD anomalies indicate that the deficits returned to seasonal norm
845 values (see Fig. 6m). Cumulative deficits in potential water balance (PCWDs, Fig. 6l) are more similar to cumulative streamflow deficits (~~CQD~~) for the variable-threshold definition ~~-(CQD, Fig. 6j (blue line))~~. This reflects the different nature of CWDs and PCWDs. ~~The Deficits based on the~~ actual water balance ~~is~~ (P-E) are more strongly tied to the actual water availability and hence the individual streamflow ~~phases. (drought) phases (Fig. 6i,k)~~. The potential water balance (P-PET), on the other hand, represents the deficit that would have been accumulated under unlimited water availability. Similar to PCWD, CQDs reflect
850 the integrated streamflow deficit over time while an actual deficit in terms of low streamflow levels does not necessarily have to exist (anymore).

A3 Composite analysis (catchment response patterns)

Composite analysis is a frequently used approach to understand the driving processes of a phenomenon such as droughts (see e.g., Bevacqua et al., 2021; Floriancic et al., 2020; Mahto and Mishra, 2024). By considering the median values of drought
855 indicators across all streamflow drought events in a catchment, typical response patterns may become more evident and may allow for more generalized inferences on typical streamflow drought response patterns e.g., to precipitation deficits accumulated over various aggregation time-scales. Here, we present a composite analysis of median SPI values associated with streamflow droughts defined by the monthly 15th-percentiles of the streamflow which corresponds to the highest of the low-flow percentile used for the Swiss national drought platform (see BAFU, 2025).

860 Note that streamflow drought characteristics and drought propagation processes may differ among catchments depending on hydro-meteorological climatologies, geological and terrestrial characteristics (e.g., aquifer, rock type, (soil) water storage capacity), seasonality of and differences in contributing streamflow (drought) generating processes and human disturbances (e.g., Van Loon and Laaha, 2015; Floriancic et al., 2022; Jehn et al., 2020; Apurv and Cai, 2020; Savelli et al., 2022; Haile et al., 2020; Brunner et al., 2022, 2021, 2023; Tjeldeman et al., 2022; de Jager et al., 2022). We therefore separate the streamflow
865 droughts and catchments by seasons winter (DJF, December–February), spring (MAM, March–May), summer (JJA, June–August) and autumn (SON, September–November) and by streamflow regime types. Six streamflow regime types are selected to capture a variety in dominant streamflow (drought) generating processes. These include glacial (*a-glaciaire*, *nivo-glaciaire*), nival (*nival alpin*, *nival méridional*) and pluvial (*pluvial jurassien*, *pluvial supérieur*) processes. The importance of precipitation deficits across scales is assessed using SPIs (SPI-1 to SPI-24). Streamflow drought events are only considered for the
870 longest common homogeneous period across catchments (1991–2022). The selection is further restricted to catchments with

at least 10 streamflow drought events in each season (over the entire time series length) with a minimum duration of at least 10 days to enhance robustness and exclude minor droughts.

Median SPI values are mostly negative across all aggregation time-scales indicating that precipitation conditions co-occurring with streamflow droughts tend to be drier than normal. Several streamflow regimetype-specific response patterns are evident
875 and change across seasons along with contributing streamflow (drought) generating processes.

Glacier melt is the dominant factor for the *a-glaciaire* regime type (Fig. A3a-d). Streamflow levels are typically lowest in winter (January–March) as a result of precipitation falling as snow (intermediate storage) and highest in summer due to large contributions of glacier melt (Aschwanden and Weingartner, 1985; Weingartner and Schwanbeck, 2020; Muelchi et al., 2021b). Streamflow droughts of strongly glaciated catchments are not associated with moderate drought conditions at any SPI scale. In
880 glacial and nival catchments a shift towards short-term precipitation deficits (SPI-1 to SPI-6) being associated with droughts is present across seasons and drought-generating processes. The transition towards shorter deficit scales emerges in summer for nival regime types (Fig. A3g,k) and in autumn for glacial regime types (Fig. A3d). In pluvial and transitional regime types short-term precipitation deficits (mostly 1- to 3 months) are relevant throughout the year (Fig. A3q-x). Seasonal shifts are also observed for pluvial and transitional regime types with mid- and long-term precipitation deficits becoming more relevant
885 in summer and autumn (Fig. A3t,w-x).

In addition to 3-monthly precipitation deficits, also mid- and long-term deficits become relevant in summer and autumn for (nivo-pluvial) catchments in the Jura region and catchments of the regime type *pluvial inférieur*. Compound moderate droughts are mainly observed for sub-yearly (1- to 9-monthly) scales with most extreme conditions on a 6-monthly scale in the Jura region (especially for nivo-pluvial catchments) and on a (6- to) 9-monthly scale for catchments of the regime type *pluvial*
890 *inférieur*. In southern Switzerland, precipitation deficits tend to be relevant on longer scales compared to similar regime types north of the Alps. In contrast to nival catchments north of the Alps (*nival alpin*, Fig. A3j-l), droughts in the nival catchments south of the Alps (*nival méridional*, Fig. A3m-p) are associated with substantial precipitation deficits at longer aggregation times (9–24 months). The deficits occur in winter and in summer, but conditions are more extreme in summer (SPI \approx -1.5) on scales longer than 15 months. Further, also 3-monthly precipitation deficits appear to be relevant for streamflow (drought)
895 generation in summer (moderate drought conditions). In spring and autumn, mid- to short-term accumulation scales are more relevant. Interpretations of the differences between the south and north sides of the Alps should however be considered with caution due to the small catchment sample sizes and the spatial proximity of the two *nival méridional* catchments. The observed response patterns may therefore not be representative of nival catchments south of the Alps in general.

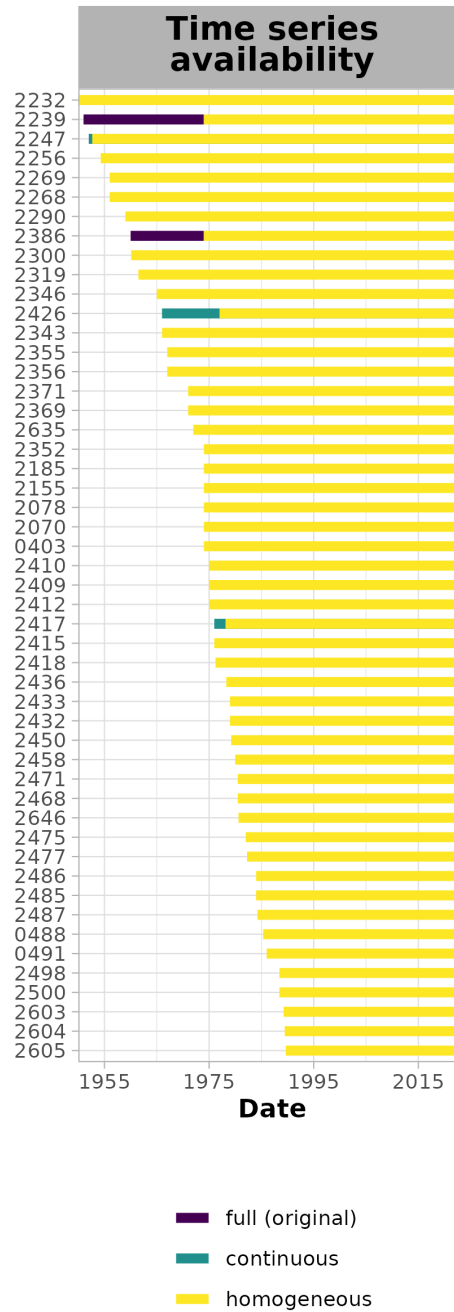


Figure 3. Streamflow time series availability for 50 example catchments. The colours indicate the periods covered by availability type. ~~Complete~~-Full is equivalent to the original time series provided by the FOEN. Continuous denotes the gap-checked time series and the homogeneous period accounts for homogeneity (starting at a breakpoint). In the case of overlapping periods, only the most important period type for analysis (e.g., homogeneous) is displayed. The importance of the periods for analysis is defined as follows: *homogeneous* is more important than *continuous* is more important than *full (original)*.

Evaluation of Standardized Indices

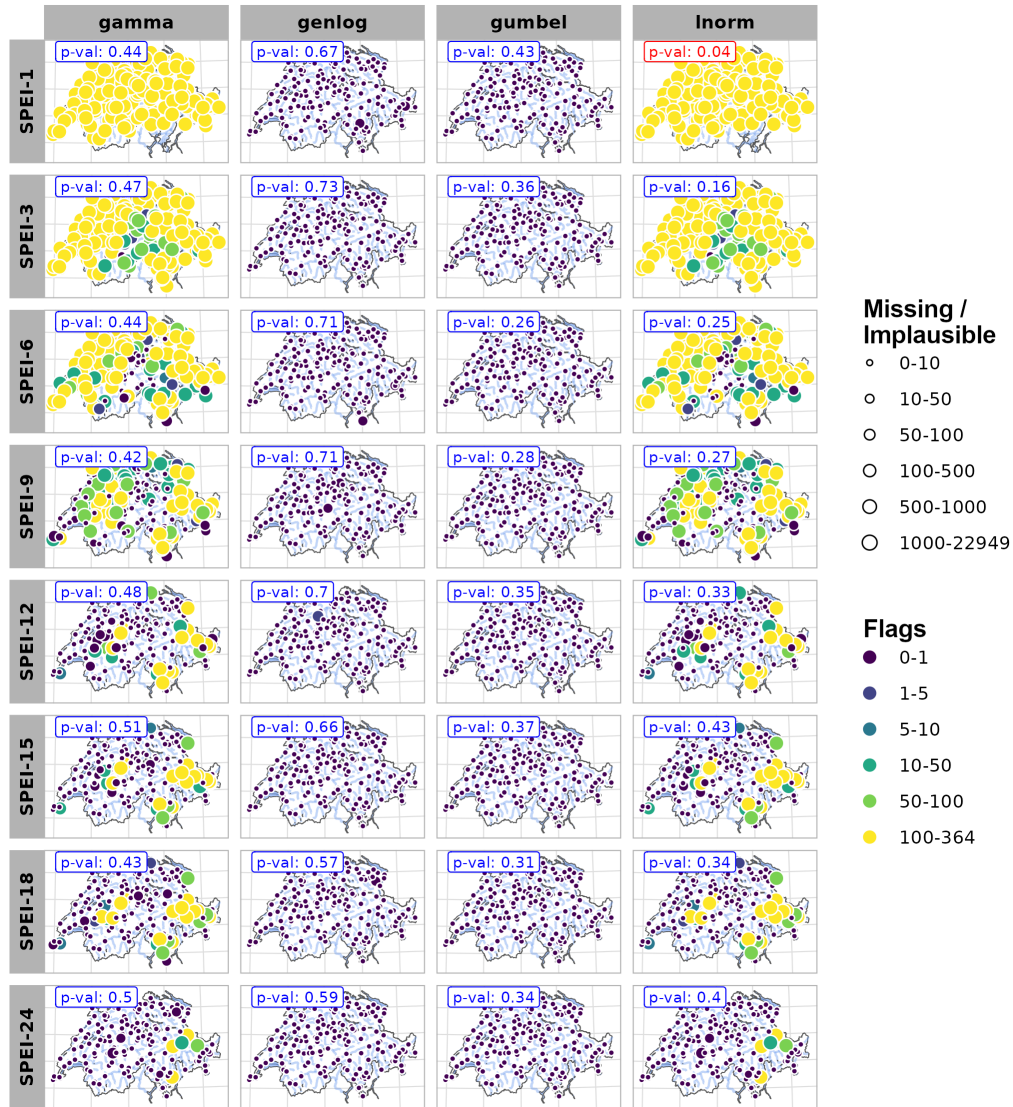


Figure 4. Evaluation statistics for the transformation of standardized (drought) indices. Information on the normality tests (p -values), flags and implausible/missing values ($SPEI \notin [-3,3]$) for four example candidate distributions for the Standardized Precipitation and Evaporation Index (SPEI; Vicente-Serrano et al., 2010). The circle size indicates the number of missing and implausible values. Colours show the number of flags (= convergence issues) returned by the fitting function of the *SCI* R-package (Stagge et al., 2015; Gudmundsson and Stagge, 2016) for all days of the year (DOY). The maximum number of flags is equivalent to 366. Median p -values of the Shapiro-Wilk normality test (Shapiro and Wilk, 1965) were calculated by considering all catchments and are coloured in red in case of rejection ($p < 0.05$). The final HYD-RESPONSES dataset only provides SPEIs fitted by the *genlog*-distribution (best choice based on the evaluation criteria).

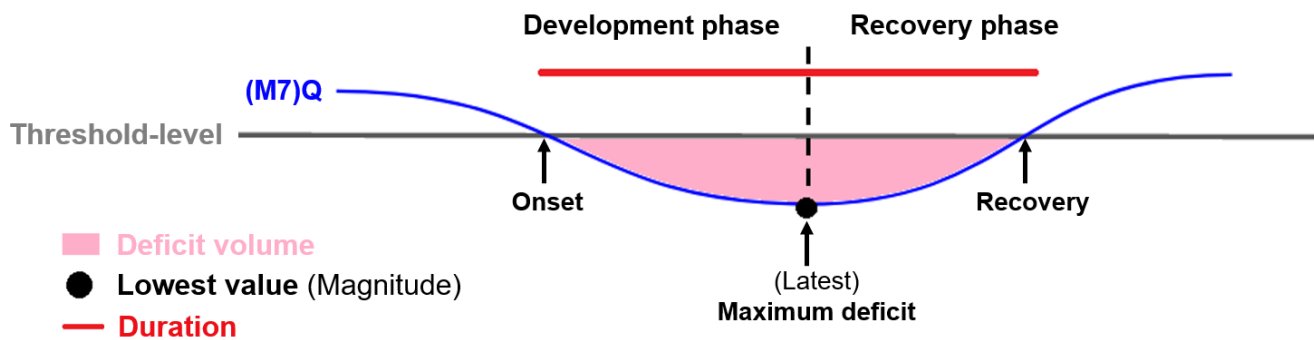


Figure 5. Schematic depiction of the event definition and phase subdivision. The extracted (streamflow) drought phases are characterized by duration, event start (onset), the latest date of the maximum streamflow deficit (anomaly), and event recovery. Additional characteristics are the drought intensity (deficit volume or accumulated deficit) and severity/magnitude (maximum streamflow deficit). The computation of other characteristics is left to the user.

Drought 2022 – Example 2034 - Broye (Payerne, Caserne d'aviation)

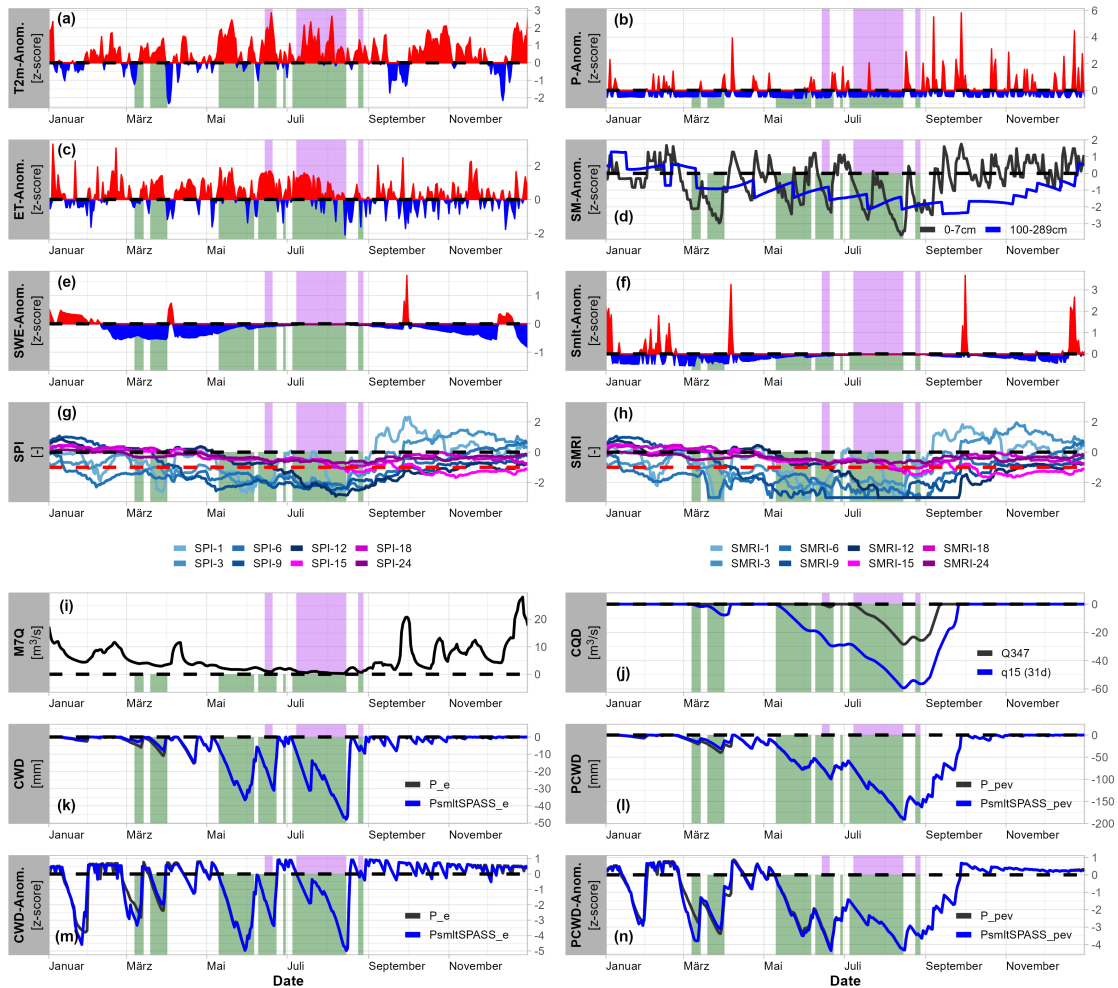


Figure 6. Schematic depiction of hydro-meteorological time series for the event definition and phase subdivision. The extracted Swiss Plateau catchment 2034 - Broye, Payerne (streamflow Caserne d'aviation) for the year 2022. Color shadings in all panels highlight streamflow drought phases are characterized by duration events for two definitions: yearly Q347 (pink, event start fixed threshold approach) and a moving monthly 15th percentile threshold (onset green, variable threshold approach). (a) Moving monthly anomalies of the 2 m-temperature (T2m), positive anomalies are shown in red and negative anomalies in blue. (b) Moving monthly anomalies of the latest date precipitation (P, RhiresD) (c) Moving monthly anomalies of the maximum streamflow deficit evaporation (anomaly ET, ERA5-land). (d) Moving monthly anomalies of the soil moisture volume (ESM ERA5-land), soil moisture anomalies are depicted for a near-surface SM-level (black, 0–7 cm) and event recovery the deepest level (blue, 100–289 cm) available from ERA5-Land. Additional characteristics are (e) Moving monthly anomalies of the snow water equivalent (SWE SPASS). (f) Moving monthly anomalies of the snowmelt (smt, SPASS). (g) SPI colored by aggregation scales from 1- to 24-months. (h) SMRI colored by aggregation scales from 1- to 24-months. (i) Seven day average streamflow (M7Q) on which streamflow drought intensity events were identified. (j) The CQD time series shows the corresponding accumulated M7Q-deficits for both the fixed threshold approach (black) and the variable threshold approach (blue). (k) Absolute cumulative water deficit volume or accumulated (CWD). (l) Potential cumulative water deficit (PCWD). (m) Monthly anomalies of the CWD (CWD anomaly). (n) Monthly anomalies of the PCWD. Time series of the cumulative water deficits for both absolute values and severity/magnitude monthly anomalies are shown for both standard (maximum streamflow deficit black, P-E (P_e)) and snowmelt-corrected (blue, $P_e + \Delta SWE$ ($P_{smltSPASS_e}$)) variants. The computation of other characteristics same is left to shown for potential cumulative water deficits which are based on the user potential water

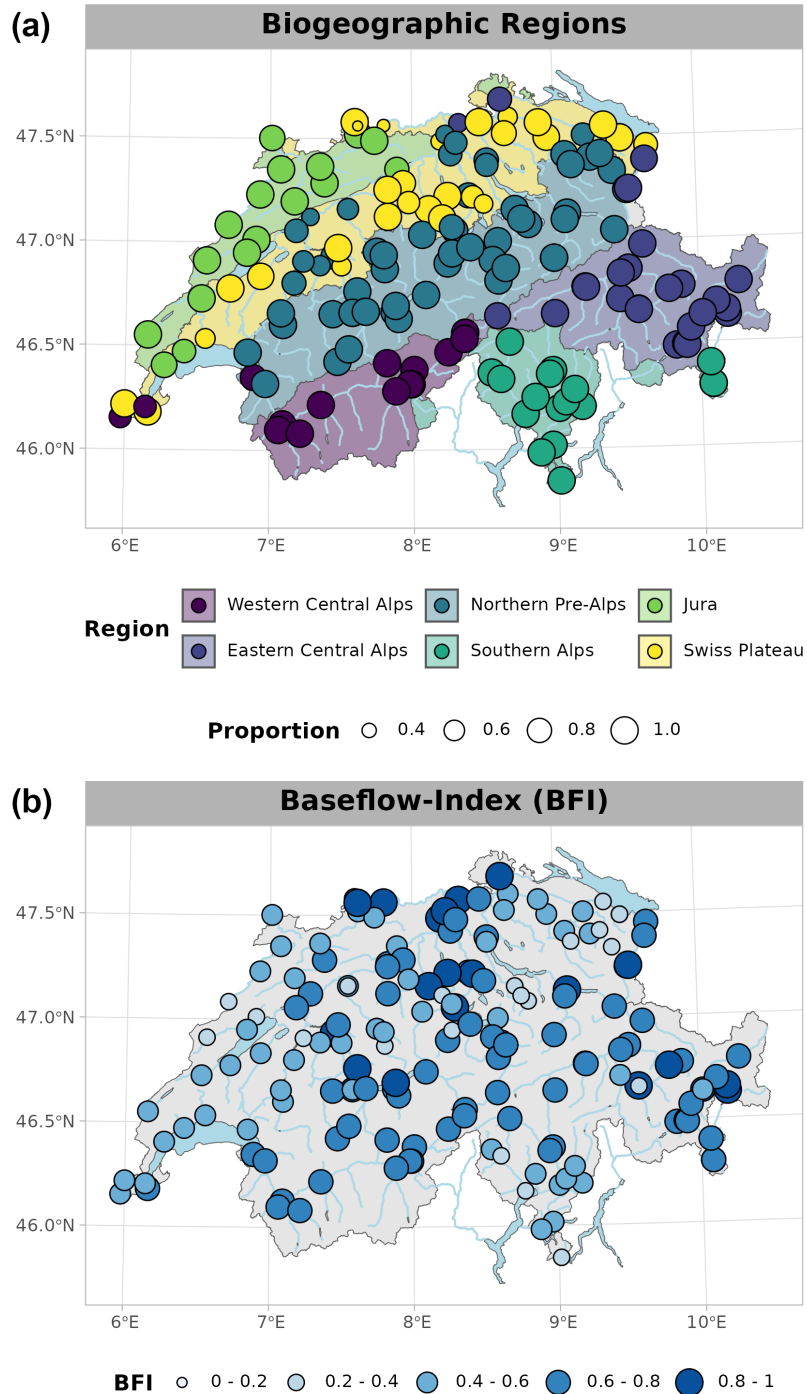


Figure 7. Catchment descriptors (examples). **Top:** (a) Dominant (largest overlap percentage with the catchment area) biogeographic region (colours). Point sizes indicate the catchment area proportion covered by the dominant biogeographic region. **Bottom:** (b) Baseflow-Index (BFI, Nathan and McMahon, 1990) for each catchment derived from the daily streamflow time series.

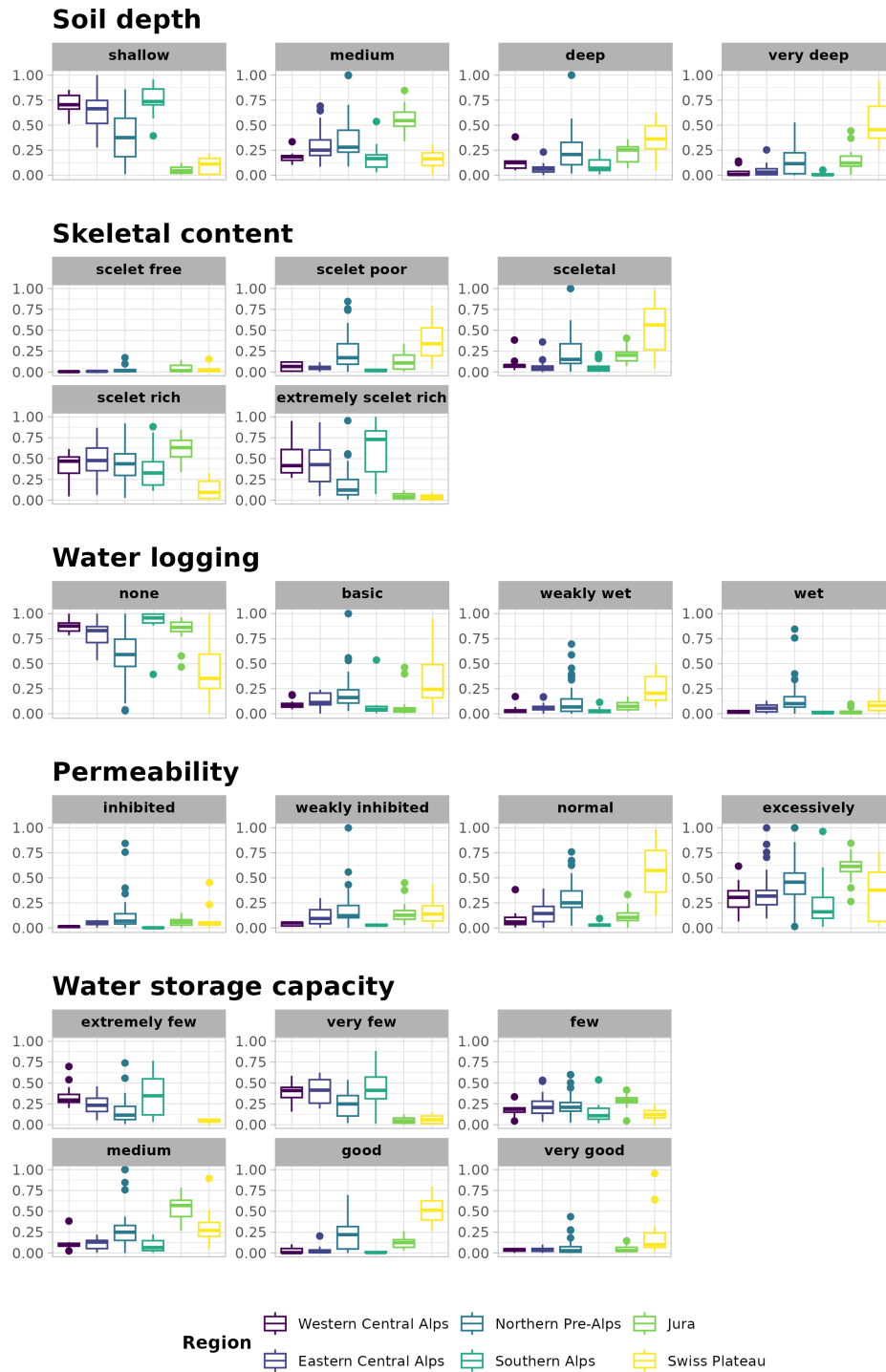


Figure A1. Catchment coverage fractions for all (sub-)categories of the soil characteristics: soil depth, skeletal content, water logging, soil permeability, and water storage capacity across regionalized catchment groups derived from the biogeographic regions of Switzerland (colours, [see also Fig. 7a](#)).

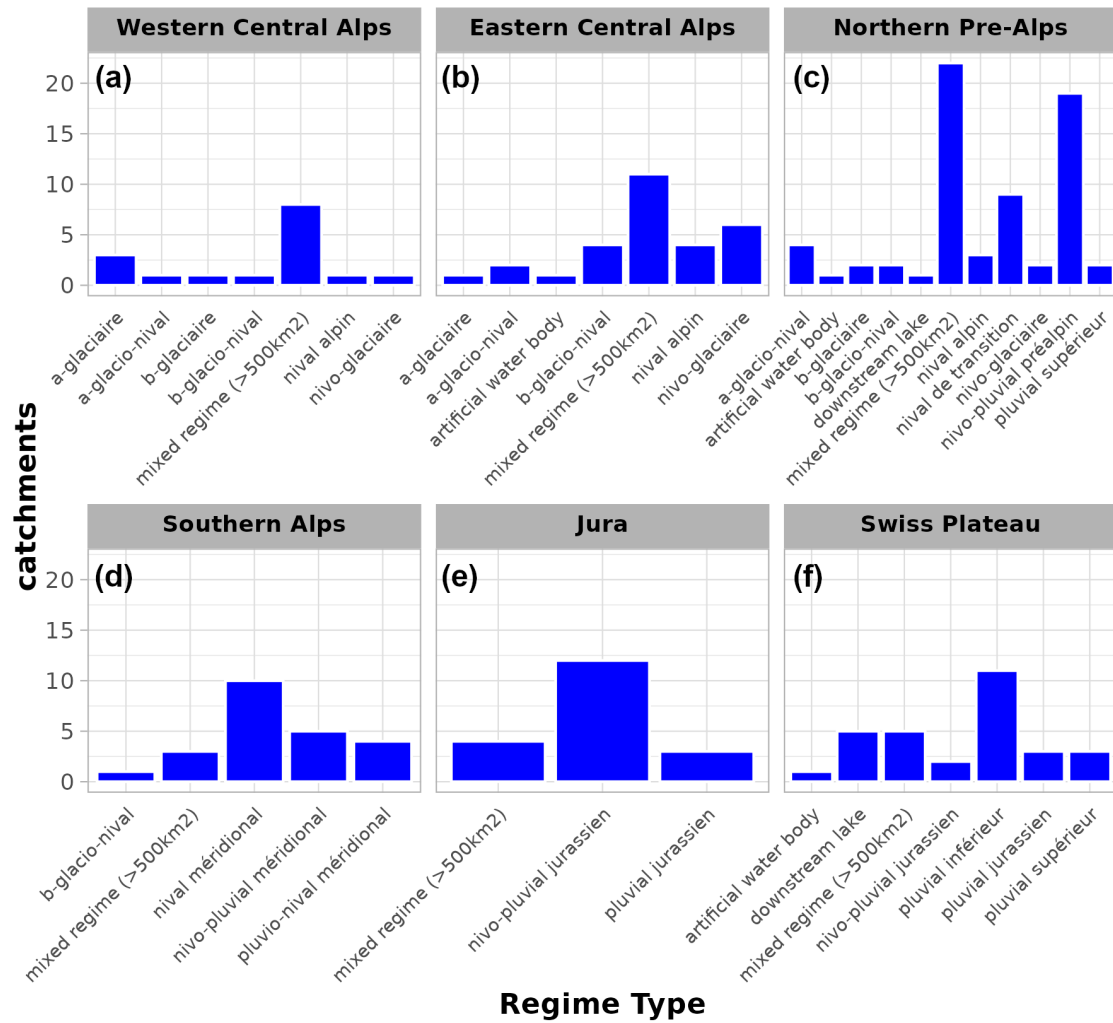


Figure A2. Streamflow regime type incidence among catchments grouped by the biogeographic regions of Switzerland (Western Central Alps, Eastern Central Alps, Northern Pre-Alps, Southern Alps, Jura and Swiss Plateau region; see Sect. 3.3 and also Fig. 7). The streamflow regime type classification was provided by the FOEN. The Y-axis shows the number of catchments associated with each category.

Median SPI-values during hydrological events

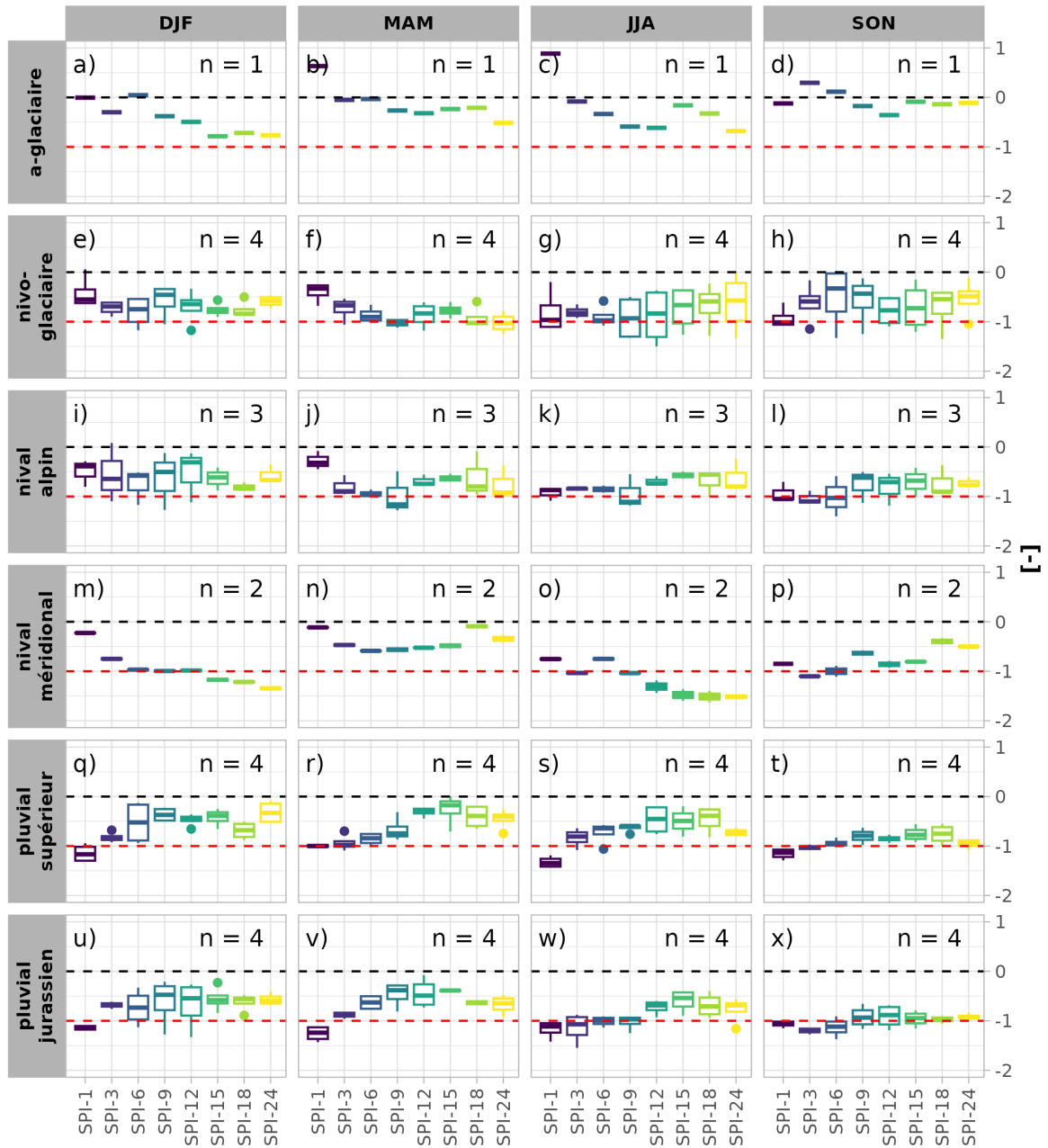


Figure A3. Median SPI values during hydrological drought conditions for all events of all catchments for six selected streamflow regime types across the four seasons winter (DJF), spring (MAM), summer (JJA) and autumn (SON). The streamflow regime types were selected to represent catchments with (dominant) glacial (a-glaciaire, nivo-glaciaire), snow (nival alpin, nival méridional) and pluvial processes (pluvial jurassien, pluvial supérieur) and spatial diversity. Hydrological drought events were defined by a moving monthly (31d) 15th-percentile (variable) threshold. Boxplots are coloured according to SPI aggregation time scales (1- to 24-months). Moderate drought conditions are indicated by the red dashed lines, the black dashed line indicates 0. ["n=" refers to the number of catchments with a specific streamflow regime type.](#)

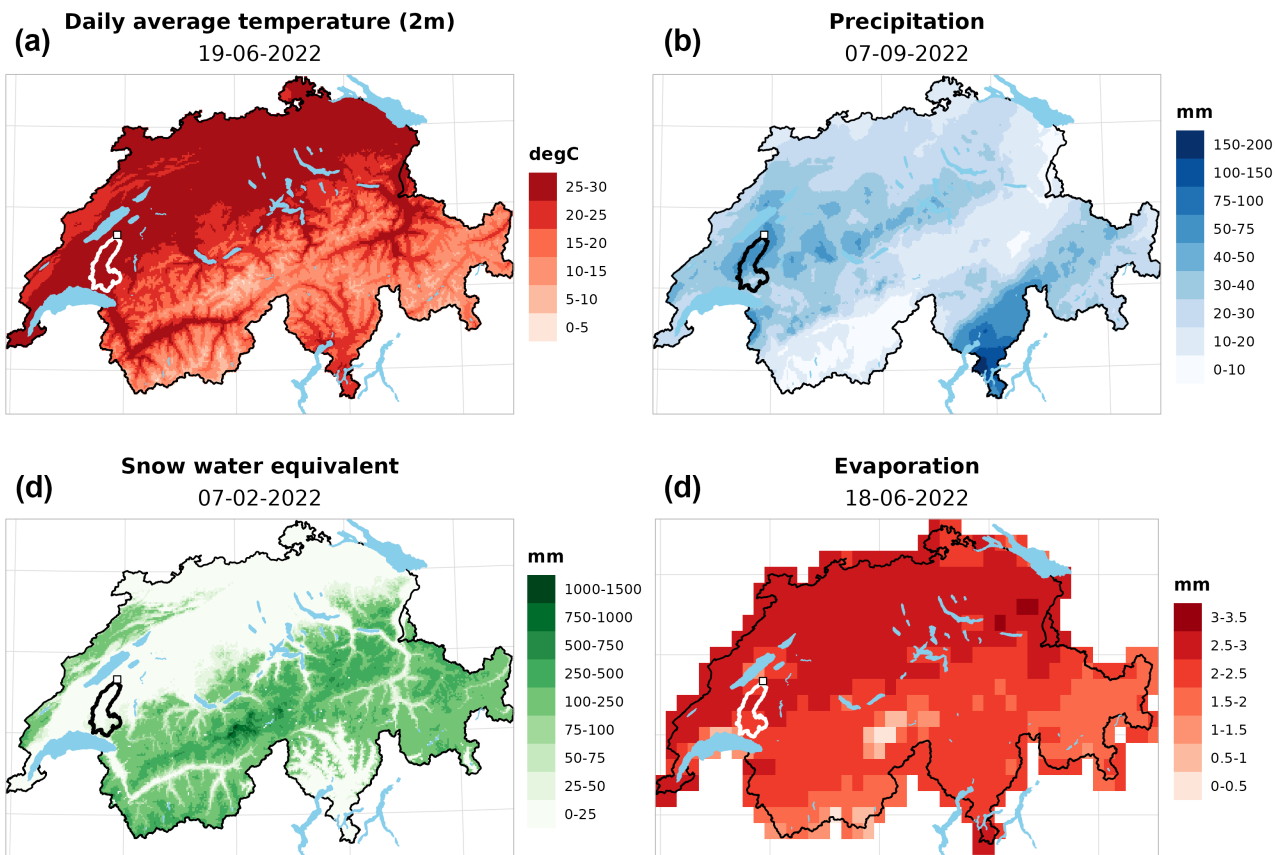


Figure A4. Overview of the spatial raster products used to extract daily time series. (a) Mean daily temperature (TabsD, MeteoSwiss). (b) Daily precipitation sun (RhiresD, MeteoSwiss). (c) Daily snow water equivalent of the Swiss snow climatology (SPASS) (SWE, MeteoSwiss & SLF). (d) Daily evaporation sum (aggregated from hourly ERA5-Land data, ECMWF). Note that the second snow climatology product (OSHD) is not shown. Contours in white/black show catchment 2034 - Broye, Payerne, Casernde d'aviation for the day with the highest observed catchment average values for each specific product for the year 2022. White squares show the catchment outlet where daily streamflow is measured. Extracted and derived time series over the year 2022 are shown for the same catchment in Figure 6.

Appendix B: [Tables](#)

900 Appendix C: **Discussion**

The HYD-RESPONSES dataset can, for example, be used to study drought dynamics and drought propagation, for streamflow forecasting using Long Short-Term Models Kratzert et al. (LSTMs; 2018); Lees et al. (LSTMs; 2022); Kratzert et al. (LSTMs; 2023), Random Forests Floriancic et al. (RFs; 2022), or to infer drought drivers using clustering and principal component analysis (e.g., Jehn et al., 2020). The information on breakpoints allows to study pre- and post-influence catchment behaviour e.g., by using the paired catchment or upstream-downstream approach (see e.g., Rangocroft et al., 2019; Van Loon et al., 2019). The availability of variables originating from multiple data sources (direct observations, reanalysis data, model data) allows for comparative analyses. The following variables are available from multiple sources: temperature (MeteoSwiss, ERA5-Land), precipitation (MeteoSwiss, ERA5-Land), and snow (MeteoSwiss, WSL, ERA5-Land). There are several known limitations related to the datasets used to compile the HYD-RESPONSES data. ERA5-Land is a state-of-the-art reanalysis product provided at a higher spatial resolution than the standard ERA5 reanalysis (Hersbach et al., 2020; Muñoz-Sabater et al., 2021). The higher spatial resolution results in a better depiction of soil moisture, lakes, river discharge estimations, and the orographic enhancement of precipitation (Muñoz-Sabater et al., 2021). However, the grid resolution of 9 km still has limitations over complex high-altitude terrain. The extracted time series related to snow depth (SWE) should be used with caution, as snow depth in ERA5-Land is of mixed quality depending on geographical location and altitude (Dalla Torre et al., 2024). Scherrer et al. (2023) showed, that ERA5-Land overestimates SWE at high elevations with larger biases in the southern compared to the northern Alps. They state that higher-resolution datasets such as SPASS (Marty et al., 2025) and OSHD (Mott, 2023; Mott et al., 2023) should be preferred over ERA5-Land. Further also note that all snow-related datasets have problems in representing small SWE amounts at low altitudes (Scherrer et al., 2023; Michel et al., 2023; Marty et al., 2025). Another limitation of the ERA5-Land dataset is the parameterization of subgrid-scale processes and the representation of subsurface storages that affect evapotranspiration (e.g., fixed maximum storage volume assumption; see Muñoz-Sabater et al., 2021). However, gridded observation-based evaporation datasets are yet to be developed for Switzerland. Caution is required when using the snow-corrected precipitation (water input) time series. The time series corrected by the Δ SWE series consider both snowfall (Δ SWE \geq 0) and snowmelt (Δ SWE $<$ 0), while the correction based on snowmelt variables only accounts for snowmelt (*smlt* in ERA5-Land and *rome* in OSHD; see Table 1 and Table B1). Snowmelt-corrected precipitation time series only account for snowmelt, they may, therefore, be of limited use during the main snow accumulation season but can still provide valuable information during the snowmelt season. The time series for standardized (drought) indices are only provided for the transformation based on the best-fitting distribution across all catchments to allow for catchment comparability (see e.g., Staudinger et al., 2014). The best-fitting distribution may however vary across catchments and climates (see e.g., Stagge et al., 2015). The HYD-RESPONSES dataset provides information on fits, missing values and flags which can be used to exclude catchments with unsatisfying fitting and transformation properties from analyses. The HYD-RESPONSES time series are provided for

product-specific periods and the spatial coverage is restricted to Swiss territory for most of the higher-resolution MeteoSwiss and SLF products (TabsD, TminD, TmaxD, SPASS, SrelD, OSHD) as well as many catchment descriptor input datasets. Full coverage over the entire hydrological Switzerland is only available for ERA5-Land (all variables) and the MeteoSwiss RhiresD product (after 1992; see MeteoSwiss, 2021a). Catchments with significant areas outside of the Swiss National borders may therefore be considered with caution or excluded from the analysis.

Appendix C: Complementary datasets

Complementary datasets provide a wide range of additional catchment descriptors and hydro-meteorological time series. An overview of datasets and variables is provided in Table 4. The FOEN provides additional geodata related to both surface and groundwater via the Hydrological Service (<https://www.hydro.ch/>). The datasets include additional catchment descriptors with information on population density, catchment areas covered by forest and agriculture (among others) as well as information on water quality aspects and sewage. The FOEN further operates both a groundwater monitoring network (NAQUA) providing continuous groundwater measurements for selected point locations (BAFU, 2019) and a water quality measurement network (NAWA) providing information on concentration and loads of important dissolved compounds (e.g., pH, electric conductivity, nutrient contents; BAFU, 2023). The “Catchment Attributes and Meteorology for Large-sample catchment Studies” (CAMELS) datasets aim at providing a consistent set of hydro-meteorological time series and catchment descriptors over a large sample of hydrological catchments on country level (Clere-Schwarzenbach et al., 2024). The catchments in the Swiss version of the CAMELS data (CAMELS-CH; Höge et al., 2023a) are largely congruent with our dataset. The only exception is station 2646, which is only contained in the HYD-RESPONSES dataset. Note that the HYD-RESPONSES dataset provides only a sample subset of 184 catchments. The CAMELS-CH dataset provides valuable complementary catchment-level information on glacier changes (based on GLAMOS, for details see Höge et al., 2023a), land use, hydro-geological and hydro-terrestrial information (e.g., the contributions of various grain size categories and bulk density) as well as anthropogenic disturbances (e.g., hydropower and reservoir capacities). CAMELS-CH further provides modelled time series based on the hydrological model PREVAH (see e.g., Höge et al., 2023a; Viviroli et al., 2009). The CAMELS-CH dataset is freely available from Zenodo (<https://zenodo.org/records/10354485>; Höge et al., 2023b). The CombiPrecip dataset (MeteoSwiss) provides high-resolution (10 minutes, 1×1 km) precipitation fields derived from a combination of radar and station measurement data (Sideris et al., 2014). The CombiPrecip dataset could be a valuable addition for studying drought recovery where extreme precipitation is often considered an important factor (Wu et al., 2022). The HydCheck project (Streeb et al., 2024) evaluated the influence of (anthropogenic) disturbance factors on streamflow at stations of the National Surface Water Quality (NAWA) Programme (BAFU, 2023). The evaluated NAWA stations are largely (87.5% of the stations) congruent with the HYD-RESPONSES dataset. The HydCheck dataset provides catchment-level information on the magnitudes for all evaluated disturbance categories including water storage and regulation, hydropower, sewage water, constructions, agriculture as well as drinking and groundwater. The overall impact on several hydrological properties including low-, mid- and high-flow regimes as well as short-term effects and hydraulics is provided as categorical information (from

"not disturbed" to "strongly disturbed"). For more information see Streeb et al. (2024). As part of the planned Swiss National drought early warning system (DEWS), both a high-resolution remote-sensing based evaporation product (V. Humphrey, pers. comm.) and an automatic soil moisture measurement network are under development at MeteoSwiss, ETH Zurich and WSL and may become a valuable addition in a future.

970 ~~Datasets compatible and complementary to the HYD-RESPONSES dataset: **Dataset** **Short description** **Provider** Includes catchment proportions of forests, agricultural (crop) land, population, built-up area and more Groundwater measurement network (NAQUA) Groundwater measurements FOEN Water quality measurement network (NAWA) Information on water quality parameters FOEN Swiss version of the Catchment Attributes and Meteorology for Large sample catchment Studies (CAMELS) dataset High-resolution precipitation fields at ground based on a combination of radar and measurement data~~

975 ~~Detailed evaluation of influences and disturbances of the streamflow at NAWA measurement stations~~

~~The HYD-RESPONSES dataset contains data for 184 Swiss catchments that cover a variety of streamflow regimes, mean altitudes, catchment areas, and anthropogenic influences/disturbances. The catchments cover all biogeographic regions of Switzerland. The HYD-RESPONSES dataset provides daily streamflow data and daily hydro-meteorological time series extracted from gridded data products of MeteoSwiss (TabsD, RhiresD, TmaxD, TminD, SrelD), Meteoswiss and SLF (SPASS), SLF (OSHD) and ECMWF (ERA5-Land). The variables include temperature, precipitation, evaporation, sunshine duration, solar radiation, snowmelt, snow water equivalent, soil moisture, surface runoff, runoff, and streamflow. HYD-RESPONSES further provides derived variables related to streamflow (e.g., M7Q), water balance (e.g., P-E) and snowfall. Additionally, three standardized drought indices (SPI, SPEI, SMRI) for accumulation periods from 1 to 24 months and information on the (non-standardized) cumulative water deficit (CWD), the potential cumulative water deficit (PCWD) and cumulative streamflow deficit (CQD) are provided. The data set also provides information on (streamflow) drought events (occurrence and duration). For each catchment, the drought events have been identified based on fixed and on seasonally varying percentile thresholds. The combination of data sources, the information on hydro-meteorological variables (mainly temperature, precipitation and snow), the derived indices (water balance, cumulative water deficits, standardized drought indices, climatology and anomalies) allow for a multi-purpose use and various analytical approaches such as time series analysis (e.g., Kratzert et al., 2018; Lees et al., 2022), drought propagation and catchment sensitivity analysis (e.g., based on principal component analysis and clustering; Jehn et al., 2020) and changes in rainfall-runoff relationships during hydrological droughts (e.g., Wu et al., 2021). The HYD-RESPONSES data set can easily be combined with complementary datasets such as CAMELS-CH (Höge et al., 2023a) and HydCheck (Streeb et al., 2024). The catchment time series vary in length (subject to station initialization), the hydrological time series are provided for the entire measurement period along with information on data homogeneity (see BAFU (2024) for more details).~~

995 ~~Limitations exist for catchments extending beyond the Swiss borders. The catchment descriptors were extracted from datasets only covering Swiss national territory. The MeteoSwiss-based datasets cover only Switzerland except for RhiresD, which covers the entire hydrological Switzerland from 1992 onward. In summary, the data set provides a state-of-the-art data basis to study droughts in Switzerland.~~

1000 ~~The HYD-RESPONSES project was funded by the Federal Office for the Environment (FOEN). The preliminary SPASS dataset was kindly provided by Regula Muelchi (MeteoSwiss). We thank Caroline Kan (FOEN) for her help with the catchment selection.~~

Appendix C

1005 ~~Streamflow regime type incidence among catchments grouped by the biogeographic regions of Switzerland (Western Central Alps, Eastern Central Alps, Northern Pre-Alps, Southern Alps, Jura and Swiss Plateau region; see Section 3.3 and also Fig. 7). The streamflow regime type classification was provided by the FOEN.~~

Table B1. Glossary of extracted time series variables, their description and units.

Dataset	Variables	Variables (fullname)	Units	Producer
Spatial Climate Analyses	TabsD	Daily 2 m mean temperature	°C	MeteoSwiss
	RhiresD	Daily precipitation sums	mm	
	TminD	Daily 2 m minimum temperature	°C	
	TmaxD	Daily 2 m maximum temperature	°C	
	SreID	Daily sunshine duration	%	
Snow Climatology for Switzerland (SPASS)	SWECLQMD	Daily snow water equivalent	mm	MeteoSwiss & SLF
Climatological snow data since 1998 (OSHD)	swee	Daily snow water equivalent	mm	SLF
	romc	Daily snowmelt-contribution to runoff	mm	
ERA5-Land	tp	Total precipitation	mm	ECMWF
	t2m	Average 2 m temperature	°C	
	e	Total evaporation	mm	
	pev	Total potential evaporation	mm	
	smlt	Snowmelt	mm	
	sd	Snow water equivalent	mm	
	ssr	Total solar radiation	MJ/m ²	
	ro	Runoff	mm	
	sro	Surface runoff	mm	
	swv11	Soil water volume level 1 (0–7cm)	mm	
	swv12	Soil water volume level 2 (7–28cm)	mm	
	swv13	Soil water volume level 3 (28–100cm)	mm	
	swv14	Soil water volume level 4 (100–289cm)	mm	
	Streamflow time series	Q	Daily mean streamflow	

Table B2. Information on the underlying processing and reliability of basic and derived time series variables.

	Type	Level	Data source	Processing	Temporal resolution	Modeling component	Variables
	Streamflow	L1	Streamflow measurements (Q-Meas.)	-	daily mean	-	Q
Sect. 4.1	<u>Precipitation</u>	<u>L2</u>	Spatial climate analyses (SCA)	<u>catchment average</u>	<u>daily total (sum)</u>	-	<u>RhiresD</u>
	<u>Sunshine Duration</u>	<u>L2</u>		<u>catchment average</u>	<u>daily relative (%)</u>	-	<u>SrelD</u>
	<u>Temperature</u>	<u>L2</u>		<u>catchment average</u>	<u>daily mean</u>	-	<u>TabSD, TmaxD, TminD</u>
	<u>Snow</u>	<u>L2</u>	<u>SPASS</u>	<u>catchment average</u>	<u>daily mean</u>	yes	<u>SWECLQMD</u>
	Snow	<u>L2</u> <u>L2</u>	OSHD	<u>catchment average</u> <u>catchment average</u>	<u>daily mean</u> <u>daily total (sum)</u>	yes yes	<u>swee</u> <u>romc</u>
	Various	<u>L2</u>	ERA5-Land	<u>catchment average, daily mean</u>	<u>daily mean</u>	-	<u>t2m</u>
		<u>L2</u>		<u>catchment average, daily mean</u>	<u>daily mean</u>	strong	<u>pev, sd, ssr, swv11, swv12, swv13, swv14</u>
		<u>L2</u>		<u>catchment average, daily total (sum)</u>	<u>daily total (sum)</u>	-	<u>tp</u>
		<u>L2</u>		<u>catchment average, daily total (sum)</u>	<u>daily total (sum)</u>	strong	<u>ro, smlt, stro, e</u>
	Streamflow	<u>L1</u> <u>L3</u>	<u>Q-Meas.</u> <u>ERA5-Land</u>	7-day average (centered)	daily	- strong	<u>M7Q</u> <u>ro7Q</u>
Sect. 4.2	Snow-related	<u>L2</u>	<u>SCA, OSHD</u>	<u>P + Snowmelt</u>	<u>daily</u>	yes	<u>P_SMLT_OSHDromc</u>
		<u>L2</u>	<u>SCA, OSHD</u>	<u>P + ΔSWE</u>	<u>daily</u>	yes	<u>P_SMLT_OSHDswe</u>
		<u>L2</u>	<u>SCA, SPASS</u>	<u>P + ΔSWE</u>	<u>daily</u>	yes	<u>P_SMLT_SPASS</u>
		<u>L2</u>	<u>OSHD</u>	<u>ΔSWE</u>	<u>daily</u>	yes	<u>SWE_diff_OSHD</u>
		<u>L2</u>	<u>SPASS</u>	<u>ΔSWE</u>	<u>daily</u>	yes	<u>SWE_diff_SPASS</u>
		<u>L2</u>	<u>OSHD</u>	<u>ΔSWE ≥ 0</u>	<u>daily</u>	yes	<u>SWE_posdiff_OSHD</u>
		<u>L2</u>	<u>SPASS</u>	<u>ΔSWE ≥ 0</u>	<u>daily</u>	yes	<u>SWE_posdiff_SPASS</u>
		<u>L3</u>	<u>ERA5-Land</u>	<u>P + Snowmelt</u>	<u>daily</u>	strong	<u>tp_smlt</u>
Water balance		<u>L3</u>	<u>SCA, ERA5-Land</u>	<u>P - E</u>	<u>daily</u>	strong	<u>P_e</u>
		<u>L3</u>	<u>SCA, ERA5-Land</u>	<u>P - PET</u>	<u>daily</u>	strong	<u>P_pev</u>
		<u>L3</u>	<u>SCA, OSHD, ERA5-Land</u>	<u>P + Snowmelt - E</u>	<u>daily</u>	strong	<u>PsmltOSHDromc_e</u>
		<u>L3</u>	<u>SCA, OSHD, ERA5-Land</u>	<u>P + Snowmelt - PET</u>	<u>daily</u>	strong	<u>PsmltOSHDromc_pev</u>
		<u>L3</u>	<u>SCA, OSHD, ERA5-Land</u>	<u>P + ΔSWE - E</u>	<u>daily</u>	strong	<u>PsmltOSHDswe_e</u>
		<u>L3</u>	<u>SCA, OSHD, ERA5-Land</u>	<u>P + ΔSWE - PET</u>	<u>daily</u>	strong	<u>PsmltOSHDswe_pev</u>
		<u>L3</u>	<u>SCA, SPASS, ERA5-Land</u>	<u>P + ΔSWE - E</u>	<u>daily</u>	strong	<u>PsmltSPASS_e</u>
		<u>L3</u>	<u>SCA, SPASS, ERA5-Land</u>	<u>P + ΔSWE - PET</u>	<u>daily</u>	strong	<u>PsmltSPASS_pev</u>
		<u>L3</u>	<u>ERA5-Land</u>	<u>P - E</u>	<u>daily</u>	strong	<u>tp_e</u>
		<u>L3</u>	<u>ERA5-Land</u>	<u>P - PET</u>	<u>daily</u>	strong	<u>tp_pev</u>
		<u>L3</u>	<u>ERA5-Land</u>	<u>P + Snowmelt - E</u>	<u>daily</u>	strong	<u>tpsmlt_e</u>
		<u>L3</u>	<u>ERA5-Land</u>	<u>P + Snowmelt - PET</u>	<u>daily</u>	strong	<u>tpsmlt_pev</u>

Table B3. Information on the underlying processing and reliability of standardized (drought) indices and cumulative deficit time series.

	Type	Level	Data source	Processing	Temporal resolution	Distributions	Index Aggregation (months)	Modeling component	Variables
	SPI	L3	SCA	fitted transformation	daily	gamma	1 - 24	yes	R hiresD
		L3	ERA5-Land	fitted transformation	daily	gamma	1 - 24	yes	tp
Sect. 4.4	SPEI	L3	SCA, ERA5-Land	fitted transformation	daily	genlog	1 - 24	strong	P_ pev
		L3	ERA5-Land	fitted transformation	daily	genlog	1 - 24	strong	tp_ pev
	SMRI	L3	SCA, SPASS	fitted transformation	daily	genlog	1 - 24	yes	P_ SMLT_ SPASS
		L3	SCA, OSHD	fitted transformation	daily	lnorm	1 - 24	yes	P_ SMLT_ OSHDromc
		L3	SCA, OSHD	fitted transformation	daily	lnorm	1 - 24	yes	P_ SMLT_ OSHDsw e
		L3	ERA5-Land	fitted transformation	daily	lnorm	1 - 24	strong	tp_ smlt
	Type	Level	Data source	Processing	Temporal resolution	Variants	Threshold-level	Modeling component	Variables
Sect. 4.3	CWD	L3	SCA, ERA5-Land	cumulative sum of negative threshold deviations	daily	multi-year, yearly	$P - E < 0$	strong	P_ e
		L3	SCA, OSHD, ERA5-Land		daily	multi-year, yearly	$P - E < 0$	strong	PsmItOSHDromc_ e
		L3	SCA, OSHD, ERA5-Land		daily	multi-year, yearly	$P - E < 0$	strong	PsmItOSHDsw e_ e
		L3	SCA, SPASS, ERA5-Land		daily	multi-year, yearly	$P - E < 0$	strong	PsmItSPASS_ e
		L3	ERA5-Land		daily	multi-year, yearly	$P - E < 0$	strong	tp_ e
		L3	ERA5-Land		daily	multi-year, yearly	$P - E < 0$	strong	tpsmIt_ e
Sect. 4.3	PCWD	L3	SCA, ERA5-Land	cumulative sum of negative threshold deviations	daily	multi-year, yearly	$P - PET < 0$	strong	P_ pev
		L3	SCA, OSHD, ERA5-Land		daily	multi-year, yearly	$P - PET < 0$	strong	PsmItOSHDromc_ pev
		L3	SCA, OSHD, ERA5-Land		daily	multi-year, yearly	$P - PET < 0$	strong	PsmItOSHDsw e_ pev
		L3	SCA, SPASS, ERA5-Land		daily	multi-year, yearly	$P - PET < 0$	strong	PsmItSPASS_ pev
		L3	ERA5-Land		daily	multi-year, yearly	$P - PET < 0$	strong	tp_ pev
		L3	ERA5-Land		daily	multi-year, yearly	$P - PET < 0$	strong	tpsmIt_ pev
Sect. 4.6	CQD	L2	Q-Meas.	cumulative sum of negative threshold deviations	daily	multi-year, yearly	monthly/seasonal: 2 nd , 5 th , 10 th , 15 th , 25 th , 50 th (median), mean yearly: Q347	-	M7Q

Table B4. Information on the underlying processing and reliability of climatology and anomaly time series.

	Type	Level	Processing	<u>Temporal resolution</u>	Variant	Statistics	<u>Window / Anomaly-Scale</u>	Variables
	climatology	L1–L2	statistical summary	<u>monthly</u> <u>seasonal</u> <u>extended season</u> <u>yearly</u>	regular	min, q05, q25, med, mean, q75, q95, max, sd, sum	–	Sect. 4.1
	climatology	L1–L3	statistical summary	<u>monthly</u> <u>seasonal</u> <u>extended season</u> <u>yearly</u>	regular	min, q05, q25, med, mean, q75, q95, max, sd, sum	–	Sect. 4.2
	climatology	L2–L3	statistical summary	<u>monthly</u> <u>seasonal</u> <u>extended season</u> <u>yearly</u>	regular	min, q05, q25, med, mean, q75, q95, max, sd, sum	–	Sect. 4.3
	climatology	L2	statistical summary	<u>monthly</u> <u>seasonal</u> <u>extended season</u> <u>yearly</u>	regular	min, q05, q25, med, mean, q75, q95, max, sd, sum	–	Sect. 4.6
Sect. 4.5	climatology	L1–L2	statistical summary	daily	window	min, q05, q25, med, mean, q75, q95, max, sd, sum	<u>no window (daily)</u> <u>31 days (monthly)</u> <u>91 days (seasonal)</u>	Sect. 4.1
	climatology	L1–L3	statistical summary	daily	window	min, q05, q25, med, mean, q75, q95, max, sd, sum	<u>no window (daily)</u> <u>31 days (monthly)</u> <u>91 days (seasonal)</u>	Sect. 4.2
	climatology	L2–L3	statistical summary	daily	window	min, q05, q25, med, mean, q75, q95, max, sd, sum	<u>no window (daily)</u> <u>31 days (monthly)</u> <u>91 days (seasonal)</u>	Sect. 4.3
	climatology	L2	statistical summary	daily	window	min, q05, q25, med, mean, q75, q95, max, sd, sum	<u>no window (daily)</u> <u>31 days (monthly)</u> <u>91 days (seasonal)</u>	Sect. 4.6
	anomalies	L1–L2	z-scores	daily	window	(value - mean) / sd	<u>no window (daily)</u> <u>31 days (monthly)</u> <u>91 days (seasonal)</u>	Sect. 4.1
	anomalies	L1–L3	z-scores	daily	window	(value - mean) / sd	<u>no window (daily)</u> <u>31 days (monthly)</u> <u>91 days (seasonal)</u>	Sect. 4.2
	anomalies	L2–L3	z-scores	daily	window	(value - mean) / sd	<u>no window (daily)</u> <u>31 days (monthly)</u>	Sect. 4.3

Table B5. Information on the underlying processing and reliability of event time series.

	<u>Type</u>	<u>Level</u>	<u>Data source</u>	<u>Processing</u>	<u>Temporal resolution</u>	<u>Threshold-level</u>	<u>Variables</u>
	<u>Cumulative water deficits</u>	<u>L3</u>	<u>Sect. 4.3</u>	<u>deficit > 0</u>	<u>daily</u>	<u>=</u>	<u>Sect. 4.3</u>
	<u>Cumulative streamflow deficits</u>	<u>L2</u>	<u>Sect. 4.6</u>	<u>deficit > 0</u>	<u>daily</u>	<u>=</u>	<u>Sect. 4.6</u>
Sect. 4.7	Streamflow droughts	L2	FOEN	M7Q < threshold-level	daily	<u>monthly/seasonal:</u> 2 nd , 5 th , 10 th , 15 th , 25 th , 50 th (median), mean <u>yearly: Q347</u>	Sect. 4.7

Table B6. Characteristics of all 184 catchments in the HYD-RESPONSES dataset (Part 1/5).

Catchment	Water name	Place	Lon / Lat EPSG:21781	Glaciation %	Area km ²	Avg. Height m asl	Regime Type	Yearly Avg. T °C	Yearly P mm	Yearly E mm	Yearly Q mm
0070	Emme	Emmenmatt	623610 / 200420	0.0	443.00	1065	nivo-pluvial préalpin	6.94	1539.26	300.29	856.45
0078	Poschiavino	Le Presse	803490 / 130520	4.0	168.00	2162	nival méridional	1.58	1324.78	175.84	1078.26
0155	Emme	Wiler, Limpachmündung	608220 / 223240	0.0	937.00	858	mixed regime (> 500km ²)	7.80	1356.58	313.03	623.66
0185	Plessur	Chur	757975 / 191925	0.0	264.00	1868	nival alpin	3.42	1179.00	194.41	915.28
0308	Goldach	Goldach, Bleiche	753190 / 261590	0.0	51.10	827	pluvial supérieur	8.33	1423.14	317.59	889.48
0352	Linth	Linthal, Ausgleichsbecken KLL	718285 / 197310	9.4	147.00	2085	a-glacio-nival	1.83	1874.45	169.98	2422.14
0403	Inn	Cinuos-chel	797700 / 168170	5.2	733.00	2456	mixed regime (> 500km ²)	-0.66	1007.10	146.31	1007.68
0488	Simme	Latterbach	610680 / 167840	1.5	563.00	1594	nival de transition	4.79	1506.56	225.96	1108.96
0491	Schächen	Bürglen, Galgenwäldli	692480 / 191800	1.5	108.00	1728	nivo-glaciaire	3.55	1854.00	188.20	1646.44
2009	Rhône	Porte du Seex	557660 / 133280	11.0	5238.00	2127	mixed regime (> 500km ²)	1.96	1292.71	148.24	1116.86
2011	Rhône	Sion	593770 / 118630	14.2	3372.00	2291	mixed regime (> 500km ²)	1.00	1240.59	127.84	966.98
2016	Aare	Brugg	657000 / 259360	1.5	11681.00	1000	mixed regime (> 500km ²)	7.34	1317.32	291.55	833.95
2018	Reuss	Mellingen	662830 / 252580	1.8	3386.00	1259	mixed regime (> 500km ²)	5.98	1592.79	239.54	1300.70
2019	Aare	Brienzwilser	649930 / 177380	15.5	555.00	2135	mixed regime (> 500km ²)	1.41	1842.89	123.14	2077.41
2020	Ticino	Bellinzona	721245 / 117025	0.2	1517.00	1679	mixed regime (> 500km ²)	4.27	1658.40	209.25	1339.14
2024	Rhône	Branson	573150 / 108300	13.0	3728.00	2235	mixed regime (> 500km ²)	1.35	1249.40	133.83	1166.41
2029	Aare	Brigg, Aegerten	588220 / 219020	2.1	8249.00	1142	mixed regime (> 500km ²)	6.73	1366.01	276.35	908.00
2030	Aare	Thun	613230 / 179280	6.9	2459.00	1746	mixed regime (> 500km ²)	3.72	1604.05	176.90	1438.59
2033	Vorderrhein	Ilanz	735000 / 182030	1.8	774.00	2030	mixed regime (> 500km ²)	2.28	1534.35	157.08	1340.76
2034	Broye	Payeme, Caserne d'aviation	561660 / 187320	0.0	416.00	715	pluvial inférieur	9.19	1186.40	322.34	564.59
2044	Thur	Andelfingen	693510 / 272500	0.0	1702.00	770	mixed regime (> 500km ²)	8.25	1392.81	333.74	857.45
2053	Dranee	Martigny, Pont de Rossetan	570930 / 105200	11.3	676.00	2250	mixed regime (> 500km ²)	1.40	1269.62	138.70	462.70
2056	Reuss	Seedorf	690085 / 193210	6.4	833.00	2013	mixed regime (> 500km ²)	1.96	1681.87	150.85	1624.38
2063	Aare	Murgenthal	629530 / 235090	1.7	10059.00	1066	mixed regime (> 500km ²)	7.04	1346.17	284.49	888.26
2070	Emme	Emmenmatt, nur Hauptstation	623610 / 200420	0.0	443.00	1065	nivo-pluvial préalpin	6.94	1539.26	300.29	835.36
2078	Poschiavino	Le Presse, stazione principale	803490 / 130520	4.0	168.00	2162	nival méridional	1.58	1324.78	175.84	1064.96
2084	Muota	Ingenbohl	688230 / 206140	0.0	317.00	1363	nival de transition	5.45	1958.67	237.00	1915.23
2085	Aare	Hagneck	580680 / 211650	3.4	5112.00	1368	mixed regime (> 500km ²)	5.61	1452.15	237.22	1068.53
2086	Brenno	Loderio	717770 / 137270	0.3	400.00	1815	nival méridional	3.68	1618.84	185.01	342.59
2087	Reuss	Andermatt	688120 / 166320	2.9	190.00	2284	b-glacio-nival	0.59	1709.03	116.01	1167.49
2091	Rhein	Rheinfelden, Messstation	627190 / 267840	0.8	34524.00	1068	mixed regime (> 500km ²)	6.68	1351.54	281.92	935.92
2099	Limmat	Zürich, Unterhard	682055 / 249430	0.8	2174.00	1194	mixed regime (> 500km ²)	6.28	1719.03	264.98	1353.24
2102	Sarner Aa	Sarnen	661460 / 194220	0.0	269.00	1281	downstream lake	5.99	1648.90	224.99	1167.84
2104	Linth	Weesen, Bäsche	725160 / 221380	1.6	1062.00	1584	mixed regime (> 500km ²)	4.39	1785.64	221.45	1538.41
2105	Inn	St. Moritzbad	783910 / 150960	3.8	155.00	2399	b-glacio-nival	-0.33	1055.10	161.39	1145.54
2106	Birs	Münchenstein, Hofmatt	613570 / 263080	0.0	887.00	728	mixed regime (> 500km ²)	8.53	1206.82	335.73	545.50
2109	Lätschine	Gsteig	633130 / 168200	13.5	381.00	2050	a-glacio-nival	2.11	1780.73	119.63	1580.50
2110	Reuss	Mühlau, Hünenberg	672520 / 230600	2.2	2902.00	1371	mixed regime (> 500km ²)	5.42	1641.78	226.17	1399.39
2112	Sitter	Appenzell	749040 / 244220	0.1	74.40	1256	nival de transition	6.22	1896.65	345.94	1421.58
2117	Dranee de Bagnes	Le Châble, Villette	582550 / 103270	22.1	254.00	2609	b-glaciaire	-0.59	1274.15	118.82	254.59
2119	Sarine	Fribourg	579420 / 183670	0.2	1271.00	1247	mixed regime (> 500km ²)	6.35	1420.49	276.29	975.93
2122	Birse	Moutier, La Charrue	595740 / 237010	0.0	186.00	921	nivo-pluvial jurassien	7.49	1371.76	333.62	520.67

T = Temperature, P = Precipitation, E = Evaporation, Q = Streamflow/Runoff

Table B7. Characteristics of all 184 catchments in the HYD-RESPONSES dataset (Part 2/5).

Catchment	Water name	Place	Lon / Lat EPSC:21781	Glaciation %	Area km ²	Avg. Height m asl	Regime Type	Yearly Avg. T °C	Yearly P mm	Yearly E mm	Yearly Q mm
2125	Lorze	Frauenthal	674715 / 229845	0.0	262.00	678	downstream lake	8.91	1427.56	309.43	911.18
2126	Murg	Wängi	714105 / 261720	0.0	80.20	652	pluvial inférieur	8.72	1282.82	340.64	693.21
2132	Töss	Nefenbach	691460 / 263820	0.0	343.00	658	pluvial inférieur	8.89	1331.52	339.46	701.10
2135	Aare	Bern, Schönau	600710 / 198000	5.8	2941.00	1596	mixed regime (>500km ²)	4.43	1542.51	196.01	1317.74
2139	Rheinlater Binnenkanal	St. Margrethen	767160 / 257780	0.0	175.00	710	artificial waterbody	9.01	1451.16	310.08	2038.65
2141	Albula	Tiefencastel	763420 / 170145	0.5	529.00	2128	mixed regime (>500km ²)	1.53	1018.61	159.38	904.27
2143	Rhein	Rekingen	667060 / 269230	0.2	14767.00	1131	mixed regime (>500km ²)	5.83	1296.20	276.20	945.75
2150	Landquart	Felsenbach	765365 / 204910	0.7	614.00	1797	mixed regime (>500km ²)	3.34	1289.45	188.82	1203.19
2151	Simme	Oberwil	600060 / 167090	2.4	344.00	1641	nival de transition	4.52	1536.17	215.10	1084.54
2152	Reuss	Luzern, Geissmattribücke	665330 / 211800	2.8	2254.00	1504	mixed regime (>500km ²)	4.72	1683.08	207.59	1526.87
2155	Emme	Wiler, Limpachmündung, nur Hauptstation	608220 / 223240	0.0	924.00	863	mixed regime (>500km ²)	7.80	1356.58	313.03	316.15
2159	Gürbe	Belp, Mülimatt	604810 / 192680	0.0	116.00	846	pluvial supérieur	8.05	1236.50	298.87	715.53
2160	Sarine	Broc, Château d'en bas	573520 / 161345	0.3	636.00	1500	mixed regime (>500km ²)	5.12	1500.63	248.29	1014.01
2161	Massa	Blatten bei Naters	643700 / 137290	56.5	196.00	2937	a-glaciaire	-2.89	2036.03	45.98	2433.50
2167	Tresa	Ponte Tresa, Rocchetta	709580 / 92145	0.0	609.00	803	mixed regime (>500km ²)	9.59	1789.28	351.80	1107.04
2170	Arve	Genève, Bout du Monde	501220 / 115120	5.1	1973.00	1370	mixed regime (>500km ²)	5.65	1505.42	249.36	1153.49
2174	Rhône	Chancy, Aux Ripes	486600 / 112340	6.6	10308.00	1569	mixed regime (>500km ²)	4.32	1324.91	216.70	1027.76
2176	Sihl	Zürich, Sihlhölzli	682145 / 246890	0.0	343.00	1045	nivo-pluvial préalpin	6.97	1787.58	294.48	621.39
2179	Sense	Thorishaus, Sense matt	593550 / 193020	0.0	351.00	1071	nivo-pluvial préalpin	7.22	1404.55	306.68	756.67
2181	Thur	Halden	733560 / 263180	0.0	1085.00	908	mixed regime (>500km ²)	7.61	1585.63	329.74	1082.92
2185	Plessur	Chur, nur Hauptstation	757975 / 191925	0.0	264.00	1868	nival alpin	3.42	1179.00	194.41	693.27
2187	Werdenberger Binnenkanal	Salz	756795 / 234005	0.0	185.00	1003	artificial waterbody	7.74	1547.48	279.64	1344.65
2199	Wiese	Basel	611800 / 269700	0.0	442.00	720	pluvial jurassien	10.67	1508.42	342.75	800.00
2200	Weisse Lütischine	Zweilütschinen	635310 / 164550	13.1	165.00	2165	a-glacio-nival	1.58	1767.24	112.23	1531.27
2202	Ergolz	Liestal	622270 / 259750	0.0	261.00	588	pluvial jurassien	9.55	1076.57	341.74	436.87
2203	Grande Eau	Aigle	563975 / 129825	0.8	132.00	1562	nival de transition	4.96	1617.15	240.72	1082.21
2205	Aare	Untersiggenthal, Stilli	659970 / 263180	1.4	17553.00	1064	mixed regime (>500km ²)	6.99	1416.13	279.19	984.66
2206	Melera	Melera (Vallée Morobbia)	726988 / 114670	0.0	1.07	1423	nivo-pluvial méridional	5.88	1712.31	290.07	1297523.71
2210	Doubs	Ocourt	572530 / 244460	0.0	1275.00	952	mixed regime (>500km ²)	7.10	1499.13	346.76	790.06
2215	Saane	Laupen	584440 / 195300	0.1	1862.00	1137	mixed regime (>500km ²)	6.87	1373.00	288.00	866.85
2219	Simme	Oberried / Lenk	602630 / 141660	22.6	34.80	2347	b-glaciaire	0.92	1779.85	171.95	2130.36
2232	Allenbach	Adelboden	608710 / 148300	0.0	28.80	1863	nival alpin	3.64	1557.08	174.36	1332.39
2239	Spöl	Punt dal Gall	811020 / 167920	0.3	295.00	2389	nivo-glaciaire	-0.61	940.86	152.75	105.09
2243	Limmatt	Baden, Limmattpromenade	665640 / 258690	0.7	2394.00	1131	mixed regime (>500km ²)	6.59	1662.82	272.41	1311.73
2244	Krummbach	Klusmatten	644500 / 119420	0.4	19.40	2271	nival méridional	1.35	1342.63	166.60	1232.18
2247	Doubs	Sortie du lac des Bremets	544560 / 214880	0.0	867.00	977	mixed regime (>500km ²)	6.41	1548.43	350.16	635.02
2251	Rotenbach	Plaffeien, Schwyberg	587980 / 170590	0.0	1.69	1455	nival de transition	5.70	1688.19	296.97	1427822.37
2252	Rotwandlbach	Plaffeien, Schwyberg	588340 / 171015	0.0	1.38	1439	nival de transition	5.76	1662.14	296.97	832954.23
2256	Rosengbach	Pontresina	788810 / 151690	21.7	66.50	2704	a-glaciaire	-1.75	1137.41	119.24	1398.90
2262	Berninabach	Pontresina	789440 / 151320	14.4	107.00	2615	a-glacio-nival	-1.18	1203.87	131.81	1411.84
2263	Chamuerabach	La Punt-Chamues-ch	791430 / 160600	0.1	73.40	2548	nivo-glaciaire	-1.10	1011.37	145.82	930.92
2265	Inn	Tarasp	816800 / 185910	3.0	1581.00	2384	mixed regime (>500km ²)	-0.37	992.18	147.59	383.43
2268	Rhone	Gletsch	670810 / 157200	41.8	39.40	2710	a-glaciaire	-1.75	1937.62	75.90	2342.03
2269	Lonza	Blatten	629130 / 140910	24.7	77.40	2624	a-glaciaire	-1.28	1566.54	86.75	1924.12
2276	Grosstalbach	Isenthal	685500 / 196050	6.7	43.90	1819	nival alpin	3.28	1731.55	227.73	1270.99

T = Temperature, P = Precipitation, E = Evaporation, Q = Streamflow/Runoff

Table B8. Characteristics of all 184 catchments in the HYD-RESPONSES dataset (Part 3/5).

Catchment	Water name	Place	Lon / Lat EPSG:21781	Glaciation %	Area km ²	Avg. Height m asl	Regime Type	Yearly Avg. T °C	Yearly P mm	Yearly E mm	Yearly Q mm
2282	Sperbelgraben	Wisen, Kurzeneitlalp	630725 / 207270	0.0	0.56	1070	nivo-pluvial préalpin	7.06	1631.78	342.53	8833404.51
2283	Rappengraben	Wisen, Riedbad	634340 / 207350	0.0	0.60	1142	nivo-pluvial préalpin	6.87	1656.81	355.40	10647734.56
2288	Rhein	Neuhausen, Flurlingerbrücke	689145 / 281975	0.3	11930.00	1239	mixed regime (>500km ²)	4.59	1295.50	261.93	960.66
2289	Rhein	Basel, Rheinhalle	613400 / 267650	0.8	35878.00	1052	mixed regime (>500km ²)	6.78	1343.83	284.04	919.47
2290	Areuse	St-Sulpice	532980 / 195880	0.0	104.00	1110	nivo-pluvial jurassien	5.67	1500.18	344.81	1408.21
2299	Alpbach	Ersfeld, Bodenberg	688560 / 185120	19.7	20.70	2205	b-glaciaire	1.07	1669.66	171.48	2406.18
2300	Minster	Euthal, Riti	704425 / 215310	0.0	59.10	1352	nival de transition	5.53	2115.46	259.83	1639.61
2303	Thur	Jonschwil, Mühlau	723675 / 252720	0.0	493.00	1021	nivo-pluvial préalpin	6.93	1757.19	320.59	1285.82
2304	Ova dal Fuorn	Zemez, Punt la Drossa	810560 / 170790	0.0	55.30	2327	nival alpin	-0.46	937.69	150.89	586.32
2305	Glatt	Herisau, Zellersmühle	737270 / 251290	0.0	16.70	829	pluvial supérieur	8.18	1491.95	329.49	1063.60
2307	Suze	Sonceboz	579810 / 227350	0.0	127.00	1036	nivo-pluvial jurassien	6.97	1332.88	340.21	1008.10
2308	Goldach	Goldach, Bleiche, nur Hauptstation	753190 / 261590	0.0	50.40	832	pluvial supérieur	8.33	1423.14	317.59	853.11
2312	Aach	Salmisach, Hungerbühl	744410 / 268400	0.0	47.40	467	pluvial inférieur	9.68	1019.41	335.09	488.00
2319	Ova da Cluozza	Zemez	804930 / 174830	0.0	27.00	2371	nivo-glaciaire	-0.47	919.61	150.80	888.70
2321	Cassarate	Pregassona	718010 / 97380	0.0	75.80	987	pluvio-nival méridional	8.52	1900.06	330.75	983.33
2327	Dischmabach	Davos, Kriegsmatte	786220 / 183370	0.7	42.90	2376	b-glacio-nival	0.15	1015.77	147.17	1242.21
2342	Salfina	Brig	642220 / 129630	2.5	76.50	2014	nivo-glaciaire	2.53	1165.38	167.60	948.67
2343	Langete	Huttwil, Häberenhud	629560 / 219135	0.0	59.90	760	pluvial inférieur	8.14	1276.02	329.38	618.66
2346	Rhone	Brig	641340 / 129700	19.2	906.00	2339	mixed regime (>500km ²)	0.31	1630.34	103.68	1481.12
2347	Riale di Roggiasca	Roveredo, Bacino di compenso	733545 / 118160	0.0	8.12	1702	nivo-pluvial méridional	4.11	1684.56	288.12	1869.20
2349	Breggia	Chiasso, Ponte di Polenta	722315 / 78320	0.0	47.10	933	pluvio-nival méridional	8.58	1726.83	382.64	712.61
2351	Vispa	Visp	634050 / 125900	23.1	786.00	2648	mixed regime (>500km ²)	-0.92	1125.42	116.03	684.02
2352	Linh	Linhthal, Ausgleichsbecken KLL., nur Haupt	718285 / 197310	9.4	147.00	2085	a-glacio-nival	1.83	1874.45	169.98	925.43
2355	Landwasser	Davos, Frauenkirch	779640 / 181200	0.3	184.00	2224	nivo-glaciaire	0.97	1063.29	151.03	926.33
2356	Riale di Calneggia	Cavigorno, Pontit	684970 / 135960	0.0	23.90	2003	nival méridional	3.08	1868.56	188.46	1922.63
2364	Ticino	Protta	694610 / 152450	0.3	159.00	2071	nival méridional	2.16	1803.44	136.09	413.29
2366	Poschiavino	La Rôsa	802120 / 142010	0.0	14.10	2285	nival méridional	0.86	1398.05	162.22	1189.26
2368	Muggia	Locarno, Soldano	703100 / 113860	0.3	927.00	1530	mixed regime (>500km ²)	5.63	1946.42	245.77	783.83
2369	Mentue	Yvonand, La Mauguettaz	545440 / 180875	0.0	105.00	675	pluvial jurassien	9.35	1081.13	328.32	457.37
2370	Doubs	Le Noirmont, La Goule	561430 / 231050	0.0	1047.00	977	mixed regime (>500km ²)	6.69	1534.75	348.30	795.29
2371	Orbe	Le Chent, Frontière	501445 / 156305	0.0	45.90	1235	nivo-pluvial jurassien	6.42	1901.34	337.96	615.79
2372	Linh	Mollis, Linthbrücke	723985 / 217965	2.9	600.00	1743	mixed regime (>500km ²)	3.49	1848.95	197.67	1687.89
2374	Necker	Mogelsberg, Aachsäge	727110 / 247290	0.0	88.10	956	nivo-pluvial préalpin	7.27	1718.29	338.15	1142.38
2378	Orbe	Orbe, Le Chalet	530080 / 175560	0.0	343.00	1139	nivo-pluvial jurassien	6.73	1692.73	341.81	1016.62
2386	Murg	Frauentfeld	709540 / 269660	0.0	213.00	597	pluvial inférieur	8.98	1178.35	343.21	567.47
2387	Hinterhein	Fürstenuw	753570 / 175730	0.6	1577.00	2127	mixed regime (>500km ²)	1.47	1147.93	165.74	767.37
2403	Inn	Cinuos-chel, nur Hauptstation	797700 / 168170	5.2	733.00	2456	mixed regime (>500km ²)	-0.66	1007.10	146.31	212.71
2409	Emme	Eggwil, Heidbüel	627910 / 191180	0.0	124.00	1281	nivo-pluvial préalpin	6.10	1604.24	270.21	1061.40
2410	Liechtensteiner Binnenkanal	Ruggell	757750 / 234590	0.0	116.00	853	artificial waterbody	8.58	1286.29	264.96	1321.13
2412	Stonge	Vuippens, Château	572420 / 167540	0.0	43.40	865	nivo-pluvial préalpin	8.10	1298.00	302.73	802.84
2414	Rieholzbach	Mosnang, Rietholz	718840 / 248440	0.0	3.19	794	pluvial supérieur	8.13	1476.78	336.69	1006909.39
2415	Glatt	Rheinsfelden	678040 / 269720	0.0	417.00	503	downstream lake	9.70	1165.36	340.63	590.10
2416	Aabach	Hitzkirch, Richensee	661390 / 230220	0.0	73.30	581	downstream lake	9.46	1163.00	317.37	535.90
2417	Suhre	Oberkirch	651320 / 223140	0.0	75.60	583	downstream lake	9.39	1139.68	312.72	510.78
2418	Julia	Tiefencastel	765570 / 169910	0.2	325.00	2196	nivo-glaciaire	1.10	1058.77	161.39	97.09
2419	Rhone	Reckingen	661910 / 146780	11.8	214.00	2305	a-glacio-nival	0.30	1814.00	105.51	1424.61
2420	Moesa	Lumino, Sassello	724765 / 120360	0.1	472.00	1667	nivo-pluvial méridional	3.98	1619.63	234.73	1339.42

T = Temperature, P = Precipitation, E = Evaporation, Q = Streamflow/Runoff

Table B9. Characteristics of all 184 catchments in the HYD-RESPONSES dataset (Part 4/5).

Catchment	Water name	Place	Lon / Lat EPSG:21781	Glaciation %	Area km ²	Avg. Height m asl	Regime Type	Yearly Avg. T °C	Yearly P mm	Yearly E mm	Yearly Q mm
2426	Seez	Mels	750410/212510	0.1	106.00	1803	nival alpin	3.55	1578.39	217.42	640.88
2430	Rein da Sumvltg	Sumvltg, Encardens	718810/167690	1.7	21.80	2457	b-glacio-nival	-0.15	1581.92	160.82	2183.90
2432	Venoge	Ecublens, Les Bois	532040/154160	0.0	228.00	686	nivo-pluvial jurassien	9.62	1148.17	332.99	539.44
2433	Aubonne	Allaman, Le Coulet	520720/147410	0.0	105.00	952	nivo-pluvial jurassien	8.21	1444.62	340.37	1587.98
2434	Dünern	Oltén, Hammermühle	634330/244480	0.0	234.00	711	pluvial jurassien	8.50	1210.83	334.79	437.11
2436	Chli Schliere	Alpnach, Chlich Erti	663800/199570	0.0	21.60	1345	nivo-pluvial préalpin	5.96	1876.39	271.62	966.44
2437	Parimbot	Ecublens, Eschiens	552060/161650	0.0	6.92	716	pluvial jurassien	9.50	1182.10	311.77	717260.34
2450	Wigger	Zofingen	637580/237080	0.0	366.00	656	pluvial inférieur	8.80	1182.26	328.47	461.60
2457	Aare	Ringenberg, Goldswil	633730/171510	12.1	1138.00	1951	mixed regime (>500km ²)	2.47	1761.77	138.78	1715.63
2458	Seyon	Valangin	559370/206810	0.0	112.00	978	nivo-pluvial jurassien	7.54	1292.29	350.00	214.91
2461	Magliasina	Magliaso, Ponte	711620/93290	0.0	34.40	926	pluvio-nival méridional	8.91	1938.53	357.01	1117.90
2468	Sitter	St. Gallen, Bruggen/Au	742540/253230	0.0	261.00	1042	nivo-pluvial préalpin	7.22	1722.67	343.20	1208.91
2471	Murg	Murgenthal, Walliswil	629340/233555	0.0	183.00	653	pluvial inférieur	8.60	1191.59	333.34	556.21
2473	Rhein	Diepoldsau, Rietbrücke	766280/250360	0.6	6299.00	1771	mixed regime (>500km ²)	3.17	1327.19	193.52	1163.69
2474	Calanca	Buseno	729440/127180	0.2	121.00	1931	nival méridional	2.65	1673.78	227.69	1113.07
2475	Maggia	Bignasco, Ponte nuovo	690040/132550	0.9	316.00	1879	nival méridional	3.67	1939.62	187.23	415.67
2477	Lotze	Zug, Letzi	680600/226070	0.0	100.00	818	downstream lake	8.15	1560.20	295.43	925.59
2478	Birse	Soyhières, Bois du Treuil	596780/249070	0.0	569.00	805	nivo-pluvial jurassien	8.06	1265.37	334.76	580.60
2480	Areuse	Boudry	554350/199940	0.0	378.00	1077	nivo-pluvial jurassien	6.27	1464.77	347.62	906.66
2481	Engelberger Aa	Buochs, Flugplatz	673555/202870	2.5	228.00	1609	b-glacio-nival	4.30	1693.58	196.94	1705.73
2485	Allaine	Boncourt, Frontière	567830/261200	0.0	212.00	562	pluvial jurassien	9.54	1108.82	343.10	464.95
2486	Veveyse	Vevey, Copet	554675/146565	0.0	64.50	1098	nivo-pluvial préalpin	7.37	1497.99	307.89	955.88
2487	Kleine Emme	Werthenstein, Chappelboden	647870/209510	0.0	311.00	1167	nivo-pluvial préalpin	6.61	1695.60	279.00	1095.28
2488	Simme	Latterbach	610680/167840	1.5	563.00	1594	nival de transition	4.79	1506.56	225.96	342.76
2490	Allondon	Dardagny, Les Granges	488880/119460	0.0	119.00	760	nivo-pluvial jurassien	10.64	1372.60	326.46	854.70
2491	Schächen	Bürglen, Galgenwäldli, nur Hauptstation	692480/191800	1.5	108.00	1728	nivo-glaciaire	3.55	1854.00	188.20	1397.24
2493	Promenthouse	Gland, Route Suisse	510080/140080	0.0	120.00	1027	nivo-pluvial jurassien	7.73	1577.83	338.92	430.80
2494	Ticino	Pollegio, Campagna	716120/135330	0.2	444.00	1796	nival méridional	3.85	1710.59	173.72	1438.77
2497	Luthem	Nebikon	640560/226740	0.0	105.00	749	pluvial inférieur	8.31	1268.69	334.87	429.99
2498	Glener	Castrisch	735330/181790	1.1	381.00	2022	nivo-glaciaire	2.11	1307.02	168.97	734.66
2500	Worble	Ittigen	603005/202455	0.0	67.10	666	pluvial inférieur	8.72	1174.24	317.69	475.10
2602	Rhein	Domat/Ems	753890/189370	0.9	3229.00	2013	mixed regime (>500km ²)	2.19	1277.76	168.28	1122.84
2603	Ilfis	Langnau	627320/198600	0.0	187.00	1039	nivo-pluvial préalpin	7.05	1619.21	318.70	882.14
2604	Biber	Biberbrugg	697240/223280	0.0	31.90	1003	nivo-pluvial préalpin	7.00	1789.15	287.37	1085.77
2605	Verzasca	Lavertezzo, Campiöi	708420/122920	0.0	185.00	1651	nivo-pluvial méridional	5.11	2013.18	260.43	1846.37
2606	Rhône	Genève, Halle de l'Île	499890/117850	7.2	8000.00	1658	mixed regime (>500km ²)	4.08	1286.36	204.12	996.79
2607	Goneri	Oberwald	670467/153932	4.0	38.50	2383	b-glacio-nival	0.07	1976.16	121.82	2011.50
2608	Sellenbodenbach	Neuenkirch	658530/218290	0.0	10.40	608	pluvial inférieur	9.33	1193.97	305.25	637.12

T = Temperature, P = Precipitation, E = Evaporation, Q = Streamflow/Runoff

Table B10. Characteristics of all 184 catchments in the HYD-RESPONSES dataset (Part 5/5).

Catchment	Water name	Place	Lon / Lat EPSG:21781	Glaciation %	Area km ²	Avg. Height m asl	Regime Type	Yearly Avg. T °C	Yearly P mm	Yearly E mm	Yearly Q mm
2609	Alp	Einsiedeln	698640 / 223020	0.0	46.70	1157	nivo-pluvial préalpin	6.35	1939.89	279.80	1459.07
2610	Scheulte	Vicques	599485 / 244150	0.0	72.70	792	nivo-pluvial jurassien	8.20	1260.81	333.18	635.64
2612	Riale di Pincascia	Lavertezzo	708060 / 123950	0.0	44.50	1705	nivo-pluvial méridional	4.89	1978.57	277.65	1911.93
2617	Rom	Müstair	830800 / 168700	0.0	128.00	2184	nival alpin	1.03	844.68	158.63	577.25
2620	Mera	Soglio	760770 / 133450	7.4	177.00	2173	b-glacio-nival	0.95	1333.42	191.09	361.81
2629	Vedeggio	Agno, stazione principale	714110 / 95680	0.0	99.90	921	pluvio-nival méridional	8.87	1904.96	334.27	656.21
2630	Sionne	Sion	594400 / 119900	0.0	27.60	1577	nival alpin	5.35	1355.03	186.55	224.58
2631	Hinterrhein	Hinterrhein, Schiessplatz	733706 / 153945	9.1	41.50	2430	a-glacio-nival	-0.38	1704.08	164.40	799.71
2634	Kleine Emme	Emmen	663700 / 213630	0.0	478.00	1054	nivo-pluvial préalpin	7.15	1610.61	284.17	994.18
2635	Grossbach	Einsiedeln, Gross	700710 / 218125	0.0	8.95	1283	nivo-pluvial préalpin	5.90	1952.69	299.45	1387.71
2640	Some	Delémont, Pré-Guillaume	593380 / 245940	0.0	214.00	779	nivo-pluvial jurassien	8.20	1233.60	335.80	603.72
2646	Kander	Emdthal	617790 / 168400	5.1	487.00	1860	b-glacio-nival	3.38	1486.71	167.85	1305.44

T = Temperature, P = Precipitation, E = Evaporation, Q = Streamflow/Runoff

References

- An, H., Ouyang, C., and Chen, X.: Real-time estimation of SMAP soil moisture in mountainous areas and its impact on rainfall-runoff simulation, *Journal of Hydrology*, 660, 133 487, <https://doi.org/10.1016/j.jhydrol.2025.133487>, 2025.
- 1010 Anderson, M. C., Kustas, W. P., Norman, J. M., Diak, G. T., Hain, C. R., Gao, F., Yang, Y., Knipper, K. R., Xue, J., Yang, Y., Crow, W. T., Holmes, T. R. H., Nieto, H., Guzinski, R., Otkin, J. A., Mecikalski, J. R., Cammalleri, C., Torres-Rua, A. T., Zhan, X., Fang, L., Colaizzi, P. D., and Agam, N.: A brief history of the thermal IR-based Two-Source Energy Balance (TSEB) model – diagnosing evapotranspiration from plant to global scales, *Agricultural and Forest Meteorology*, 350, 109 951, <https://doi.org/10.1016/j.agrformet.2024.109951>, 2024.
- Apurv, T. and Cai, X.: Drought Propagation in Contiguous U.S. Watersheds: A Process-Based Understanding of the Role of Climate and Watershed Properties, *Water Resources Research*, 56, e2020WR027 755, <https://doi.org/10.1029/2020WR027755>, [_eprint: https://onlinelibrary.wiley.com/doi/pdf/10.1029/2020WR027755](https://onlinelibrary.wiley.com/doi/pdf/10.1029/2020WR027755), 2020.
- 1015 Apurv, T., Sivapalan, M., and Cai, X.: Understanding the Role of Climate Characteristics in Drought Propagation, *Water Resources Research*, 53, 9304–9329, <https://doi.org/10.1002/2017WR021445>, [_eprint: https://onlinelibrary.wiley.com/doi/pdf/10.1002/2017WR021445](https://onlinelibrary.wiley.com/doi/pdf/10.1002/2017WR021445), 2017.
- Aschwanden, H.: Die Niedrigwasserabflussmenge Q347 – Bestimmung und Abschätzung in alpinen schweizerischen Einzugsgebieten., Tech. Rep. 18, Bern, 1992.
- 1020 Aschwanden, H. and Kan, C.: Die Abflussmenge Q347 – eine Standortbestimmung., Tech. Rep. 27, Bern, 1999.
- Aschwanden, H. and Weingartner, R.: Die Abflussregimes der Schweiz., Tech. Rep. 65, Geographisches Institut der Universität Bern (GIUB), Bern, <https://boris.unibe.ch/133660/>, 1985.
- Avanzi, F., Munerol, F., Milelli, M., Gabellani, S., Massari, C., Giroto, M., Cremonese, E., Galvagno, M., Bruno, G., Morra di Cella, U., Rossi, L., Altamura, M., and Ferraris, L.: Winter snow deficit was a harbinger of summer 2022 socio-hydrologic drought in the Po Basin, Italy, *Commun Earth Environ*, 5, 1–12, <https://doi.org/10.1038/s43247-024-01222-z>, publisher: Nature Publishing Group, 2024.
- 1025 Bachmair, S., Stahl, K., Collins, K., Hannaford, J., Acreman, M., Svoboda, M., Knutson, C., Smith, K. H., Wall, N., Fuchs, B., Crossman, N. D., and Overton, I. C.: Drought indicators revisited: the need for a wider consideration of environment and society, *WIREs Water*, 3, 516–536, <https://doi.org/10.1002/wat2.1154>, [_eprint: https://onlinelibrary.wiley.com/doi/pdf/10.1002/wat2.1154](https://onlinelibrary.wiley.com/doi/pdf/10.1002/wat2.1154), 2016.
- 1030 Bachmair, S., Tanguy, M., Hannaford, J., and Stahl, K.: How well do meteorological indicators represent agricultural and forest drought across Europe?, *Environ. Res. Lett.*, 13, 034 042, <https://doi.org/10.1088/1748-9326/aaafda>, publisher: IOP Publishing, 2018.
- Baez-Villanueva, O. M., Zambrano-Bigiarini, M., Miralles, D. G., Beck, H. E., Siegmund, J. F., Alvarez-Garreton, C., Verbist, K., Garreaud, R., Boisier, J. P., and Galleguillos, M.: On the timescale of drought indices for monitoring streamflow drought considering catchment hydrological regimes, *Hydrology and Earth System Sciences*, 28, 1415–1439, <https://doi.org/10.5194/hess-28-1415-2024>, publisher: Copernicus GmbH, 2024.
- 1035 BAFU: Hitze und Trockenheit im Sommer 2015. Auswirkungen auf Mensch und Umwelt. Bundesamt für Umwelt BAFU, Bern. Umwelt-Zustand Nr. 1629: 108 S., Tech. rep., 2016.
- BAFU: Nationale Grundwasserbeobachtung NAQUA, <https://www.bafu.admin.ch/bafu/de/home/themen/thema-wasser/wasser-fachinformationen/zustand-der-gewaesser/zustand-des-grundwassers/nationale-grundwasserbeobachtung-naqua.html>, 2019.
- 1040 BAFU: Trockenheit: Bundesrat will nationales System zur Früherkennung und Warnung, <https://www.bafu.admin.ch/bafu/de/home/dokumentation/medienmitteilungen/anzeige-nsb-unter-medienmitteilungen.msg-id-88854.html>, 2022.
- BAFU: Nationale Beobachtung Oberflächengewässerqualität (NAWA), <https://www.bafu.admin.ch/bafu/de/home/themen/thema-wasser/wasser-daten-indikatoren-und-karten/wasser-messnetze/nationale-beobachtung-oberflaechengewaesserqualitaet--nawa-.html>, 2023.

- BAFU: Stationsbericht Niedrigwasserstatistik - Leitfaden, <https://www.bafu.admin.ch/dam/bafu/de/dokumente/hydrologie/fachinfo-daten/leitfaden-stationsberichte-niedrigwasserstatistik-bafu.pdf.download.pdf/leitfaden-stationsberichte-niedrigwasserstatistik-bafu.pdf>, 2024.
- 1045 BAFU: Der kombinierte Trockenheitsindex - Nationale Trockenheitsplattform, <https://www.trockenheit.admin.ch/de/trockenheit/trockenheitsindex>, 2025.
- BAFU (Eds.): Auswirkungen des Klimawandels auf die Schweizer Gewässer. Hydrologie, Gewässerökologie und Wasserwirtschaft. Bundesamt für Umwelt BAFU, Bern. Umwelt-Wissen Nr. 2101: 134 S., Tech. rep., 2021.
- 1050 BAFU (Eds.): Die biogeographischen Regionen der Schweiz. 1. aktualisierte Auflage 2022. Erstausgabe 2001. Bundesamt für Umwelt, Bern, Umwelt-Wissen Nr. 2214: p.28, Tech. rep., Bundesamt für Umwelt, https://www.bafu.admin.ch/dam/bafu/de/dokumente/landschaft/uw-umwelt-wissen/die_biogeographischenregionenderschweiz.pdf.download.pdf/die_biogeographischenregionenderschweiz.pdf, 2022.
- BAFU (Eds.): Hydrologisches Jahrbuch der Schweiz 2022. Abfluss, Wasserstand und Wasserqualität der Schweizer Gewässer., Tech. rep., Bundesamt für Umwelt, Ittigen, Bern, https://www.bafu.admin.ch/dam/bafu/de/dokumente/hydrologie/uz-umwelt-zustand/hydrologisches-jahrbuch-2022.pdf.download.pdf/de_BAFU_UZ_2215_Hydrologisches_Jahrbuch_2022_bf.pdf, 2023.
- 1055 BAFU et al. (Eds.): Hitze und Trockenheit im Sommer 2018. Auswirkungen auf Mensch und Umwelt. Bundesamt für Umwelt, Bern. Umwelt-Zustand Nr. 1909: 91 S., Tech. rep., 2019.
- Bai, J. and Perron, P.: Estimating and Testing Linear Models with Multiple Structural Changes, *Econometrica*, 66, 47–78, <https://doi.org/10.2307/2998540>, publisher: [Wiley, Econometric Society], 1998.
- 1060 Baker, D. B., Richards, R. P., Loftus, T. T., and Kramer, J. W.: A New Flashiness Index: Characteristics and Applications to Midwestern Rivers and Streams, *JAWRA Journal of the American Water Resources Association*, 40, 503–522, <https://doi.org/10.1111/j.1752-1688.2004.tb01046.x>, <https://onlinelibrary.wiley.com/doi/pdf/10.1111/j.1752-1688.2004.tb01046.x>, 2004.
- Barker, L. J., Hannaford, J., Chiverton, A., and Svensson, C.: From meteorological to hydrological drought using standardised indicators, *Hydrology and Earth System Sciences*, 20, 2483–2505, <https://doi.org/10.5194/hess-20-2483-2016>, publisher: Copernicus GmbH, 2016.
- 1065 Baston, D.: exactextractr: Fast Extraction from Raster Datasets using Polygons. R package version 0.10.0, <https://cran.r-project.org/web/packages/exactextractr/index.html>, 2023.
- Besso, H., Shean, D., and Lundquist, J. D.: Mountain snow depth retrievals from customized processing of ICESat-2 satellite laser altimetry, *Remote Sensing of Environment*, 300, 113 843, <https://doi.org/10.1016/j.rse.2023.113843>, 2024.
- Bevacqua, E., De Michele, C., Manning, C., Couasnon, A., Ribeiro, A. F. S., Ramos, A. M., Vignotto, E., Bastos, A., Blesić, S., Durante, F., Hillier, J., Oliveira, S. C., Pinto, J. G., Ragno, E., Rivoire, P., Saunders, K., van der Wiel, K., Wu, W., Zhang, T., and Zscheischler, J.: Guidelines for Studying Diverse Types of Compound Weather and Climate Events, *Earth’s Future*, 9, e2021EF002 340, <https://doi.org/10.1029/2021EF002340>, <https://onlinelibrary.wiley.com/doi/pdf/10.1029/2021EF002340>, 2021.
- Biegel, S., Schindler, K., and Stocker, B. D.: Unrecognised water limitation is a main source of uncertainty for models of terrestrial photosynthesis, *Biogeosciences*, 22, 7455–7481, <https://doi.org/10.5194/bg-22-7455-2025>, publisher: Copernicus GmbH, 2025.
- 1075 Bloomfield, J. P., Gong, M., Marchant, B. P., Coxon, G., and Addor, N.: How is Baseflow Index (BFI) impacted by water resource management practices?, *Hydrology and Earth System Sciences*, 25, 5355–5379, <https://doi.org/10.5194/hess-25-5355-2021>, publisher: Copernicus GmbH, 2021.
- BLW, B. f. L.: Bodeneignungskarte der Schweiz, <https://www.blw.admin.ch/blw/de/home/politik/datenmanagement/geografisches-informationssystem-gis/bodeneignungskarte.html>, 2022.
- 1080 Brocca, L., Barbetta, S., Camici, S., Ciabatta, L., Dari, J., Filippucci, P., Massari, C., Modanesi, S., Tarpanelli, A., Bonaccorsi, B., Mosaffa, H., Wagner, W., Vreugdenhil, M., Quast, R., Alfieri, L., Gabellani, S., Avanzi, F., Rains, D., Miralles, D. G., Mantovani, S., Briese, C.,

- Domeneghetti, A., Jacob, A., Castelli, M., Camps-Valls, G., Volden, E., and Fernandez, D.: A Digital Twin of the terrestrial water cycle: a glimpse into the future through high-resolution Earth observations, *Front. Sci.*, 1, <https://doi.org/10.3389/fsci.2023.1190191>, publisher: Frontiers, 2024a.
- 1085 Brocca, L., Gaona, J., Bavera, D., Fioravanti, G., Puca, S., Ciabatta, L., Filippucci, P., Mosaffa, H., Esposito, G., Roberto, N., Dari, J., Vreugdenhil, M., and Wagner, W.: Exploring the actual spatial resolution of 1 km satellite soil moisture products, *Science of The Total Environment*, 945, 174 087, <https://doi.org/10.1016/j.scitotenv.2024.174087>, 2024b.
- Brunner, M. I. and Chartier-Rescan, C.: Drought Spatial Extent and Dependence Increase During Drought Propagation From the Atmosphere to the Hydrosphere, *Geophysical Research Letters*, 51, e2023GL107 918, <https://doi.org/10.1029/2023GL107918>, [_eprint: https://onlinelibrary.wiley.com/doi/pdf/10.1029/2023GL107918](https://onlinelibrary.wiley.com/doi/pdf/10.1029/2023GL107918), 2024.
- 1090 Brunner, M. I., Björnson Gurung, A., Zappa, M., Zekollari, H., Farinotti, D., and Stähli, M.: Present and future water scarcity in Switzerland: Potential for alleviation through reservoirs and lakes, *Science of The Total Environment*, 666, 1033–1047, <https://doi.org/10.1016/j.scitotenv.2019.02.169>, 2019a.
- Brunner, M. I., Farinotti, D., Zekollari, H., Huss, M., and Zappa, M.: Future shifts in extreme flow regimes in Alpine regions, *Hydrology and Earth System Sciences*, 23, 4471–4489, <https://doi.org/10.5194/hess-23-4471-2019>, publisher: Copernicus GmbH, 2019b.
- 1095 Brunner, M. I., Liechti, K., and Zappa, M.: Extremeness of recent drought events in Switzerland: dependence on variable and return period choice, *Natural Hazards and Earth System Sciences*, 19, 2311–2323, <https://doi.org/10.5194/nhess-19-2311-2019>, publisher: Copernicus GmbH, 2019c.
- Brunner, M. I., Slater, L., Tallaksen, L. M., and Clark, M.: Challenges in modeling and predicting floods and droughts: A review, *WIREs Water*, 8, e1520, <https://doi.org/10.1002/wat2.1520>, [_eprint: https://onlinelibrary.wiley.com/doi/pdf/10.1002/wat2.1520](https://onlinelibrary.wiley.com/doi/pdf/10.1002/wat2.1520), 2021.
- 1100 Brunner, M. I., Van Loon, A. F., and Stahl, K.: Moderate and Severe Hydrological Droughts in Europe Differ in Their Hydrometeorological Drivers, *Water Resources Research*, 58, e2022WR032 871, <https://doi.org/10.1029/2022WR032871>, [_eprint: https://onlinelibrary.wiley.com/doi/pdf/10.1029/2022WR032871](https://onlinelibrary.wiley.com/doi/pdf/10.1029/2022WR032871), 2022.
- Brunner, M. I., Götte, J., Schlemper, C., and Van Loon, A. F.: Hydrological Drought Generation Processes and Severity Are Changing in the Alps, *Geophysical Research Letters*, 50, e2022GL101 776, <https://doi.org/10.1029/2022GL101776>, [_eprint: https://onlinelibrary.wiley.com/doi/pdf/10.1029/2022GL101776](https://onlinelibrary.wiley.com/doi/pdf/10.1029/2022GL101776), 2023.
- 1105 BUWAL, BWG, MeteoSchweiz: Auswirkungen des Hitzesommers 2003 auf die Gewässer. Schriftenreihe Umwelt Nr. 369. Bern: Bundesamt für Umwelt, Wald und Landschaft, 174 S., Tech. rep., 2004.
- Calanca, P.: Climate change and drought occurrence in the Alpine region: How severe are becoming the extremes?, *Global and Planetary Change*, 57, 151–160, <https://doi.org/10.1016/j.gloplacha.2006.11.001>, 2007.
- 1110 Cammalleri, C., Barbosa, P., and Vogt, J. V.: Analysing the Relationship between Multiple-Timescale SPI and GRACE Terrestrial Water Storage in the Framework of Drought Monitoring, *Water*, 11, 1672, <https://doi.org/10.3390/w11081672>, number: 8 Publisher: Multidisciplinary Digital Publishing Institute, 2019.
- CH2018: CH2018 – Climate Scenarios for Switzerland, Technical Report, National Centre for Climate Services, Zurich, 271 pp. ISBN: 978-3-9525031-4-0., Tech. rep., 2018.
- 1115 Clerc-Schwarzenbach, F., Selleri, G., Neri, M., Toth, E., van Meerveld, I., and Seibert, J.: Large-sample hydrology – a few camels or a whole caravan?, *Hydrology and Earth System Sciences*, 28, 4219–4237, <https://doi.org/10.5194/hess-28-4219-2024>, publisher: Copernicus GmbH, 2024.

- Cui, G., Ma, Q., and Bales, R.: Assessing multi-year-drought vulnerability in dense Mediterranean-climate forests using water-balance-based indicators, *Journal of Hydrology*, 606, 127 431, <https://doi.org/10.1016/j.jhydrol.2022.127431>, 2022.
- Dalla Torre, D., Di Marco, N., Menapace, A., Avesani, D., Righetti, M., and Majone, B.: Suitability of ERA5-Land re-analysis dataset for hydrological modelling in the Alpine region, *Journal of Hydrology: Regional Studies*, 52, 101 718, <https://doi.org/10.1016/j.ejrh.2024.101718>, 2024.
- Das, B. C., Islam, A., and Sarkar, B.: Drainage Basin Shape Indices to Understanding Channel Hydraulics, *Water Resour Manage*, 36, 2523–2547, <https://doi.org/10.1007/s11269-022-03121-4>, 2022.
- de Jager, A., Corbane, C., and Szabo, F.: Recent Developments in Some Long-Term Drought Drivers, *Climate*, 10, 31, <https://doi.org/10.3390/cli10030031>, number: 3 Publisher: Multidisciplinary Digital Publishing Institute, 2022.
- Ding, Y., Gong, X., Xing, Z., Cai, H., Zhou, Z., Zhang, D., Sun, P., and Shi, H.: Attribution of meteorological, hydrological and agricultural drought propagation in different climatic regions of China, *Agricultural Water Management*, 255, 106 996, <https://doi.org/10.1016/j.agwat.2021.106996>, 2021.
- Dingman, S. L.: Drainage density and streamflow: A closer look, *Water Resources Research*, 14, 1183–1187, <https://doi.org/10.1029/WR014i006p01183>, _eprint: <https://onlinelibrary.wiley.com/doi/pdf/10.1029/WR014i006p01183>, 1978.
- Eekhout, J. P. C., Hunink, J. E., Terink, W., and de Vente, J.: Why increased extreme precipitation under climate change negatively affects water security, *Hydrology and Earth System Sciences*, 22, 5935–5946, <https://doi.org/10.5194/hess-22-5935-2018>, publisher: Copernicus GmbH, 2018.
- European Commission: Standardized Precipitation Index (SPI). EDO Indicator Factsheet. European Drought Observatory (EDO)., https://edo.jrc.ec.europa.eu/documents/factsheets/factsheet_spi.pdf, 2020.
- Floriancic, M. G., Berghuijs, W. R., Jonas, T., Kirchner, J. W., and Molnar, P.: Effects of climate anomalies on warm-season low flows in Switzerland, *Hydrology and Earth System Sciences*, 24, 5423–5438, <https://doi.org/10.5194/hess-24-5423-2020>, publisher: Copernicus GmbH, 2020.
- Floriancic, M. G., Spies, D., van Meerveld, I. H. J., and Molnar, P.: A multi-scale study of the dominant catchment characteristics impacting low-flow metrics, *Hydrological Processes*, 36, e14 462, <https://doi.org/10.1002/hyp.14462>, _eprint: <https://onlinelibrary.wiley.com/doi/pdf/10.1002/hyp.14462>, 2022.
- Fluhrer, A., Baur, M. J., Piles, M., Bayat, B., Rahmati, M., Chaparro, D., Dubois, C., Hellwig, F. M., Montzka, C., Kübert, A., Mueller, M. M., Augscheller, I., Jonard, F., Schellenberg, K., and Jagdhuber, T.: Assessing evapotranspiration dynamics across central Europe in the context of land–atmosphere drivers, *Biogeosciences*, 22, 3721–3746, <https://doi.org/10.5194/bg-22-3721-2025>, publisher: Copernicus GmbH, 2025.
- Fowler, K., Peel, M., Saft, M., Nathan, R., Horne, A., Wilby, R., McCutcheon, C., and Peterson, T.: Hydrological Shifts Threaten Water Resources, *Water Resources Research*, 58, e2021WR031 210, <https://doi.org/10.1029/2021WR031210>, _eprint: <https://onlinelibrary.wiley.com/doi/pdf/10.1029/2021WR031210>, 2022.
- Frei, C.: Interpolation of temperature in a mountainous region using nonlinear profiles and non-Euclidean distances, *International Journal of Climatology*, 34, 1585–1605, <https://doi.org/10.1002/joc.3786>, _eprint: <https://onlinelibrary.wiley.com/doi/pdf/10.1002/joc.3786>, 2014.
- Frei, C. and Schär, C.: A precipitation climatology of the Alps from high-resolution rain-gauge observations, *International Journal of Climatology*, 18, 873–900, [https://doi.org/10.1002/\(SICI\)1097-0088\(19980630\)18:8<873::AID-JOC255>3.0.CO;2-9](https://doi.org/10.1002/(SICI)1097-0088(19980630)18:8<873::AID-JOC255>3.0.CO;2-9), _eprint: <https://onlinelibrary.wiley.com/doi/pdf/10.1002/%28SICI%291097-0088%2819980630%2918%3A8%3C873%3A%3AAID-JOC255%3E3.0.CO%3B2-9>, 1998.

- Gebrechorkos, S. H., Sheffield, J., Vicente-Serrano, S. M., Funk, C., Miralles, D. G., Peng, J., Dyer, E., Talib, J., Beck, H. E., Singer, M. B., and Dadson, S. J.: Warming accelerates global drought severity, *Nature*, 642, 628–635, <https://doi.org/10.1038/s41586-025-09047-2>, publisher: Nature Publishing Group, 2025.
- 1160 Gudmundsson, L. and Stagge, J. H.: SCI: Standardized Climate Indices such as SPI, SRI or SPEIR package version 1.0-2., 2016.
- Guo, Y., Zhang, Y., Zhang, L., and Wang, Z.: Regionalization of hydrological modeling for predicting streamflow in ungauged catchments: A comprehensive review, *WIREs Water*, 8, e1487, <https://doi.org/10.1002/wat2.1487>, _eprint: <https://onlinelibrary.wiley.com/doi/pdf/10.1002/wat2.1487>, 2021.
- Haile, G. G., Tang, Q., Li, W., Liu, X., and Zhang, X.: Drought: Progress in broadening its understanding, *WIREs Water*, 7, e1407, <https://doi.org/10.1002/wat2.1407>, _eprint: <https://onlinelibrary.wiley.com/doi/pdf/10.1002/wat2.1407>, 2020.
- 1165 Hammond, J. C., Simeone, C., Hecht, J. S., Hodgkins, G. A., Lombard, M., McCabe, G., Wolock, D., Wiczorek, M., Olson, C., Caldwell, T., Dudley, R., and Price, A. N.: Going Beyond Low Flows: Streamflow Drought Deficit and Duration Illuminate Distinct Spatiotemporal Drought Patterns and Trends in the U.S. During the Last Century, *Water Resources Research*, 58, e2022WR031930, <https://doi.org/10.1029/2022WR031930>, _eprint: <https://onlinelibrary.wiley.com/doi/pdf/10.1029/2022WR031930>, 2022.
- 1170 Hao, Z. and Singh, V. P.: Drought characterization from a multivariate perspective: A review, *Journal of Hydrology*, 527, 668–678, <https://doi.org/10.1016/j.jhydrol.2015.05.031>, 2015.
- Haslinger, K., Koffler, D., Schöner, W., and Laaha, G.: Exploring the link between meteorological drought and streamflow: Effects of climate-catchment interaction, *Water Resources Research*, 50, 2468–2487, <https://doi.org/10.1002/2013WR015051>, _eprint: <https://onlinelibrary.wiley.com/doi/pdf/10.1002/2013WR015051>, 2014.
- 1175 Haslinger, K., Holawe, F., and Blöschl, G.: Spatial characteristics of precipitation shortfalls in the Greater Alpine Region—a data-based analysis from observations, *Theor Appl Climatol*, 136, 717–731, <https://doi.org/10.1007/s00704-018-2506-5>, 2019.
- Henne, P. D., Bigalke, M., Büntgen, U., Colombaroli, D., Conedera, M., Feller, U., Frank, D., Fuhrer, J., Grosjean, M., Heiri, O., Luterbacher, J., Mestrot, A., Rigling, A., Rössler, O., Rohr, C., Rutishauser, T., Schwikowski, M., Stampfli, A., Szidat, S., Theurillat, J.-P., Weingartner, R., Wilcke, W., and Tinner, W.: An empirical perspective for understanding climate change impacts in Switzerland, *Reg Environ Change*, 18, 205–221, <https://doi.org/10.1007/s10113-017-1182-9>, 2018.
- 1180 Hersbach, H., Bell, B., Berrisford, P., Hirahara, S., Horányi, A., Muñoz-Sabater, J., Nicolas, J., Peubey, C., Radu, R., Schepers, D., Simmons, A., Soci, C., Abdalla, S., Abellan, X., Balsamo, G., Bechtold, P., Biavati, G., Bidlot, J., Bonavita, M., De Chiara, G., Dahlgren, P., Dee, D., Diamantakis, M., Dragani, R., Flemming, J., Forbes, R., Fuentes, M., Geer, A., Haimberger, L., Healy, S., Hogan, R. J., Hólm, E., Janisková, M., Keeley, S., Laloyaux, P., Lopez, P., Lupu, C., Radnoti, G., de Rosnay, P., Rozum, I., Vamborg, F., Villaume, S., and Thépaut, J.-N.: The ERA5 global reanalysis, *Quarterly Journal of the Royal Meteorological Society*, 146, 1999–2049, <https://doi.org/10.1002/qj.3803>, _eprint: <https://onlinelibrary.wiley.com/doi/pdf/10.1002/qj.3803>, 2020.
- Hijmans, R.: terra: Spatial Data Analysis. R package version 1.7-29., <https://cran.r-project.org/web/packages/terra/>, 2023.
- Hirschi, M., Davin, E. L., Schwingshackl, C., Wartenburger, R., Meier, R., Gudmundsson, L., and Seneviratne, S. I.: Soil moisture and evapotranspiration, Report, ETH Zurich, <https://doi.org/10.3929/ethz-b-000389455>, accepted: 2020-06-05T07:44:43Z, 2020.
- 1190 Hisdal, H. and Tallaksen, L. M.: Drought event definition. Technical Report to the ARIDE project No. 6. Department of Geophysics, University of Oslo., Tech. rep., 2000.
- Horton, R. E.: Drainage-basin characteristics, *Eos, Transactions American Geophysical Union*, 13, 350–361, <https://doi.org/10.1029/TR013i001p00350>, _eprint: <https://agupubs.onlinelibrary.wiley.com/doi/pdf/10.1029/TR013i001p00350>, 1932.

- 1195 Höge, M., Kauzlaric, M., Siber, R., Schönenberger, U., Horton, P., Schwanbeck, J., Floriancic, M. G., Viviroli, D., Wilhelm, S., Sikorska-Senoner, A. E., Addor, N., Brunner, M., Pool, S., Zappa, M., and Fenicia, F.: CAMELS-CH: hydro-meteorological time series and landscape attributes for 331 catchments in hydrologic Switzerland, *Earth System Science Data*, 15, 5755–5784, <https://doi.org/10.5194/essd-15-5755-2023>, publisher: Copernicus GmbH, 2023a.
- 1200 Höge, M., Kauzlaric, M., Siber, R., Schönenberger, U., Horton, P., Schwanbeck, J., Floriancic, M. G., Viviroli, D., Wilhelm, S., Sikorska-Senoner, A. E., Addor, N., Brunner, M., Pool, S., Zappa, M., and Fenicia, F.: Catchment attributes and hydro-meteorological time series for large-sample studies across hydrologic Switzerland (CAMELS-CH), <https://doi.org/10.5281/zenodo.10354485>, 2023b.
- Imfeld, N., Stucki, P., Brönnimann, S., Bürgi, M., Calanca, P., Holzkämper, A., Isotta, F., Nussbaumer, S. U., Scherrer, S., Staub, K., Vicedo-Cabrera, A., Wohlgenuth, T., and Zumbühl, H. J.: 2022: Ein ziemlich normaler zukünftiger Sommer, *Geographica Bernensia*, G100, 1–3, <https://doi.org/10.4480/GB2022.G100>, publisher: Geographisches Institut Universität Bern, 2022.
- 1205 Jehn, F. U., Bestian, K., Breuer, L., Kraft, P., and Houska, T.: Using hydrological and climatic catchment clusters to explore drivers of catchment behavior, *Hydrology and Earth System Sciences*, 24, 1081–1100, <https://doi.org/10.5194/hess-24-1081-2020>, publisher: Copernicus GmbH, 2020.
- Kchouk, S., Melsen, L. A., Walker, D. W., and van Oel, P. R.: A geography of drought indices: mismatch between indicators of drought and its impacts on water and food securities, *Natural Hazards and Earth System Sciences*, 22, 323–344, <https://doi.org/10.5194/nhess-22-323-2022>, publisher: Copernicus GmbH, 2022.
- 1210 Koehler, J., Dietz, A. J., Zellner, P., Baumhoer, C. A., Dirscherl, M., Cattani, L., Vlahović, , Alasawedah, M. H., Mayer, K., Haslinger, K., Bertoldi, G., Jacob, A., and Kuenzer, C.: Drought in Northern Italy: Long Earth Observation Time Series Reveal Snow Line Elevation to Be Several Hundred Meters Above Long-Term Average in 2022, *Remote Sensing*, 14, 6091, <https://doi.org/10.3390/rs14236091>, number: 23 Publisher: Multidisciplinary Digital Publishing Institute, 2022.
- 1215 Kotlarski, S., Gobiet, A., Morin, S., Olefs, M., Rajczak, J., and Samacoits, R.: 21st Century alpine climate change, *Clim Dyn*, 60, 65–86, <https://doi.org/10.1007/s00382-022-06303-3>, 2023.
- Kratzert, F., Klotz, D., Brenner, C., Schulz, K., and Herrnegger, M.: Rainfall–runoff modelling using Long Short-Term Memory (LSTM) networks, *Hydrology and Earth System Sciences*, 22, 6005–6022, <https://doi.org/10.5194/hess-22-6005-2018>, publisher: Copernicus GmbH, 2018.
- 1220 Kratzert, F., Klotz, D., Shalev, G., Klambauer, G., Hochreiter, S., and Nearing, G.: Towards learning universal, regional, and local hydrological behaviors via machine learning applied to large-sample datasets, *Hydrology and Earth System Sciences*, 23, 5089–5110, <https://doi.org/10.5194/hess-23-5089-2019>, publisher: Copernicus GmbH, 2019.
- Kratzert, F., Nearing, G., Addor, N., Erickson, T., Gauch, M., Gilon, O., Gudmundsson, L., Hassidim, A., Klotz, D., Nevo, S., Shalev, G., and Matias, Y.: Caravan - A global community dataset for large-sample hydrology, *Sci Data*, 10, 61, <https://doi.org/10.1038/s41597-023-01975-w>, publisher: Nature Publishing Group, 2023.
- 1225 Laaha, G. and Koffler, D.: Ifstat: Calculation of Low Flow Statistics for Daily Stream Flow Data. R package version 0.9.12, 2022.
- Lee, S. and Ajami, H.: Comprehensive assessment of baseflow responses to long-term meteorological droughts across the United States, *Journal of Hydrology*, 626, 130–256, <https://doi.org/10.1016/j.jhydrol.2023.130256>, 2023.
- 1230 Lees, T., Reece, S., Kratzert, F., Klotz, D., Gauch, M., De Bruijn, J., Kumar Sahu, R., Greve, P., Slater, L., and Dadson, S. J.: Hydrological concept formation inside long short-term memory (LSTM) networks, *Hydrology and Earth System Sciences*, 26, 3079–3101, <https://doi.org/10.5194/hess-26-3079-2022>, publisher: Copernicus GmbH, 2022.

- Mahto, S. S. and Mishra, V.: Global evidence of rapid flash drought recovery by extreme precipitation, *Environ. Res. Lett.*, 19, 044 031, <https://doi.org/10.1088/1748-9326/ad300c>, publisher: IOP Publishing, 2024.
- 1235 Marty, C., Michel, A., Jonas, T., Steijn, C., Muelchi, R., and Kotlarski, S.: SPASS – new gridded climatological snow datasets for Switzerland: Potential and limitations, *EGUsphere*, pp. 1–21, <https://doi.org/10.5194/egusphere-2025-413>, publisher: Copernicus GmbH, 2025.
- Massari, C., Avanzi, F., Bruno, G., Gabellani, S., Penna, D., and Camici, S.: Evaporation enhancement drives the European water-budget deficit during multi-year droughts, *Hydrology and Earth System Sciences*, 26, 1527–1543, <https://doi.org/10.5194/hess-26-1527-2022>, publisher: Copernicus GmbH, 2022.
- Matanó, A., Berghuijs, W. R., Mazzoleni, M., Ruiten, M. C. d., Ward, P. J., and Loon, A. F. V.: Compound and consecutive drought-flood events at a global scale, *Environ. Res. Lett.*, 19, 064 048, <https://doi.org/10.1088/1748-9326/ad4b46>, publisher: IOP Publishing, 2024.
- 1240 McKee, T., Doesken, N., and Kleist, J.: THE RELATIONSHIP OF DROUGHT FREQUENCY AND DURATION TO TIME SCALES, Eight conference on applied climatology, 17-22 January 1993, Anaheim, California, <https://www.semanticscholar.org/paper/THE-RELATIONSHIP-OF-DROUGHT-FREQUENCY-AND-DURATION-McKee-Doesken/c3f7136d6cb726b295eb34565a8270177c57f40f>, 1993.
- 1245 Melsen, L. A. and Guse, B.: Hydrological Drought Simulations: How Climate and Model Structure Control Parameter Sensitivity, *Water Resources Research*, 55, 10 527–10 547, <https://doi.org/10.1029/2019WR025230>, _eprint: <https://onlinelibrary.wiley.com/doi/pdf/10.1029/2019WR025230>, 2019.
- Menapace, A., Dhawan, P., Dalla Torre, D., Kaffas, K., Crespi, A., Larcher, M., Righetti, M., and Cannon, A. J.: Review of bias correction methods for climate model outputs in hydrology, *Journal of Hydrology*, 660, 133 213, <https://doi.org/10.1016/j.jhydrol.2025.133213>, 2025.
- 1250 MeteoSwiss: Daily Precipitation (final analysis): RhiresD, https://www.meteoswiss.admin.ch/dam/jcr:4f51f0f1-0fe3-48b5-9de0-15666327e63c/ProdDoc_RhiresD.pdf, 2021a.
- MeteoSwiss: Daily Mean, Minimum and Maximum Temperature: TabsD, TminD, TmaxD, https://www.meteoswiss.admin.ch/dam/jcr:818a4d17-cb0c-4e8b-92c6-1a1bdf5348b7/ProdDoc_TabsD.pdf, 2021b.
- MeteoSwiss: Daily Relative Sunshine Duration: SrelD, https://www.meteoswiss.admin.ch/dam/jcr:981891db-30d1-47cc-a2e1-50c270bdaf22/ProdDoc_SrelD.pdf, 2021c.
- 1255 MeteoSwiss: Spatial Climate Analyses - MeteoSwiss, <https://www.meteoswiss.admin.ch/climate/the-climate-of-switzerland/spatial-climate-analyses.html>, 2024.
- MeteoSwiss: Open Data - MeteoSchweiz, <https://www.meteoswiss.admin.ch/service-und-publikationen/service/open-data.html>, 2025.
- Michel, A., Aschauer, J., Jonas, T., Gubler, S., Kotlarski, S., and Marty, C.: SnowQM 1.0: A fast R Package for bias-correcting spatial fields of snow water equivalent using quantile mapping, *Geoscientific Model Development Discussions*, pp. 1–28, <https://doi.org/10.5194/gmd-2022-298>, publisher: Copernicus GmbH, 2023.
- 1260 Miller, V. C.: A quantitative geomorphic study of drainage basin characteristics in the Clinch Mountain Area, Virginia and Tennessee. New York: Columbia University, Office of Naval Research Project NR 389 - 042, Technical Report No. 3., Project NR 389 - 042, Technical Report 3, Columbia University, Office of Naval Research, New York, <https://apps.dtic.mil/sti/citations/tr/AD0057755>, 1953.
- 1265 Mishra, A. K. and Singh, V. P.: A review of drought concepts, *Journal of Hydrology*, 391, 202–216, <https://doi.org/10.1016/j.jhydrol.2010.07.012>, 2010.
- Mott, R.: Climatological snow data since 1998, OSHD. *EnviDat*. <https://www.doi.org/10.16904/envidat.401>, 2023.

- Mott, R., Winstral, A., Cluzet, B., Helbig, N., Magnusson, J., Mazzotti, G., Quéno, L., Schirmer, M., Webster, C., and Jonas, T.: Operational snow-hydrological modeling for Switzerland, *Front. Earth Sci.*, 11, <https://doi.org/10.3389/feart.2023.1228158>, publisher: Frontiers, 2023.
- 1270 Muelchi, R., Rössler, O., Schwanbeck, J., Weingartner, R., and Martius, O.: River runoff in Switzerland in a changing climate – changes in moderate extremes and their seasonality, *Hydrology and Earth System Sciences*, 25, 3577–3594, <https://doi.org/10.5194/hess-25-3577-2021>, publisher: Copernicus GmbH, 2021a.
- Muelchi, R., Rössler, O., Schwanbeck, J., Weingartner, R., and Martius, O.: River runoff in Switzerland in a changing climate – runoff regime changes and their time of emergence, *Hydrology and Earth System Sciences*, 25, 3071–3086, <https://doi.org/10.5194/hess-25-3071-2021>, publisher: Copernicus GmbH, 2021b.
- 1275 Mukherjee, S., Mishra, A., and Trenberth, K. E.: Climate Change and Drought: a Perspective on Drought Indices, *Curr Clim Change Rep*, 4, 145–163, <https://doi.org/10.1007/s40641-018-0098-x>, 2018.
- Muñoz-Sabater, J., Dutra, E., Agustí-Panareda, A., Albergel, C., Arduini, G., Balsamo, G., Boussetta, S., Choulga, M., Harrigan, S., Hersbach, H., Martens, B., Miralles, D. G., Piles, M., Rodríguez-Fernández, N. J., Zsoter, E., Buontempo, C., and Thépaut, J.-N.: ERA5-Land: a state-of-the-art global reanalysis dataset for land applications, *Earth System Science Data*, 13, 4349–4383, <https://doi.org/10.5194/essd-13-4349-2021>, publisher: Copernicus GmbH, 2021.
- Mwinjuma, M., Wang, R., Mtupili, M., and Twaha, M.: Comparisons of SPI and SPEI in capturing drought dynamics: A Global assessment across arid and humid regions, *Atmospheric Research*, 329, 108 475, <https://doi.org/10.1016/j.atmosres.2025.108475>, 2026.
- Myronidis, D., Fotakis, D., Ioannou, K., and Sgouropoulou, K.: Comparison of ten notable meteorological drought indices on tracking the effect of drought on streamflow, *Hydrological Sciences Journal*, 63, 2005–2019, <https://doi.org/10.1080/02626667.2018.1554285>, publisher: Taylor & Francis _eprint: <https://doi.org/10.1080/02626667.2018.1554285>, 2018.
- 1285 Najafi, H., Lagerwall, G. L., Obeysekera, J., and Liu, J.: Machine Learning in Climate Downscaling: A Critical Review of Methodologies, Physical Consistency, and Operational Applications, *Water*, 18, 271, <https://doi.org/10.3390/w18020271>, publisher: Multidisciplinary Digital Publishing Institute, 2026.
- 1290 Nathan, R. J. and McMahon, T. A.: Evaluation of automated techniques for base flow and recession analyses, *Water Resources Research*, 26, 1465–1473, <https://doi.org/10.1029/WR026i007p01465>, _eprint: <https://onlinelibrary.wiley.com/doi/pdf/10.1029/WR026i007p01465>, 1990.
- Naumann, G., Cammalleri, C., Mentaschi, L., and Feyen, L.: Increased economic drought impacts in Europe with anthropogenic warming, *Nat. Clim. Chang.*, 11, 485–491, <https://doi.org/10.1038/s41558-021-01044-3>, number: 6 Publisher: Nature Publishing Group, 2021.
- 1295 NCCS, N. C. f. C. S.: South side of the Alps - Current climate., <https://www.nccs.admin.ch/nccs/en/home/regionen/grossregionen/alpensuedseite/klima-heute-alpensuedseite.html>, 2025.
- Orth, R. and Destouni, G.: Drought reduces blue-water fluxes more strongly than green-water fluxes in Europe, *Nat Commun*, 9, 3602, <https://doi.org/10.1038/s41467-018-06013-7>, 2018.
- Otero, N., Horton, P., Martius, O., Allen, S., Zappa, M., Wechsler, T., and Schaeffli, B.: Impacts of hot-dry conditions on hydropower production in Switzerland, *Environ. Res. Lett.*, 18, 064 038, <https://doi.org/10.1088/1748-9326/acd8d7>, publisher: IOP Publishing, 2023.
- 1300 Parry, S., Prudhomme, C., Wilby, R. L., and Wood, P. J.: Drought termination: Concept and characterisation, *Progress in Physical Geography: Earth and Environment*, 40, 743–767, <https://doi.org/10.1177/0309133316652801>, publisher: SAGE Publications Ltd, 2016.
- Parry, S., Wilby, R., Prudhomme, C., Wood, P., and McKenzie, A.: Demonstrating the utility of a drought termination framework: prospects for groundwater level recovery in England and Wales in 2018 or beyond, *Environ. Res. Lett.*, 13, 064 040, <https://doi.org/10.1088/1748-9326/aac78c>, publisher: IOP Publishing, 2018.
- 1305

- Pebesma, E.: Simple Features for R: Standardized Support for Spatial Vector Data, *The R Journal*, 10, 439–446, <https://journal.r-project.org/archive/2018/RJ-2018-009/index.html>, 2018.
- Pebesma, E. and Bivand, R.: *Spatial Data Science: With Applications in R*, Chapman and Hall/CRC, New York, <https://doi.org/10.1201/9780429459016>, 2023.
- 1310 Peña-Angulo, D., Vicente-Serrano, S. M., Domínguez-Castro, F., Lorenzo-Lacruz, J., Murphy, C., Hannaford, J., Allan, R. P., Tramblay, Y., Reig-Gracia, F., and El Kenawy, A.: The Complex and Spatially Diverse Patterns of Hydrological Droughts Across Europe, *Water Resources Research*, 58, e2022WR031976, <https://doi.org/10.1029/2022WR031976>, _eprint: <https://onlinelibrary.wiley.com/doi/pdf/10.1029/2022WR031976>, 2022.
- Peña-Gallardo, M., Vicente-Serrano, S. M., Hannaford, J., Lorenzo-Lacruz, J., Svoboda, M., Domínguez-Castro, F., Maneta, M., Tomas-Burguera, M., and Kenawy, A. E.: Complex influences of meteorological drought time-scales on hydrological droughts in natural basins of the contiguous United States, *Journal of Hydrology*, 568, 611–625, <https://doi.org/10.1016/j.jhydrol.2018.11.026>, 2019.
- 1315 Pisupati, S. L. and Ratnakar, P.: Morphometric analysis and prioritization of sub-watersheds in the Gosthani River Basin of southern India using PCA-WSM and geospatial techniques, *Journal of Water and Climate Change*, 16, 2006–2031, <https://doi.org/10.2166/wcc.2025.727>, 2025.
- 1320 Poussin, C., Massot, A., Ginzler, C., Weber, D., Chatenoux, B., Lacroix, P., Piller, T., Nguyen, L., and Giuliani, G.: Drying conditions in Switzerland – indication from a 35-year Landsat time-series analysis of vegetation water content estimates to support SDGs, *Big Earth Data*, 5, 445–475, <https://doi.org/10.1080/20964471.2021.1974681>, publisher: Taylor & Francis _eprint: <https://doi.org/10.1080/20964471.2021.1974681>, 2021.
- Qiu, J., Shen, Z., Leng, G., and Wei, G.: Synergistic effect of drought and rainfall events of different patterns on watershed systems, *Sci Rep*, 11, 18957, <https://doi.org/10.1038/s41598-021-97574-z>, number: 1 Publisher: Nature Publishing Group, 2021.
- 1325 Ranasinghe, R., Ruane, A. C., Vautard, R., Arnell, N., Coppola, E., Cruz, F. A., Dessai, S., Islam, A. S., Rahimi, M., Ruiz Carrascal, D., Sillmann, J., Sylla, M. B., Tebaldi, C., Wang, W., and Zaaboul, R.: Climate Change Information for Regional Impact and for Risk Assessment., in: *Climate Change 2021: The Physical Science Basis. Contribution of Working Group I to the Sixth Assessment Report of the Intergovernmental Panel on Climate Change.*, pp. 1767–1926, Cambridge University Press, Cambridge, United Kingdom and New York, NY, USA, doi:10.1017/9781009157896.014, 2021.
- 1330 Rangelcroft, S., Van Loon, A. F., Maureira, H., Verbist, K., and Hannah, D. M.: An observation-based method to quantify the human influence on hydrological drought: upstream–downstream comparison, *Hydrological Sciences Journal*, 64, 276–287, <https://doi.org/10.1080/02626667.2019.1581365>, 2019.
- Raposo, V. d. M. B., Costa, V. A. F., and Rodrigues, A. F.: A review of recent developments on drought characterization, propagation, and influential factors, *Science of The Total Environment*, 898, 165550, <https://doi.org/10.1016/j.scitotenv.2023.165550>, 2023.
- 1335 Rodell, M. and Reager, J. T.: Water cycle science enabled by the GRACE and GRACE-FO satellite missions, *Nat Water*, 1, 47–59, <https://doi.org/10.1038/s44221-022-00005-0>, publisher: Nature Publishing Group, 2023.
- Saft, M., Western, A. W., Zhang, L., Peel, M. C., and Potter, N. J.: The influence of multiyear drought on the annual rainfall-runoff relationship: An Australian perspective, *Water Resources Research*, 51, 2444–2463, <https://doi.org/10.1002/2014WR015348>, _eprint: <https://onlinelibrary.wiley.com/doi/pdf/10.1002/2014WR015348>, 2015.
- 1340 Samaniego, L., Kumar, R., and Zink, M.: Implications of Parameter Uncertainty on Soil Moisture Drought Analysis in Germany, *Journal of Hydrometeorology*, 14, 47–68, <https://doi.org/10.1175/JHM-D-12-075.1>, publisher: American Meteorological Society Section: Journal of Hydrometeorology, 2013.

- 1345 Samaniego, L., Thober, S., Kumar, R., Wanders, N., Rakovec, O., Pan, M., Zink, M., Sheffield, J., Wood, E. F., and Marx, A.: Anthropogenic warming exacerbates European soil moisture droughts, *Nature Clim Change*, 8, 421–426, <https://doi.org/10.1038/s41558-018-0138-5>, number: 5 Publisher: Nature Publishing Group, 2018.
- Sarailidis, G., Vasiliades, L., and Loukas, A.: Analysis of streamflow droughts using fixed and variable thresholds, *Hydrological Processes*, 33, 414–431, <https://doi.org/10.1002/hyp.13336>, _eprint: <https://onlinelibrary.wiley.com/doi/pdf/10.1002/hyp.13336>, 2019.
- 1350 Savelli, E., Rusca, M., Cloke, H., and Di Baldassarre, G.: Drought and society: Scientific progress, blind spots, and future prospects, *WIREs Climate Change*, 13, e761, <https://doi.org/10.1002/wcc.761>, _eprint: <https://onlinelibrary.wiley.com/doi/pdf/10.1002/wcc.761>, 2022.
- Scherrer, S. C., Hirschi, M., Spirig, C., Maurer, F., and Kotlarski, S.: Trends and drivers of recent summer drying in Switzerland, *Environ. Res. Commun.*, <https://doi.org/10.1088/2515-7620/ac4fb9>, 2022.
- Scherrer, S. C., Göldi, M., Gubler, S., Steger, C. R., and Kotlarski, S.: Towards a spatial snow climatology for Switzerland: Comparison and validation of existing datasets, *Meteorologische Zeitschrift*, <https://doi.org/10.1127/metz/2023/1210>, publisher: Schweizerbart'sche Verlagsbuchhandlung, 2023.
- 1355 Schürch, M., Kozel, R., and Jemelin, L.: Hydrogeological mapping in Switzerland, *Hydrogeol J*, 15, 799–808, <https://doi.org/10.1007/s10040-006-0136-y>, 2007.
- Shapiro, S. S. and Wilk, M. B.: An Analysis of Variance Test for Normality (Complete Samples), *Biometrika*, 52, 591–611, <https://doi.org/10.2307/2333709>, publisher: [Oxford University Press, Biometrika Trust], 1965.
- 1360 Sideris, I. V., Gabella, M., Erdin, R., and Germann, U.: Real-time radar–rain-gauge merging using spatio-temporal co-kriging with external drift in the alpine terrain of Switzerland, *Quarterly Journal of the Royal Meteorological Society*, 140, 1097–1111, <https://doi.org/10.1002/qj.2188>, _eprint: <https://onlinelibrary.wiley.com/doi/pdf/10.1002/qj.2188>, 2014.
- Stagge, J. H., Tallaksen, L. M., Gudmundsson, L., Van Loon, A. F., and Stahl, K.: Candidate Distributions for Climatological Drought Indices (SPI and SPEI), *International Journal of Climatology*, 35, 4027–4040, <https://doi.org/10.1002/joc.4267>, _eprint: <https://onlinelibrary.wiley.com/doi/pdf/10.1002/joc.4267>, 2015.
- 1365 Stahl, K., Vidal, J.-P., Hannaford, J., Tjeldeman, E., Laaha, G., Gauster, T., and Tallaksen, L. M.: The challenges of hydrological drought definition, quantification and communication: an interdisciplinary perspective, in: *Proceedings of IAHS*, vol. 383, pp. 291–295, Copernicus GmbH, <https://doi.org/10.5194/piahs-383-291-2020>, iSSN: 2199-8981, 2020.
- Staudinger, M., Stahl, K., and Seibert, J.: A drought index accounting for snow, *Water Resources Research*, 50, 7861–7872, <https://doi.org/10.1002/2013WR015143>, _eprint: <https://onlinelibrary.wiley.com/doi/pdf/10.1002/2013WR015143>, 2014.
- 1370 Staudinger, M., Stoelzle, M., Seeger, S., Seibert, J., Weiler, M., and Stahl, K.: Catchment water storage variation with elevation, *Hydrological Processes*, 31, 2000–2015, <https://doi.org/10.1002/hyp.11158>, _eprint: <https://onlinelibrary.wiley.com/doi/pdf/10.1002/hyp.11158>, 2017.
- Stocker, B. D.: *cwd v1.0: R package for cumulative water deficit calculation (v1.0)*. Zenodo. <https://doi.org/10.5281/zenodo.5359053>, 2021.
- Stocker, B. D., Tumber-Dávila, S. J., Konings, A. G., Anderson, M. C., Hain, C., and Jackson, R. B.: Global patterns of water storage in the rooting zones of vegetation, *Nat. Geosci.*, 16, 250–256, <https://doi.org/10.1038/s41561-023-01125-2>, number: 3 Publisher: Nature Publishing Group, 2023.
- 1375 Stoelzle, M., Schuetz, T., Weiler, M., Stahl, K., and Tallaksen, L. M.: Beyond binary baseflow separation: a delayed-flow index for multiple streamflow contributions, *Hydrology and Earth System Sciences*, 24, 849–867, <https://doi.org/10.5194/hess-24-849-2020>, publisher: Copernicus GmbH, 2020.
- 1380 Streeb, N., Lustenberger, F., and Zappa, M.: Beurteilung der Beeinflussung des Abflusses an NAWA-Messstellen. Detailbericht des BAFU-Projekts HydCheck., Tech. rep., Eidg. Forschungsanstalt WSL, Birmensdorf, <https://www.bafu.admin.ch/dam/bafu/de/>

- dokumente/wasser/externe-studien-berichte/beurteilung-der-beeinflussung-des-abflusses-an-nawa-messstellen.pdf.download.pdf/20241007_HydCheck_Detailbericht.pdf, 2024.
- 1385 Sur, C., Park, S.-Y., Kim, J.-S., and Lee, J.-H.: Prognostic and diagnostic assessment of hydrological drought using water and energy budget-based indices, *Journal of Hydrology*, 591, 125–149, <https://doi.org/10.1016/j.jhydrol.2020.125549>, 2020.
- Sutanto, S. J. and Van Lanen, H. A. J.: Catchment memory explains hydrological drought forecast performance, *Sci Rep*, 12, 2689, <https://doi.org/10.1038/s41598-022-06553-5>, number: 1 Publisher: Nature Publishing Group, 2022.
- Swiss Confederation: Nationale Trockenheitsplattform, <https://www.trockenheit.admin.ch/de>, 2025.
- 1390 Swisstopo: Bodeneignungskarte der Schweiz, <https://www.bfs.admin.ch/bfs/de/home/dienstleistungen/geostat/geodaten-bundesstatistik/boden-nutzung-bedeckung-eignung/abgeleitete-und-andere-daten/bodeneignungskarte-schweiz.html>, 2020.
- Swisstopo: swissALTI3D - Das hoch aufgelöste Terrainmodell der Schweiz, <https://backend.swisstopo.admin.ch/fileservice/sdweb-docs-prod-swisstepoch-files/files/2023/11/14/6d40e558-c3df-483a-bd88-99ab93b88f16.pdf>, 2022.
- Tallaksen, L. M. and Van Lanen, H. A. J., eds.: Hydrological drought: processes and estimation methods for streamflow and groundwater., no. 48 in *Developments in Water Science*, Elsevier Science B.V., Amsterdam, the Netherlands, 2004.
- 1395 Tallaksen, L. M., Madsen, H., and Clausen, B.: On the definition and modelling of streamflow drought duration and deficit volume, *Hydrological Sciences Journal*, 42, 15–33, <https://doi.org/10.1080/02626669709492003>, publisher: Taylor & Francis _eprint: <https://doi.org/10.1080/02626669709492003>, 1997.
- Tarasova, L., Gnann, S., Yang, S., Hartmann, A., and Wagener, T.: Catchment characterization: Current descriptors, knowledge gaps and future opportunities, *Earth-Science Reviews*, 252, 104–139, <https://doi.org/10.1016/j.earscirev.2024.104739>, 2024.
- 1400 Tijdeman, E., Barker, L. J., Svoboda, M. D., and Stahl, K.: Natural and Human Influences on the Link Between Meteorological and Hydrological Drought Indices for a Large Set of Catchments in the Contiguous United States, *Water Resources Research*, 54, 6005–6023, <https://doi.org/10.1029/2017WR022412>, _eprint: <https://onlinelibrary.wiley.com/doi/pdf/10.1029/2017WR022412>, 2018.
- Tijdeman, E., Stahl, K., and Tallaksen, L. M.: Drought Characteristics Derived Based on the Standardized Streamflow Index: A Large Sample Comparison for Parametric and Nonparametric Methods, *Water Resources Research*, 56, e2019WR026315, <https://doi.org/10.1029/2019WR026315>, _eprint: <https://onlinelibrary.wiley.com/doi/pdf/10.1029/2019WR026315>, 2020.
- 1405 Tijdeman, E., Blauhut, V., Stoelzle, M., Menzel, L., and Stahl, K.: Different drought types and the spatial variability in their hazard, impact, and propagation characteristics, *Natural Hazards and Earth System Sciences*, 22, 2099–2116, <https://doi.org/10.5194/nhess-22-2099-2022>, publisher: Copernicus GmbH, 2022.
- Tripathy, K. P. and Mishra, A. K.: How Unusual Is the 2022 European Compound Drought and Heat-wave Event?, *Geophysical Research Letters*, 50, e2023GL105453, <https://doi.org/10.1029/2023GL105453>, _eprint: <https://onlinelibrary.wiley.com/doi/pdf/10.1029/2023GL105453>, 2023.
- 1410 Tschurr, F., Feigenwinter, I., Fischer, A. M., and Kotlarski, S.: Climate Scenarios and Agricultural Indices: A Case Study for Switzerland, *Atmosphere*, 11, 535, <https://doi.org/10.3390/atmos11050535>, number: 5 Publisher: Multidisciplinary Digital Publishing Institute, 2020.
- USGS: Drainage Density | U.S. Geological Survey, <https://www.usgs.gov/media/images/drainage-density>, 2023.
- 1415 Van Lanen, H. a. J., Wanders, N., Tallaksen, L. M., and Van Loon, A. F.: Hydrological drought across the world: impact of climate and physical catchment structure, *Hydrology and Earth System Sciences*, 17, 1715–1732, <https://doi.org/10.5194/hess-17-1715-2013>, publisher: Copernicus GmbH, 2013.
- Van Loon, A. F.: Hydrological drought explained, *WIREs Water*, 2, 359–392, <https://doi.org/10.1002/wat2.1085>, _eprint: <https://onlinelibrary.wiley.com/doi/pdf/10.1002/wat2.1085>, 2015.

- 1420 Van Loon, A. F. and Laaha, G.: Hydrological drought severity explained by climate and catchment characteristics, *Journal of Hydrology*, 526, 3–14, <https://doi.org/10.1016/j.jhydrol.2014.10.059>, 2015.
- Van Loon, A. F. and Van Lanen, H. a. J.: A process-based typology of hydrological drought, *Hydrology and Earth System Sciences*, 16, 1915–1946, <https://doi.org/10.5194/hess-16-1915-2012>, publisher: Copernicus GmbH, 2012.
- Van Loon, A. F., Rangecroft, S., Coxon, G., Breña Naranjo, J. A., Van Ogtrop, F., and Van Lanen, H. A. J.: Using paired catchments to quantify
1425 the human influence on hydrological droughts, *Hydrology and Earth System Sciences*, 23, 1725–1739, <https://doi.org/10.5194/hess-23-1725-2019>, publisher: Copernicus GmbH, 2019.
- Vicente-Serrano, S. M., Beguería, S., and López-Moreno, J. I.: A Multiscalar Drought Index Sensitive to Global Warming: The Standardized Precipitation Evapotranspiration Index, *Journal of Climate*, 23, 1696–1718, <https://doi.org/10.1175/2009JCLI2909.1>, publisher: American Meteorological Society Section: *Journal of Climate*, 2010.
- 1430 Vicente-Serrano, S. M., Peña-Angulo, D., Beguería, S., Domínguez-Castro, F., Tomás-Burguera, M., Noguera, I., Gimeno-Sotelo, L., and El Kenawy, A.: Global drought trends and future projections, *Philosophical Transactions of the Royal Society A: Mathematical, Physical and Engineering Sciences*, 380, 20210285, <https://doi.org/10.1098/rsta.2021.0285>, publisher: Royal Society, 2022.
- Viviroli, D., Zappa, M., Gurtz, J., and Weingartner, R.: An introduction to the hydrological modelling system PREVAH and its pre- and post-processing-tools, *Environmental Modelling & Software*, 24, 1209–1222, <https://doi.org/10.1016/j.envsoft.2009.04.001>, 2009.
- 1435 von Matt, C. N., Muelchi, R., Gudmundsson, L., and Martius, O.: Compound droughts under climate change in Switzerland, *Natural Hazards and Earth System Sciences*, 24, 1975–2001, <https://doi.org/10.5194/nhess-24-1975-2024>, publisher: Copernicus GmbH, 2024.
- von Matt, C. N., Martius, O., and Stocker, B. D.: HYD-RESPONSES: High-resolution daily catchment-level time series for relevant hydro-meteorological variables, (water) deficit accumulation and streamflow droughts for Switzerland, <https://doi.org/10.5281/zenodo.14713275>, 2025.
- 1440 von Matt, C. N., Martius, O., and Stocker, B.: HYD-RESPONSES: High-resolution daily catchment-level time series for relevant hydro-meteorological variables, (water) deficit accumulation and streamflow droughts for Switzerland, <https://doi.org/10.5281/zenodo.15748821>, 2026.
- Weingartner, R. and Schwanbeck, J.: Veränderung der Niedrigwasserabflüsse und der kleinsten saisonalen Abflüsse in der Schweiz im Zeitraum 1961 – 2018. Im Auftrag des Bundesamts für Umwelt (BAFU), Bern, Schweiz, 41 S., Tech. rep., Bern, Schweiz, 2020.
- 1445 Wickham, H., Averick, M., Bryan, J., Chang, W., McGowan, L. D., François, R., Grolemund, G., Hayes, A., Henry, L., Hester, J., Kuhn, M., Pedersen, T. L., Miller, E., Bache, S. M., Müller, K., Ooms, J., Robinson, D., Seidel, D. P., Spinu, V., Takahashi, K., Vaughan, D., Wilke, C., Woo, K., and Yutani, H.: Welcome to the Tidyverse, *Journal of Open Source Software*, 4, 1686, <https://doi.org/10.21105/joss.01686>, 2019.
- WMO and GWP: Handbook of Drought Indicators and Indices (M. Svoboda and B. A. Fuchs). Integrated Drought Management Programme (IDMP), Integrated Drought Management Tools and Guidelines Series 2. Geneva., 2016.
- 1450 Wood, R. R., Janzing, J., van Hamel, A., Götte, J., Schumacher, D. L., and Brunner, M. I.: Comparison of high-resolution climate reanalysis datasets for hydro-climatic impact studies, *Hydrology and Earth System Sciences*, 29, 4153–4178, <https://doi.org/10.5194/hess-29-4153-2025>, publisher: Copernicus GmbH, 2025.
- Wu, J., Chen, X., Love, C. A., Yao, H., Chen, X., and AghaKouchak, A.: Determination of water required to recover from
1455 hydrological drought: Perspective from drought propagation and non-standardized indices, *Journal of Hydrology*, 590, 125227, <https://doi.org/10.1016/j.jhydrol.2020.125227>, 2020.

- Wu, J., Chen, X., Yuan, X., Yao, H., Zhao, Y., and AghaKouchak, A.: The interactions between hydrological drought evolution and precipitation-streamflow relationship, *Journal of Hydrology*, 597, 126 210, <https://doi.org/10.1016/j.jhydrol.2021.126210>, 2021.
- 1460 Wu, J., Mallakpour, I., Yuan, X., Yao, H., Wang, G., and Chen, X.: Impact of the false intensification and recovery on the hydrological drought internal propagation, *Weather and Climate Extremes*, 36, 100 430, <https://doi.org/10.1016/j.wace.2022.100430>, 2022.
- Xu, Z., Wu, Z., Guo, X., and He, H.: Estimation of water required to recover from agricultural drought: Perspective from regression and probabilistic analysis methods, *Journal of Hydrology*, 617, 128 888, <https://doi.org/10.1016/j.jhydrol.2022.128888>, 2023.
- 1465 Yi, K., Senay, G. B., Fisher, J. B., Wang, L., Suvočarev, K., Chu, H., Moore, G. W., Novick, K. A., Barnes, M. L., Keenan, T. F., Mallick, K., Luo, X., Missik, J. E. C., Delwiche, K. B., Nelson, J. A., Good, S. P., Xiao, X., Kannenberg, S. A., Ahmadi, A., Wang, T., Bohrer, G., Litvak, M. E., Reed, D. E., Oishi, A. C., Torn, M. S., and Baldocchi, D.: Challenges and Future Directions in Quantifying Terrestrial Evapotranspiration, *Water Resources Research*, 60, e2024WR037 622, <https://doi.org/10.1029/2024WR037622>, <https://agupubs.onlinelibrary.wiley.com/doi/pdf/10.1029/2024WR037622>, 2024.
- Yihdego, Y., Vaheddoost, B., and Al-Weshah, R. A.: Drought indices and indicators revisited, *Arab J Geosci*, 12, 69, <https://doi.org/10.1007/s12517-019-4237-z>, 2019.
- 1470 Zambrano-Bigiarini, M.: hydroTSM: Time Series Management, Analysis and Interpolation for Hydrological ModellingR package version 0.6-0. URL <https://github.com/hzambran/hydroTSM>. DOI:10.5281/zenodo.839864., 2020.
- Zhang, L., Yan, Z., Huang, K., and Zhang, W.: Evaluation and statistical bias correction of ERA5-Land meteorological variables for a humid river basin in Southwest China, *Sci Rep*, 15, 41 101, <https://doi.org/10.1038/s41598-025-24942-4>, publisher: Nature Publishing Group, 2025.
- 1475 Zhou, Z., Shi, H., Fu, Q., Ding, Y., Li, T., and Liu, S.: Investigating the Propagation From Meteorological to Hydrological Drought by Introducing the Nonlinear Dependence With Directed Information Transfer Index, *Water Resources Research*, 57, e2021WR030 028, <https://doi.org/10.1029/2021WR030028>, <https://onlinelibrary.wiley.com/doi/pdf/10.1029/2021WR030028>, 2021.